Trafficking of lysosomal proteins via the sortilin sorting receptor

Maryssa Canuel
Department of Anatomy and Cell Biology
McGill University
Montréal, Canada
December 2007

A thesis submitted to McGill University in partial fulfillment of the requirements of the degree Doctor of Philosophy in Science

Your file Votre référence
ISBN: 978-0-494-50787-2
Our file Notre référence
ISBN: 978-0-494-50787-2

Abstract

Delivery of soluble lysosomal proteins from the Golgi apparatus to the lysosomes is dependent primarily on the mannose 6-phosphate receptor (M6PR). The M6PR has been demonstrated to achieve and be recycled from the endosomal compartment through interactions with GGA, AP-1, and retromer adaptor proteins. However, in I-cell disease (ICD), in which the M6PR pathway is non-functional, many soluble lysosomal proteins continue to traffic to the lysosomes. The novel sortilin sorting receptor has been implicated in the M6PR-independent targeting of sphingolipid activator proteins. We therefore tested the hypothesis that soluble proteases that exhibit M6PR-independent trafficking are targeted to the lysosomes by sortilin in a process dependent upon AP-1 and retromer. Using a dominant-negative sortilin construct and an RNA interference (RNAi), we demonstrated that while cathepsin D transport is partially dependent upon sortilin, cathepsin H requires sortilin, whereas cathepsins K and L do not. Similarly, using RNAi, we observed that the anterograde trafficking of sortilin and its cargo required AP-1, while the retrograde recycling pathway necessitated retromer through an interaction with a YXXΦ consensus site in the cytosolic tail of sortilin. Furthermore, analysis of detergent-resistant membrane (DRM) microdomains demonstrated the presence of sortilin and its ligands, but the absence of the M6PR and its ligands. Our results suggest that sortilin functions as an alternative sorting receptor to the M6PR and that uniquely sortilin and its ligands interact on sphingomyelin rich platforms in the Golgi apparatus.

Résumé

La distribution des protéines lysosomales solubles aux lysosomes dépend principalement du récepteur mannose 6-phosphate (RM6P). Il a été démontré que le RM6P atteint le compartiment endosomale et y est recyclé à travers l'interaction avec le GGA, le AP-1 et les protéines retromères adapteures. Cependant, dans la maladie I-cell (MIC), dans laquelle la voie du RM6P est non-fonctionnelle, plusieurs protéines lysosomales solubles continuent de circuler vers les lysosomes. Le nouveau récepteur de triage de la sortiline est impliqué dans la vectorisation indépendante des protéines activatrices de sphingolipides du RM6P. C'est pourquoi nous avons testé l'hypothèse selon laquelle les protéases solubles qui présentent une circulation indépendante du RM6P sont associées aux lysosomes par la sortiline dans un processus dépendant du AP-1 et du retromer. En utilisant un modèle de sortiline à dominance négative et une interférence du RNA (iRNA), nous démontrons que le transport de la cathepsine D est partiellement dépendant de la sortiline, que la cathepsine H requiert la sortiline et que les cathepsines K et L n'en ont aucun besoin. De façon similaire, en utilisant l'iRNA, nous observons que la circulation anterograde de la sortiline et de ses charges requiert le AP-1, et que la voie de recyclage retrogarde nécessite le retromer à travers une interaction avec un site de consensus YXXΦ dans la queue cytosolique de la sortiline. De plus, l'analyse des microdomaines de la membrane résistante au détergent démontre la présence de sortiline et de ses ligands, mais l'absence du RM6P et de ses ligands. Nos résultats suggèrent que la sortiline fonctionne comme récepteur de triage alternatif au RM6P et que, de façon unique, la sortiline et ses ligands interagissent sur les plates-formes riches de sphingomyeline dans l'appareil de Golgi.

To my family, for their unwavering support and encouragement.

Acknowledgements

I would like to begin by expressing my gratitude and appreciation to my supervisor, Dr. Carlos R. Morales. He has been a great guide and mentor throughout my studies and research in his laboratory.

I would also like to recognize and thank Drs. Hermo, Presley, and Lefrancois for the many hours of support and advice they provided me with over the years. Furthermore, I would like to acknowledge Dr. Pchejetski for his guidance, suggestions, and experimental help.

Additionally, profound thanks must be expressed to Dr. John Mort for providing me with antibodies for cathepsins B and H, as well as for LAMP-1.

To my fellow students and lab-mates, both past and present, I would like to communicate my appreciation for the support and advice they provided me. Time spent with them, as well as the undergraduate students I had the privilege of working with, not only improved my research, but also made it more enjoyable.

Finally, I would like to extend a most sincere and profound thanks to my loving parents and husband. Their support began early on and never faltered.

Abbreviations

CD-M6PR: Cation dependent mannose 6-phosphate receptor

CI-M6PR: Cation independent mannose 6-phosphate receptor

CO-IP: Co-immunoprecipitation

COP: Coat protein complex

DMEM: Dulbecco's modified Eagle's medium

DRMs: Detergent-resistant membranes

FBS: Fetal bovine serum

GGA: Golgi-localized, γ-ear containing, Arf binding protein

$G_{M2}AP$: G_{M2} activator protein

ICD: Inclusion-cell disease

IGF: Insulin-like growth factor

LAMP: Lysosome-associated membrane protein

LAP: Lysosomal acid phosphatase

LEP: Lysosomal-endosomal protein

LIMP: Lysosome integral membrane proteins

LpL: Lipoprotein lipase

LRP: Low-density lipoprotein receptor-related protein-1

LSD: Lysosomal storage disorder

M6PR: Mannose 6-phosphate receptor

MVB: Multi-vesicular body

NTR: Neurotensin receptor

PACS-1: Phosphofurin acidic cluster sorting protein

PBS: Phosphate buffered saline

Pro-NGF: Nerve growth factor precursor

RAP: Receptor-associated protein

SAP: Sphingolipid activator protein

shRNA: Short-hairpin RNA

siRNA: Short-interfering RNA

SNAREs: Soluble N-ethylmaleimide-sensitive fusion protein (NSF) attachment proteins receptors

TGN: Trans-Golgi network

TIP-47: Tail-interacting protein 47

VPS: Vacuolar sorting protein

Table of Contents

List of Tables and Figures

Chapter 1: Introduction

Lysosomal proteins are synthesized in the endoplasmic reticulum (ER) and are subsequently processed in the Golgi apparatus. In order to attain the lysosomal compartment from the *trans*-Golgi network (TGN), newly synthesized proteins employ a vesicular transport system. Soluble hydrolases require a trans-membrane sorting receptor to interact with adaptor molecules, which in turn mediate sorting from the TGN (Lobel et al., 1989).

It has been well established that the majority of soluble lysosomal proteases employ the canonical mannose-6-phosphate receptor (M6PR) to traffic to the lysosomes. In this pathway, a phosphotransferase found in the *cis*-Golgi recognizes and tags the newly synthesized enzyme with mannos-6-phosphate residues. Upon arrival in the TGN, the mannose-6-phosphate tagged protease is recognized by the luminal domain of the M6PR (Reitman et al., 1981; Varki et al., 1981; Waheed et al., 1982). This receptor has a cytoplasmic tail containing an acidic cluster di-leucine motif that recruits adaptor proteins and ultimately drives clathrin-coated vesicle formation, as well as lysosomal targeting (Puertollano et al., 2001; Zhu et al., 2001).

Examination of the lysosomal contents of fibroblasts from patients with I-cell disease (ICD) revealed near normal levels of sphingolipid activator proteins (SAPs), as well as several soluble proteases. ICD results from a mutation in the phosphotransferase gene that adds the M6P tag to soluble lysosomal proteins (Reitman et al., 1981; Rijnboutt et al., 1991a). This finding is an indication of the existence of an alternative mechanism of trafficking for certain soluble lysosomal proteins independently of the M6PR.

Sortilin is a 100 kDa type I sorting receptor recently implicated in the transport of a subtype of soluble lysosomal proteins, the SAPs (Lefrancois et al., 2003). It is therefore our hypothesis that sortilin may represent a general alternative pathway to the M6PR for other lysosomal proteins that exhibit M6PR-independent trafficking. In this context, our study pursues two objectives: **1) Identification of novel sortilin cargo; 2) Determination of the adaptor proteins and complexes that mediate the anterograde and retrograde sorting of sortilin.** To test the proposed hypothesis, we have used both RNAi targeting of sortilin and of the adaptor proteins that we postulated were implicated in sorting sortilin. Additionally, we have employed a dominant-negative sortilin construct lacking its cytoplasmic tail.

Moreover, in an attempt to distinguish and differentiate the sortilin and M6PR sorting pathways, we have examined whether the interaction between soluble proteins and their sorting receptors occurs in lipid microdomains. Recent studies have demonstrated that prosaposin, a known ligand of sortilin, requires sphingomyelin for its translocation to the lysosomes (Lefrancois et al., 2002). Depletion of sphingomyelin with D609 resulted in the inhibition of the lysosomal transport of prosaposin and consequently in its misrouting to the secretory pathway (Lefrancois et al., 1999). Since sphingomyelin is enriched in detergent resistant membrane (DRM) domains which serve as scaffolds for cellular signaling and trafficking events (Helms and Zurzolo, 2004; Ikonen, 2001; Simons and Ikonen, 1997; Simons and Toomre, 2000), **we propose that sortilin resides in a DRM domain, possibly in the TGN.** To test this hypothesis we have compared the localizations of sortilin, the M6PR, and a variety of their ligands, with the lipid raft marker, flotillin-1.

Chapter 2: Review of the Literature

Objectives

Given that sortilin is a sorting receptor that traffics between the TGN and the endosomal compartment, the first objective of the present review will be to describe the biogenesis and function of lysosomes. Further to this, lysosomal proteins will be categorized into four different groups and the mechanism of vesicular trafficking and sorting of the various types of lysosomal protein examined. Specific attention will be given to sorting receptors, M6PR and sortilin, that mediate targeting of soluble lysosomal proteins, as well as the adaptor proteins implicated in this process.

Since lysosomes are dynamic structures involved in the regulation of various metabolic pathways, there are many possible points of mutation and disruption in the biogenesis of lysosomes and the targeting of proteins to these organelles. Once thought to be rare, the number and frequency of diagnosis of lysosomal storage disorders (LSDs) is growing rapidly. More and more powerful techniques are driving the identification of markers of LSDs. These markers extend beyond those related to classical lysosomal proteins (enzymes and activators) and now include proteins that function as sorting receptors and adaptor proteins involved in lysosomal trafficking and lysosomal biogenesis. Further research into lysosomal biogenesis and function will help to spur a better understanding of the enzymology, cell biology, and pathology of LSDs. The final objective of this review will therefore be to discuss LSDs and provide a summary of the most important details related to the research conducted herein.

Biogenesis of Lysosomes

Lysosomes are intracytoplasmic organelles that contain 60 different hydrolases responsible for the digestion of material of intracellular and extracellular origin (Morales et al., 1995; Steinman et al., 1983; Suzuki, 1995). In addition, lysosomes have been implicated in other specialized cellular processes such as antigen presentation, bone remodeling, and regulation of various growth factors (Dell'Angelica et al., 2000a; Marks et al., 1995; Marks, 1989; Renfrew and Hubbard, 1991). When viewed under the electron microscope, lysosomes are morphologically heterogeneous (Morales et al., 1999). The typical lysosome, however, is surrounded by a single membrane, ranges between 0.2 and 0.4 μm in diameter, contains electron dense material, has an acidic pH, and is enriched in acid phosphatase as well as in a variety of soluble hydrolases (Bainton, 1981; Maxfield, 1982; Morales et al., 1999; Steinman et al., 1983). Also visible by the electron microscope are electron-lucent endosomes that are free of acid-phosphatases and multivesicular bodies (MVBs) containing numerous membrane-bound structures and moderate acid phosphatase activity (Morales et al., 1999; Steinman et al., 1983). MVBs are considered intermediate structures in the pathway to lysosome formation and clear distinction of MVBs from late endosomes may sometimes prove to be difficult (Morales et al., 1999).

There are three known mechanisms by which lysosomes are formed: bulk and receptor-mediated endocytosis, phagocytosis, and autophagy (Clermont et al., 1987; Geuze et al., 1983; Morales et al., 1999; Steinman et al., 1983; Tang et al., 1988). Endocytosis exists in most cell types whereas phagocytosis is predominant in

professional phagocytes such as macrophages and Sertoli cells, and involves cellular uptake of large particulate matter such as bacteria, erythrocytes, cellular debris, and apoptotic cells (Clermont et al., 1987; Morales et al., 1999; Steinman et al., 1983). Autophagy also exists in most cell types and is the process responsible for intracellular degradation of various aged organelles through formation of autophagocytic structures (Tang et al., 1988; Terman and Brunk, 2005). Nonetheless, lysosomal formation via the endocytic pathway is considered the prevalent mechanism (Clermont et al., 1987).

Two main models have been proposed, and extensively debated, to explain how endocytosis results in formation of lysosomes: the "stationary model" and the "maturational model" (Mellman, 1996; Morales et al., 1999). According to the "stationary model", the structures that comprise the endocytic pathway (endosome, MVB, and lysosome) are all permanent and functionally distinct. The lysosomes then arise from vesicles budding off the late endosomal compartment. Vesicles from the endosomal compartment deliver soluble and membrane components to the lysosomes (Mellman, 1996). According to this model, endosomal resident proteins necessitate a retrograde trafficking from the lysosomal compartment to the endosomes. Unfortunately, little direct evidence has been obtained to support the "stationary model" of lysosomal biogenesis. The second model, the "maturational model", predicts that endocytosis results in the translocation of plasma membrane to pinocytotic vesicles that mature into endosomes, multivesicular bodies, and finally lysosomes (Geuze et al., 1983). According to this view, the endosome and MVB are transient structures where endocytic vesicles fuse together to form the endosomal

compartment (Clermont et al., 1987). Subsequent formation of the lysosomes then depends upon vesicular transport of lysosomal proteins from the Golgi apparatus to endosomes to initiate the maturational process (Morales et al., 2001; Morales et al., 1999). This model has also been called into question, primarily for the implication that the lysosome is a terminal compartment (Storrie and Desjardins, 1996). Small fluorescently labeled dextran and sucrose molecules have been previously demonstrated to be rapidly recycled from the lysosomal compartment, this suggests that the lysosome is not a terminal compartment and that vesicular trafficking plays a role in lysosomal biogenesis and maintenance (Besterman et al., 1981; Buckmaster et al., 1987; Jahraus et al., 1994). Given that neither the "stationary model" nor the "maturational model" entirely account for the diverse nature and function of the lysosomes and their biogenesis, recent work has continued to examine lysosome formation. Controversial new data has led to the proposal of hybrid models, such as the "kiss-and-run" hypothesis, that have only added further complexity to the issue (Storrie and Desjardins, 1996). The "kiss-and-run" hypothesis predicts that endosomes and lysosomes "bump into" each other and fusion between the two organelles results in transfer of material from the endosome to the lysosomes. The main evidence for the "kiss-and-run" model comes from cell-free assays that examined the transfer of material from endosomes to lysosomes, resulting in a new hybrid organelle (Storrie and Desjardins, 1996). Although there has been extensive debate, a complete understanding of the biogenesis of lysosomes has not yet been attained.

Nevertheless, it is by these various endocytic, phagocytic, and autophagocytic mechanisms that lysosomes acquire integral membrane proteins of protective function or of specialized function (such as proton pump ATPases) (Braun et al., 1989; Ogata and Fukuda, 1994; Rohrer et al., 1996; Stevens and Forgac, 1997). These specialized transmembrane proteins are essential in generating and maintaining the acidic environment found within the lysosomes by pumping protons into the lumen in an ATP-dependent manner (Stevens and Forgac, 1997). The acidic environment is in turn essential for the optimal activity of hydrolytic enzymes found within the lysosomal lumen (Stoka et al., 2005).

Protection of the lysosomal membrane, as well as of other organelles, from the acidic environment and hydrolytic enzymes within, is provided by a carbohydrate coat of heavily glycosylated membrane proteins found therein (Ogata and Fukuda, 1994; Rohrer et al., 1996; Sandhoff and Kolter, 1996). However, in addition to the contribution of the endocytic pathway to the biogenesis of the lysosomal membrane there is additional contribution from the Golgi apparatus which traffics not only soluble hydrolases such as cathepsins, but also integral membrane proteins like lysosome-associated membrane proteins (LAMPs) to the lysosomes (Lobel et al., 1989).

The diverse mechanisms by which lysosomes are formed account in part for their heterogeneous morphology and content (Bagshaw et al., 2005b; Morales et al., 1999). Interestingly, a proteomic assessment of highly purified tritosomes (Triton WR 1339-filled lysosomes) revealed over 215 different membrane proteins, some of which had previously been observed to associate with the endoplasmic reticulum,

Golgi apparatus, cytoplasm, plasma membrane, and lipid rafts (Bagshaw et al., 2005b). These results reflect a higher degree of complexity for the biogenesis and functions of these organelles.

Lysosomal Proteins

The lysosomal proteome encompasses four classes of proteins that include soluble hydrolases, membrane hydrolases, protective membrane proteins, and activator proteins (Morales et al., 1999).

Soluble Hydrolases

Soluble hydrolases comprise a vast group of diverse lysosomal proteins that are synthesized as pre-proenzymes (Hasilik, 1992). The pre-proenzymes undergo subsequent N-linked glycosylation and carbohydrate processing that allows for recognition by lysosomal sorting receptors and may protect the proenzyme from degradation within the lysosomal compartment (Bohley and Seglen, 1992). This group of lysosomal proteins includes proteases, nucleases, lipases, glycosidases, phosphatases, and sulfatases (Morales et al., 1999). A large number of soluble hydrolases are in fact proteases, the most abundant of which are the cathepsins. The proteolytic capacity of these proteases may be divided into endo- or exo-peptidase activity depending upon the location of their targeted cleavage (Bohley and Seglen, 1992). Additionally, proteases can be classified according to the catalytic residue found in the enzyme's active site. Endopeptidases that are cysteine proteases include cathepsins B, F, H, K, L, O, S, and W. Endopeptidases that are aspartic proteases

include cathepsins D, and E. Endopeptidases that are serine proteases include cathepsin G. Exopeptidases may be divided into aminopeptidases (cathepsin H and C) and carboxypeptidases (cathepsins A, B, and X). These enzymes function optimally at the acidic pH found within the lysosomes, although cathepsin E and G have been found to function outside the lysosome at neutral pH (Winchester, 2005). While neutral pH acts as an inhibitor of cathepsin activity, there are numerous factors such as stefins, cystatins, serpins, and thyropins that also inhibit activity of cathepsins in the cell (Turk et al., 2002). Many cathepsins, including cathepsins B, H, and L are ubiquitously expressed, whereas other cathepsins, such as cathepsins S and K, have restricted expression patterns (primarily in lymphatic tissue and osteoclasts respectively).

While cathepsins function primarily in the degradation and turnover of proteins within the lysosomal compartment, they possess several other important features. Cathepsins are responsible for the processing of antigens for presentation to MHC class II molecules (Turk et al., 2000; Turk et al., 2001). It has been suggested that cathepsins play a role in cell death through destabilization of the mitochondria via Bid activation, as well as cleavage of anti-apoptotic Bcl-2 family members (Turk and Stoka, 2007). Therefore the proper distribution and function of cathepsins is essential for efficient lysosomal and cellular functioning. There is growing evidence that imbalance in the localization of cathepsins is related to familial forms of Alzheimer's disease (Urbanelli et al., 2006). Increased levels of cathepsin H in sera have also been identified as a marker in colorectal cancer (Schweiger et al., 2004).

Membrane Hydrolases

A second type of lysosomal hydrolase is an integral membrane protein, the ubiquitously expressed lysosomal acid phosphatase (LAP). LAP is targeted to the plasma membrane and translocated to the lysosome via endocytic flow (Braun et al., 1989). Once LAP attains the lysosome, it is released from the membrane by limited proteolysis (Gottschalk et al., 1989). *In vivo* the substrates and functional role of LAP are unclear. *In vitro* LAP has been demonstrated to be capable of cleaving phosphomonoesters like adenosine monophosphate and glucose 6-phosphate (Gieselmann et al., 1984). LAP-deficient mice showed lysosomal storage in podocytes and tubular epithelial cells of the kidneys and subsets of glial cells, although the mice had normal levels of phosphomonoesters (Suter et al., 2001).

Protective Membrane Proteins

Other lysosomal integral membrane proteins are not enzymatically active, but rather have either a membrane protective role or function as ion transporters. Protective membrane proteins include the lysosomal associated membrane proteins (LAMPs), lysosome integral membrane proteins (LIMPs), lysosomal-endosomal protein (LEP) (Morales et al., 1999). It has been proposed that in order to serve their protective membrane function LAMPs and LIMPs are highly glycosylated and pack together tightly to comprise greater than 50 % of the total lysosomal membrane (Eskelinen et al., 2003). LAMPs are type I transmembrane proteins. LAMP-2 spans the lysosomal membrane twice whereas LIMP-1 spans the lysosomal membrane 4 times (Fukuda, 1991; Metzelaar et al., 1991; Vega et al., 1991b). Although not

considered a protective membrane protein, the best characterized example of a lysosomal integral membrane protein is the H^+-ATPase pump. This transporter is composed of a protein-complex of at least 13 different subunits and is responsible for the translocation of protons into the lysosomal compartment leading to acidification of the lysosome. Acidification of the vacuole involves the reversible dissociation and reassembly of the various subunits of the H^+-ATPase pump (Forgac, 1999). Mutation of a subunit of the proton pump that is specifically expressed in osteoclasts leads to osteopetrosis since demineralization of the bone matrix is inhibited by defective acidification of resorption lacunae which function as "extracellular lysosomes" (Eskelinen et al., 2003; Frattini et al., 2000).

Sphingolipid Activator Proteins

Sphingolipid activator proteins (SAPs) are a category of soluble lysosomal co-factors involved in the non-enzymatic degradation of sphingolipids in lysosomes. This category includes 5 activators, the G_{M2} activator protein ($G_{M2}AP$) and saposins A, B, C, and D. SAPs act as biological detergents to facilitate the interaction of glycosphingolipid substrates with their respective enzymes for degradation, since glycosphingolipids are unable to interact directly with hydrolytic enzymes in a hydrosoluble milieu (Furst and Sandhoff, 1992; Mahuran, 1998; O'Brien and Kishimoto, 1991). According to the "liftase hypothesis", $G_{M2}AP$ recognizes G_{M2} gangliosides within the membrane, binds to and lifts it out of the bilayer to then present it in a water-soluble format to β-hexosaminidase A (Giehl et al., 1999). However, a second hypothesis proposes that $G_{M2}AP$ binds to an already solubilized

ganglioside to insure its recognition by the β-hexosaminidase A enzyme responsible for its degradation (Furst and Sandhoff, 1992; Li et al., 1999).

The remaining SAPs result from a common precursor, prosaposin, which is the product of a gene different from that of the $G_{M2}AP$. Prosaposin is proteolytically cleaved in the lysosomal compartment to generate saposins A, B, C, and D (Furst and Sandhoff, 1992; Nakano et al., 1989; O'Brien et al., 1988; Sandhoff and Kolter, 1996). The saposins resemble each other in that they are all approximately 80 amino acids in length, they are glycosylated, and they all form three internal disulfide bridges in their hydrophobic core (Morimoto et al., 1988; O'Brien and Kishimoto, 1991; O'Brien et al., 1988).

Saposin B was the first identified activator protein. Saposin B activates the hydrolysis of sulfatide by arylsulfatase A, the hydrolysis of GM1 ganglioside by β-galactosidase, and globotriaosylceramide by α-galactosidase (Inui and Wenger, 1984; Li et al., 1988). While many other lipids (such as G_{M2} ganglioside) interact with saposin B, this activator is not responsible for stimulating their hydrolysis (Inui and Wenger, 1984). Saposin C, was identified in 1971, and shown to activate the hydrolysis of glucosylceramide by β-glucosidase and galactocerebroside by β-galactosidase (Glew et al., 1988; Ho and O'Brien, 1971; Morimoto et al., 1989; Radin, 1984). Unlike saposin B, saposin C does not interact directly with its lipid substrates, but rather binds to and activates its effecter enzymes. The activation effect of saposin C has been proposed to be either due to its ability to induce a conformational change in the effecter enzyme allowing for optimal catalysis or more likely by reconstituting enzyme activity by favoring enzyme localization to

appropriate lipid surfaces (Fabbro and Grabowski, 1991; Peters et al., 1977; Qi et al., 1994; Vaccaro et al., 1995; Vaccaro et al., 1993). Saposin A stimulates acid β-glucosidase (glucocerebrosidase) to hydrolyze glucocerebroside (Fabbro and Grabowski, 1991). Saposin D, the final and least characterized SAP, has been implicated in the activation of both sphingomyelin and ceramide hydrolysis (Azuma et al., 1998; Morimoto et al., 1988).

Vesicular Transport

Under most circumstances, the transfer of material between various organelles requires vesicles. Four main processes have been described in vesicle transport: budding, transport, tethering, and fusion (Bonifacino and Glick, 2004).

The budding of vesicles necessitates a wide variety of coat proteins that function to generate membrane curvature, and participate in cargo selection of transmembrane proteins (Cai et al., 2007). Coat proteins are primarily composed of adaptor proteins, clathrin, coat protein complex I (COPI), COPII, and SNAREs (soluble N-ethylmaleimide-sensitive fusion protein (NSF) attachment proteins receptors) (Barlowe et al., 1994; Pearse, 1975; Waters et al., 1991). The recruitment of coat proteins involve small GTPases from the Arf family (Springer et al., 1999). Molecular motors such as kinesin, dynein, and myosin may then drive transport of the vesicle to its destination (Hammer and Wu, 2002; Matanis et al., 2002).

Once at the desired destination, a vesicle may then attach, or tether to the recipient membrane. Tethers are responsible for directing specific interactions between vesicular and destination membranes (Cai et al., 2007). They function by

physically bringing vesicles together with their target compartment or by promoting formation of SNARE complexes to mediate membrane fusion (Malsam et al., 2005; Shorter et al., 2002). Tethers may be sub-categorized as either long coiled-coil proteins (such as Uso1p, p115, GM130/golgin-95) or multi-subunit protein complexes (such as transport protein particle (TRAPP) complexes I and II) (Hammer and Wu, 2002; Matanis et al., 2002). Rabs are small GTPases that belong to the Ras superfamily of proteins and play an important role in vesicular tethering. Over 60 known Rabs have been identified in mammals. Rabs are present in the cytosol under a GDP-bound format but are recruited and inserted into membranes via prenyl groups. Specific GEFs (guanine nucleotide exchange factors) then activate Rabs through the exchange of GDP with GTP (Soldati et al., 1994; Ullrich et al., 1994). Activated Rabs then interact with downstream effectors to mediate membrane tethering. GTP is hydrolyzed to GDP by specific GAPs (GTPase-activating protein) to terminate Rab activity and release Rabs back into the cytosol (Rybin et al., 1996). Rabs 4, 5, and 11 have been shown to be localized to the early endosomal compartment, whereas Rabs 7 and 9 are found on the membrane of the late endosomal compartment (Feng et al., 1995; Soldati et al., 1995; Sonnichsen et al., 2000).

Vesicular and donor membranes then fuse. SNAREs are trans-membrane proteins implicated in mediating membrane fusion events (Chen and Scheller, 2001; Jahn and Grubmuller, 2002; Pelham and Rothman, 2000). Vesicles that bud from the TGN are associated with specific vesicle-membrane SNAREs (v-SNAREs) that recognize and mediate interaction with specific target-SNAREs (t-SNAREs) found on

endosomal membranes (Hong, 2005). As a result of fusion, a pore is formed joining the distal leaflets of the fusing membranes. It is postulated that the role of SNAREs in such a process is to exert mechanical force upon the membranes in order to force fusion. Alternatively, SNAREs may cause the formation of non-bilayer membranes by disrupting hydrophilic-hydrophobic boundaries (Jahn and Scheller, 2006). It is by thus mechanism that material is transported between subcellular compartments in vesicles.

Trafficking of Lysosomal Proteins

Depending on the physical nature of a protein, trafficking to the lysosomes occurs through two different pathways. Given their localization to the Golgi membrane, lysosomal integral membrane proteins with the appropriate sorting signals may interact directly with adaptor proteins to recruit clathrin and be transported to lysosomes. For the same reason, soluble lysosomal proteins found within the Golgi lumen must interact with trans-membrane lysosomal sorting receptors which in turn recruit clathrin for lysosomal transport.

Lysosomal Integral Membrane Proteins

Integral membrane proteins that are lysosomally bound may reach their target destination via two different routes. For LAMP-1, LAMP-2, and LIMP-2 the route from the Golgi to the endosomes and then lysosomes is direct, whereas in the case of LAP the route taken is indirect and involves passage through the secretory pathway and the plasma membrane where LAP is endocytosed (Barriocanal et al., 1986; Braun

et al., 1989; Traub et al., 1996; Vega et al., 1991a). The two different sorting signals responsible for targeting these proteins from the Golgi to the lysosomes are both found in their short cytosolic tails. The first sorting signal found in lysosomally bound integral membrane proteins is based upon a tyrosine containing motif. This signal has been shown to be implicated in the trafficking of LAMP-1, LAMP-2, LIMP-1, and LAP (Harter and Mellman, 1992; Honing and Hunziker, 1995; Peters et al., 1990). The second signal that has been demonstrated to play a role in lysosomal transport of integral membrane proteins is a "dileucine" motif. This signal is found in LIMP-2 (Sandoval et al., 1994). The presence of these lysosomal sorting signals in the cytosolic domains of integral membrane proteins allows for the interaction with the multimeric adaptor protein 3 (AP-3) which can then drive formation of clathrin-coated vesicles destined to the lysosomes (Ohno et al., 1997; Robinson and Bonifacino, 2001).

Lysosomal Sorting Receptors

It is well established that to reach the lysosome, a soluble lysosomal protein must interact with a trans-membrane sorting receptor containing a cytoplasmic domain that binds adaptor proteins (Lobel et al., 1989; Nielsen et al., 2001). The mannose 6-phosphate receptor (M6PR) binds and routes most soluble lysosomal proteases, including several cathepsins (Lobel et al., 1989). The recognition of soluble proteases by the M6PR occurs in the TGN and depends upon the tagging of M6P residues to the newly synthesized enzyme by a specific phosphotransferase (Reitman et al., 1981; Varki et al., 1981; Waheed et al., 1982). Sortilin, a 100 kDa,

TGN-localized sorting receptor, has also been implicated in the transport of soluble lysosomal proteins, namely the SAPs, prosaposin and G_{M2} activator protein ($G_{M2}AP$) (Lefrancois et al., 2003).

To exit the Golgi compartment the sorting receptors must in turn interact with cytoplasmic coat proteins such as monomeric adaptor proteins, Arf-1, clathrin, as well as a host of other proteins. Transport of the M6PR and sortilin to the lysosomes is achieved through the binding of monomeric adaptor proteins (GGAs) to an acidic cluster dileucine motif in the cytoplasmic tail of the M6PR (Nielsen et al., 2001; Puertollano et al., 2001; Zhu et al., 2001).

M6PR

There exist two distinct forms of the M6PR, the 46 kDa cation-dependent (CD) M6PR and the 300 kDa cation-independent (CI) M6PR. Original sequence analysis of the bovine CD-M6PR has revealed that it is comprised of a 28-residue N-terminal signal sequence, a 159-residue luminal domain, a 25-residue transmembrane region, and a 67-residue C-terminus that is highly homologous to that of humans. The CD-M6PR receptor has five potential N-linked glycosylation sites and has little homology (20 %) to the CI-M6PR other than the presence of a 13 amino acid consensus sequence in the luminal domain (Dahms et al., 1987; Hancock et al., 2002). The CI-M6PR, also known as the insulin-like growth factor II (IGF II) receptor, is a multifunctional receptor that binds not only lysosomal proteins bearing the M6P tag, but to IGF II as well. The CI-M6PR consists of a 44-residue N-terminus containing the signal peptide, a luminal domain that contains 15 repeats of

the 13 amino acid consensus sequence, a single transmembrane domain, and a 163 amino acid cytoplasmic tail (Morgan et al., 1987). Although binding of M6P and IGF II to the CI-M6PR occurs at distinct sites (consensus sequences 3 and 9 for the M6PR and consensus site 11 for IGF II), binding of either type of ligand to the M6PR is inhibitory to the other (MacDonald et al., 1988; Waheed et al., 1988). Ligands of the M6PR include most soluble lysosomal hydrolases, including cathepsins and various sulfatases, IGF-II, pro-renin, renin, granzyme B, proliferin, retinoic acid, uPAR, and plasminogen (Griffiths and Isaaz, 1993; Kang et al., 1997; Lee and Nathans, 1988; Lobel et al., 1989; MacDonald et al., 1988; Nguyen, 2006; Nykjaer et al., 1998; Oesterreicher et al., 2005).

Sorting of soluble lysosomal proteins by the M6PR is dependent upon the addition of a M6P tag to the soluble protein. Subsequent to the acquisition of a preformed oligosaccharide from a lipid intermediate in the endoplasmic reticulum, soluble hydrolases are transported to the Golgi where they obtain the M6P tag that is essential for their translocation to lysosomes (Kornfeld and Kornfeld, 1985). The M6P tag is added to the newly synthesized hydrolases in a two-step process that is initiated by the addition of N-acetylglucosamine-1-phosphate to mannose residues from UDP-GlcNAc by an N-acetylglucosamine-1-phosphotransferase (Hasilik et al., 1981; Kornfeld, 1986). The M6P tag is then exposed by the trimming of N-acetylglucosamine residues by N-acetylglucosamine-1-phosphodiester α-N-acetylglucosaminidase (Varki and Kornfeld, 1980). Exposure of the M6P tag allows for recognition of the soluble hydrolase by the M6PR and subsequent transport to the lysosomes in clathrin-coated vesicles (Kaplan et al., 1977). While both forms of

M6PR bind M6P with similar affinity (7-8 x 10^{-6} M) and are implicated in lysosomal sorting, the CI-M6PR is the dominant lysosomal targeting receptor for soluble hydrolases (Ludwig et al., 1994; Tong and Kornfeld, 1989). Interestingly, the luminal domain of the CI-M6PR was demonstrated to confer specificity in the localization of the receptor. Chimeric studies of the CI-M6PR showed by live-cell image analysis that removal of the luminal domain greatly altered the distribution of the receptor. Mutation of the luminal domain to inhibit the binding to M6P did not alter the distribution as compared to the wild type receptor, suggesting that the localization specificity conferred by the luminal domain is not attributable to the ligand binding situation (Waguri et al., 2006).

Once the clathrin-coated vesicles fuse with the endosomal compartment, the acidic environment therein causes dissociation of the hydrolase from the sorting receptor (von Figura and Hasilik, 1986). Recent studies using pH perturbing chemicals, ammonium chloride and monesin, however suggest that efficient delivery of CD-M6PR ligands does not require acidification of the endosomal compartment (Probst et al., 2006). Receptors freed from cargo may then be recycled the Golgi apparatus from the endosomal compartment (von Figura and Hasilik, 1986).

M6PR-Independent Trafficking

Although the M6PR is the primary sorting receptor implicated in lysosomal targeting, it is clear that an alternative receptor is also involved in the lysosomal sorting of some soluble proteins. Evidence for this hypothesis originally came from fibroblasts of patients with mucolipidosis type II, a lysosomal storage disorder in

which the M6PR sorting pathway is blocked due to mutation of the UDP-N-acetylglucoasmine-1-phosphotransferase thereby inhibiting formation of M6P residues. Under such conditions, soluble proteins such as the SAPs (prosaposin and $G_{M2}AP$) and cathepsin D, are transferred to the lysosomes in a M6PR-independent manner (Kornfeld, 1986; Rijnboutt et al., 1991a).

Various biochemical studies have suggested that additional soluble lysosomal proteins exhibit M6PR-independent sorting. Primary cultures of rat hepatocytes metabolically labeled with ^{32}P and ^{35}S were used to examine the subcellular localization and different pro-forms of cathepsin H. It was determined that only the pro-form of cathepsin H obtained an M6P tag on its high mannose oligosaccharide, and that regardless of this tag, pro-cathepsin H was secreted into the medium with no correlate targeting to the lysosomes. Therefore in at least rat hepatocytes, cathepsin H is targeted from the TGN in an M6PR-independent manner (Tanaka et al., 2000).

Similarly, when M6P was exogenously added to CHO cells expressing cathepsin K in an attempt to out-compete binding of endogenous ligands of the M6PR, the subcellular localization of cathepsin K was unaffected. This result again implies that an M6PR-independent pathway exists and that cathepsin K may use this alternative pathway (Claveau and Riendeau, 2001).

Different lines of evidence suggest that cathepsin L, a lysosomal cysteine protease, also traffics from the TGN in a manner that is independent of the M6PR. While cathepsin L carries an M6P tag in its proform, it is synthesized at high levels but has very low affinity for the M6PR (Gottesman, 1978). Further to this, mutagenic analysis of vacuolar sorting determinants suggested that the nature of the vacuolar

sorting signal was proteinaceous and not due to oligosaccharide chains (Johnson et al., 1987; Valls et al., 1987). These results again suggested a pathway for transport from the Golgi to the endosomes that was independent of the M6PR, this being true at least in the case of certain soluble lysosomal proteins.

Sortilin

The sortilin sorting receptor/neurotensin receptor-3 is a member of the Vps10 family of type I transmembrane receptors. In addition to sortilin, the mammalian Vps10 family includes the SorLA and SorCS1-3 receptors (Hermey et al., 1999; Jacobsen et al., 1996; Petersen et al., 1997). In Saccharomyces cerevisiae the Vps10 receptor family also includes the Vps10p receptor for which the family was named. Receptors in this family all possess the following: a short cytoplasmic tail that interacts with cytosolic adaptor proteins for targeting and a luminal domain characterized by a region homologous to the yeast Vps10p receptor (Nielsen et al., 2001). The Vps10 receptors are expressed in many tissues and target a variety of different ligands (Hermey et al., 1999; Jacobsen et al., 2001).

Sortilin was first cloned and purified with a receptor associated protein (RAP) affinity column from human brain extracts. The human sortilin protein is a 100 kDa receptor consisting of a 44 amino acid N-terminal propeptide, a long luminal domain, a single transmembrane domain, and a short cytoplasmic tail (Petersen et al., 1997). The N-terminal propeptide is followed by a furin cleavage site (RWRR) that when recognized in the Golgi apparatus leads to conversion of the sortilin precursor to a mature form. The cleaved propeptide has high affinity to the mature sortilin protein

and competes for binding with RAP and neurotensin. It has been hypothesized that the propeptide of sortilin has a role in both directing the proper folding of sortilin, as well as acting as a molecular safeguard against the formation of death-signaling complexes involving sortilin (Nielsen et al., 1999; Westergaard et al., 2004). This mechanism of activation is unique to sortilin since other receptors processed by furin-cleavage (including the insulin and LRP receptors) are cleaved in order to generate functional subunits and do not involve interaction of the propeptide with the receptor (Ullrich et al., 1986).

Sortilin is a multifunctional receptor capable of binding several different ligands including neurotensin, RAP, lipoprotein lipase (LpL), and SAPs (prosaposin and $G_{M2}AP$) via its Vps domain (Lefrancois et al., 2003; Mazella et al., 1998; Nielsen et al., 1999; Petersen et al., 1997). Sortilin's multifunctionality is reflected in its localization in the trans-Golgi network and cytoplasmic vesicles, as well as approximately 10 % at the plasma membrane (Petersen et al., 1997). Intracellularly, the lysosomal sorting function of sortilin has been demonstrated for newly synthesized SAPs and acid sphingomyelinase (Lefrancois et al., 2003; Ni and Morales, 2006). Recent studies also suggest that sortilin interacts with conotoxin-Tx VI in the ER to facilitate its ER export to the Golgi apparatus (Conticello et al., 2003).

In the case of SAPs, trafficking to the lysosomal compartment requires more than just a protein-protein interaction with sortilin. Recent studies have shown that the transport of prosaposin requires sphingomyelin for its translocation to the lysosomes (Zhao and Morales, 2000). It has also been hypothesized that a region

within the prosaposin molecule (the D domain) interacts with sphingomyelin to bring this protein into close proximity of the Golgi membrane and to facilitate the binding of prosaposin to sortilin (Lefrancois et al., 2002). Depletion of sphingomyelin with specific biochemical inhibitors results in the misrouting of prosaposin to the secretory pathway (Lefrancois et al., 1999). Sphingomyelin is one of the main components of detergent resistant membranes (DRM) domains (Simons and Ikonen, 1997). DRMs have been postulated to exist in the TGN and to function as sorting platforms (Simons and Ikonen, 1997; Simons and van Meer, 1988). Sortilin has also been shown to interact with G proteins present in lipid rafts at the plasma membrane via an interaction with the neurotensin receptor 1 (NTR1) (Gkantiragas et al., 2001; Martin et al., 2002).

At the plasma membrane, sortilin has been demonstrated to mediate the endocytosis of LpL, neurotensin, and the nerve growth factor precursor (pro-NGF) (Mazella et al., 1998; Nielsen et al., 1999; Nykjaer et al., 2004). The endocytosis and modulation of neurotensin signaling by sortilin requires an interaction with the G-protein coupled neurotensin receptor-1. The role of sortilin in the endocytosis of neurotensin and its homology to the NTR3 led to the observation that sortilin and the non-G-coupled neurotensin receptor-3 are the same protein (Mazella et al., 1998). Analysis comparing the molecular weight of sortilin/NTR3 obtained from both the plasma membrane and the TGN of human carcinoma HT29 cells show differing sizes. The sortilin/NTR3 isolated from the plasma membrane exhibited a higher molecular weight than that from the TGN. This led to the hypothesis that while sortilin and the NTR3 are the same protein, their different functions may be accounted for through

differential glycosylation (Morinville et al., 2004). Additionally, the interaction of sortilin with $p75^{NTR}$ at the plasma membrane is essential for induction of death signals via pro-NGF (Nykjaer et al., 2004).

The cytoplasmic tail of sortilin is important in mediating the localization of the receptor and has been demonstrated to be functionally important and highly homologous to that of the CI-M6PR. The cytoplasmic domain of sortilin contains a YXXϕ (Tyr- any two amino acids- bulky hydrophobic amino acid) and a DXXLL (dileucine) sorting motif that are responsible for mediating both the rapid endocytosis and Golgi to endosomal sorting of sortilin. Chimeras comprised of the luminal and the transmembrane domains of the M6PR and the cytoplasmic domain of sortilin rescued the trafficking of M6PR-dependent proteins to the endosomal compartment in M6PR deficient cells (Nielsen et al., 2001). Additionally, the GGA adaptor protein that binds to the cytoplasmic tail of the M6PR was also demonstrated to interact with sortilin and mediate its targeting to the endosomes (Nielsen et al., 2001; Puertollano et al., 2001; Takatsu et al., 2001).

Peripherally Associated Proteins

The trafficking of other lysosomal proteins is more complex. Within the lysosomal compartment sialidase 1 and cathepsin A (protective protein/carboxypeptidase A) form a high molecular weight complex that is required for the functional activity of sialidase 1 (Pshezhetsky and Ashmarina, 2001). The role of cathepsin A in the complex is to maintain sialidase in a catalytically active conformation while protecting it from proteolytic degradation (D'Azzo et al., 1982;

Vinogradova et al., 1998). Also associated with this complex are β-galactosidase and N-acetyl-galactosamine-6-sulphate sulphatase (Pshezhetsky and Ashmarina, 2001).

Transport of sialidase 1 to the endo-lysosomal compartment occurs as an integral membrane protein and requires a tyrosine-based signal for delivery (Lukong et al., 2001). Upon translocation to the endo-lysosomal compartment it is hypothesized that the enzyme is cleaved to generate a soluble, as well as a membrane bound pool of sialidase 1 (Seyrantepe et al., 2003). Subsequently, sialidase 1 may be transferred to the plasma membrane as a complex with cathepsin A (Liang et al., 2006). Evidence for lysosome-to-plasma membrane transport has been previously observed for MHC II complexed to various peptides in antigen-presenting cells (Turley et al., 2000). Once at the cell surface, sialidase 1 is believed to play a role in antigen presentation, cell-cell interactions, and elastogenesis via interaction with β-galactosidase at the plasma membrane (Hinek et al., 2006; Liang et al., 2006). These findings emphasize that the lysosome is a dynamic organelle that is implicated in more than terminal degradation.

Unlike sialidase 1, cathepsin A is a soluble protease that is sorted to the endosomal compartment via the M6PR pathway (Lukong et al., 1999). Reports suggest that the transport of β-galactosidase, and possibly sialidase 1, to lysosomes requires an interaction with cathepsin A in the biosynthetic pathway (van der Spoel et al., 1998).

Disruption of the various elements of the multi-enzyme complex result in different lysosomal storage disorders (LSDs). Mutations affecting cathepsin A cause galactosialidosis. Galactosialidosis is characterized by the combined deficiency of

cathepsin A, sialidase 1, and β-galactosidase, highlighting the role of cathepsin A in transporting and stabilizing the protein complex (d'Azzo, 2001). Mutations affecting the NEU 1 gene result in deficiency of only neuraminidase 1 and trigger sialidosis (Seyrantepe et al., 2003).

Adaptor Proteins Involved in Lysosomal Trafficking

The delivery of proteins to various cellular locations depends upon a group of proteins termed adaptor proteins. The adaptor proteins are responsible for providing a link between the cargo and the cytoplasmic components implicated in cellular targeting such as clathrin, Arf1, γ-synergin, epsinR, and others (Traub, 2005). Based upon their structure, two categories of adaptor proteins have been identified to traffic between the Golgi apparatus and the endosomal compartments, namely the multimeric adaptor proteins and the monomeric adaptor proteins also termed Golgi-localized, γ-ear containing, Arf binding protein (GGA) (Dell'Angelica et al., 2000b; Hirst et al., 2001). The multimeric adaptor protein family includes AP-1, AP-2, AP-3, and AP-4 (Robinson, 2004).

Multimeric Adaptor Proteins

This family of multimeric adaptor proteins consists of four different adaptor proteins (AP 1-4), each of which is composed of four subunits: two large subunits (γ, α, δ, or ε, and β), a medium subunit (μ), and a small subunit (σ). The four domains are said to be organized into globular structures with a core composed of the medium and small subunits, as well as the N-terminal domains of the two large subunits.

Respectively, the "ears" consist of the C-terminal domains of the two large subunits, connected by flexible hinge domains (Robinson and Bonifacino, 2001). Immunofluorescence microscopy has localized AP-1 and AP-3 to the TGN and TGN-derived vesicles, while AP-2 is found at the plasma membrane, and AP-4 is implicated in TGN trafficking to the basolateral membrane (Ahle et al., 1988; Robinson, 1987; Simmen et al., 2002). AP-3 has been shown to be essential in the transport of lysosomal integral membrane proteins (such as the LAMPs) to the lysosomes (Dell'Angelica et al., 1999). The AP-1A adaptor protein has been found to play a role in the sorting events at the TGN that involve the M6PR, whereas the AP-1B isoform is implicated in sorting integral membrane proteins from the TGN or endosomes to the basolateral domains (Meyer et al., 2000). An interaction between AP-1 and full-length sortilin has not yet been definitively demonstrated. However, while the cytoplasmic acid cluster dileucine signal of the M6PR is required to mediate lysosomal trafficking, AP-1 does not interact with the M6PR at these sites (Honing et al., 1997; Johnson and Kornfeld, 1992). What is clear, however, is that the μ subunit of AP-1 binds to a YXXϕ motif in the cytosolic tail of the M6PR (Ohno et al., 1995; Owen and Evans, 1998). Despite this, examination of fibroblasts deficient in the μ subunit of AP-1 revealed that both the CI- and CD-M6PRs were capable of reaching the lysosomes (Meyer et al., 2001). Together this evidence helped pave the way for the discovery of a second group of adaptor proteins implicated in sorting the M6PR, the GGAs (Dell'Angelica et al., 2000b).

Monomeric Adaptor Proteins

The GGAs are a family of three similar proteins (GGAs1, 2 and 3) that were identified by searching databases for AP subunit homologues (Boman et al., 2000; Dell'Angelica et al., 2000b; Hirst et al., 2000). GGA1 and GGA2 were identified in yeast, whereas all three forms were found to be present and conserved throughout eukaryotes (Boman, 2001). The GGAs are 60-80 kDa monomeric adaptor proteins composed of four domains: N-terminal VHS domain, GAT domain, hinge domain, and EAR domain (Ghosh and Kornfeld, 2004). The VHS domain was also identified in Vps27, Hrs, and STAM (hence the term VHS) and shown to be the domain implicated in interacting with the cytoplasmic tail of sorting receptors (Misra et al., 2000; Nielsen et al., 2001; Puertollano et al., 2001). The VHS domain recognizes a DXXLL motif in the cytosolic tails of both sortilin and the M6PR (Nielsen et al., 2001; Puertollano et al., 2001). The GAT domain is the most highly conserved domain amongst the three GGAs (with 65 % identity) and is responsible for mediating the interaction with Arf1 and Arf3. The interaction of GGAs and GTP bound Arfs is essential for the recruitment of GGAs to the Golgi membrane (Collins et al., 2003; Dell'Angelica et al., 2000b). The hinge domain of the GGAs interacts with clathrin, whereas the EAR domain, which is highly homologous to the γ-adaptin subunit of AP-1, interacts with coat proteins such as clathrin, γ-synergin, p56, and rabaptin-5 (Bonifacino, 2004; Dell'Angelica et al., 2000b).

While the GGAs have been demonstrated to be essential for delivery of soluble proteins to the lysosomes via the M6PR and sortilin receptors, there has been controversy over the exact role played by the GGAs (Doray et al., 2002a; Lefrancois

et al., 2003). The most supported hypothesis to date is that GGAs and AP-1 function together to recruit cargo into the same transport vesicles and that the GGAs "hand-off" cargo to AP-1 for transport. Evidence for this model is supported by several lines of evidence, mainly that AP-1, but not GGAs, are enriched in purified clathrin-coated vesicles, and that the association of AP-1 with the membrane is stable while that of the GGAs is transient (Hirst et al., 2001; Hirst et al., 2000). Additionally, Kornfeld and colleagues demonstrated that the hinge region of the GGAs does in fact interact with the EAR domain of AP-1, γ-adaptin at the TGN region (Doray et al., 2002b). However, what is clear is that both GGAs and AP-1 are important for the efficient delivery of sorting receptors and their cargo to the lysosomes.

Recycling Complexes

Crucial to maintaining the lysosomal transport of hydrolases is the efficient retrieval of the sorting/trafficking receptors from endosomes to the TGN. Failure to recycle will lead to disruption of the lysosomes (Seaman et al., 1997; Seaman et al., 1998). Recent evidence has shown that lysosomal sorting receptors are indeed recycled from the endosomes to the Golgi apparatus and that this process is mediated by a protein complex called "retromer" (Seaman et al., 1997; Seaman et al., 1998). The retromer complex was first identified in *Saccharomyces cerevisiae* and was demonstrated to play a role in the recycling of Vps10p, the yeast homologue of the M6PR (Seaman et al., 1997; Seaman et al., 1998). The mammalian retromer complex consists of Vps26, Vps29, Vps35, and sorting nexins 1 and 2 (SNX1 and SNX2), whereas the originally identified yeast homologue consists of Vps35p, Vps29p,

Vps26p, Vps17p, and Vps5p (Haft et al., 2000; Seaman et al., 1997; Seaman et al., 1998). The mammalian Vps35 domain, and possibly the Vps26 as well, have been demonstrated to interact with cargo proteins such as the M6PR, while SNX1 is capable of reshaping the endosomal membrane, and Vps26 is a phosphoesterase that dephosphorylates the serine preceding the DXXLL motif in the M6PR tail (Arighi et al., 2004; Collins et al., 2005; Damen et al., 2006; Seaman, 2007).

While it has been well established that this complex is responsible for the recycling of the M6PR, the recycling pathway of sortilin is less clear. However, preliminary evidence suggests that the retromer complex may also play a role in sortilin recycling (Arighi et al., 2004; Seaman, 2004). Recently, a conserved WLM sequence in the cytosolic tail of the M6PR was confirmed as being important for the interaction of the receptor with retromer. Mutation of the WLM motif resulted in the failure of the M6PR to be recycled and in its rapid degradation (Seaman, 2007).

Retromer is not the only factor important in mediating recycling of sorting receptors from the endosomal compartment to the TGN. Golgi-localized SNAREs include: syntaxin 5, 6, 10, 11 and 16 (Bennett et al., 1993; Bock et al., 1996; Tang et al., 1998a; Tang et al., 1998b; Valdez et al., 1999). Inhibition of the SNARE proteins syntaxin 5 and 16 by RNA interference abrogated recycling of the M6PR from endosomes and resulted in increased degradation of the receptor. It was therefore postulated that syntaxin 5 and 16 are important mediators of M6PR recycling. Transport protein phosphofurin acidic cluster sorting protein (PACS-1), tail-interacting protein 47 (TIP-47), and the intracellular adaptor epsinR have also been

demonstrated to help regulate recycling from the endosomal compartment (Diaz and Pfeffer, 1998; Saint-Pol et al., 2004; Scott et al., 2006).

Lysosomal Storage Disorders

Lysosomal storage disorder (LSDs) is the term given to a group of more than 50 inherited diseases that are caused by the malfunction of lysosomal enzymes, activators, or adaptors involved in enzyme targeting and lysosomal biogenesis (Meikle et al., 1999; Parkinson-Lawrence et al., 2006). The combined frequency of all LSDs has been estimated to be approximately 1:7700 live births, however this number is growing as there is more biochemical and genetic characterization of disorders (Meikle et al., 1999).

The first reported case of a LSD was in the early 1880s by physicians Warren Tay and Bernard Sachs, at a time when the lysosome had not yet been identified (Fernandes Filho and Shapiro, 2004). Noting the cherry red foveala centralis of the eye, cessation of mental development, flaccid or spastic paralysis in one to two year old children, the physicians identified the main characteristics of the LSD presently known as infantile Tay-Sachs disease or the B-variant of G_{M2} gangliosidosis (Kolter and Sandhoff, 1998; Sachs, 1896; Tay, 1884). Only in the 1960s was the cause of infantile Tay-Sachs identified as an autosomal recessive mutation in the α-subunit of β-hexosaminidase A, an enzyme involved in the lysosomal degradation of the G_{M2} ganglioside (Okada and O'Brien, 1969; Sandhoff, 1969; Sandhoff, 2001). Since this time additional characterization has led to identification of the various polypeptides involved in the degradation of the G_{M2} ganglioside to G_{M3} and which result in a

family of LSD known as G_{M2} gangliosidosis. The α subunit of β-hexosaminidase A (αβ) and β-hexosaminidase S (αα) are encoded by the HEXA gene, while the β subunit in β-hexosaminidase A and β-hexosaminidase B (ββ) is encoded by the HEXB gene (Kolter and Sandhoff, 1998). Mutation of the HEXA gene leads to deficient activity of β-hexosaminidase A and S but normal levels of β-hexosaminidase B. Mutation of the HEXB gene results in Sandhoff disease or the 0-variant form of G_{M2} gangliosidosis which is characterized by deficient enzyme activity of β-hexosaminidases A and B (Gravel RA, 1995; Kolter and Sandhoff, 1998). The final member of the family of G_{M2} gangliosidosis is the AB-variant form which does not affect the β-hexosaminidase enzymes but rather the activator of β-hexosaminidase A, the $G_{M2}AP$ (Conzelmann and Sandhoff, 1978). Point mutations in the $G_{M2}A$ gene result in early degradation of the gene product and accumulation of G_{M2} within lysosomes since the β-hexosaminidase A enzyme requires the $G_{M2}AP$ to form a water-soluble complex with the ganglioside in order to access the ganglioside (Furst and Sandhoff, 1992; Meier et al., 1991; Xie et al., 1998).

LSDs have also been associated with the other activator proteins derived from the prosaposin precursor. Deficiency of saposin B results in a variant form of metachromatic leukodystrophy that is characterized by the absence of saposin B and normal activity of arylsulfatase A (Gieselmann, 2003; Stevens et al., 1981). Similar to many LSDs, metachromatic leukodystrophy results in progressive neurological deterioration (marked by sulfatide, globotriaosylceramide, and G_{M3} ganglioside accumulation and demyelination) and mental retardation (Gieselmann et al., 2003;

Holtschmidt et al., 1991; Nalini and Christopher, 2004). As with deficiency of saposin B, deficiency of saposin C results in a variant form of a LSD, namely Gaucher's disease (Christomanou et al., 1986). Over 200 mutations have been identified in the glucosylceramide β-glucosidase enzyme responsible for the hydrolysis of glucocerebroside, leading to glucocerebroside accumulation in Gaucher's disease (Beutler, 1991). However, in the variant of Gaucher's disease in which saposin C is affected, there is normal glucosylceramide β-glucosidase activity but accumulation of glucocerebroside (Christomanou et al., 1986; O'Brien and Kishimoto, 1991). Although mutations of saposins A and D have not been implicated in any known LSD, a mouse model suggests that deficiency of saposin A can cause a LSD similar to globoid cell leukodystrophy (Krabbe's disease) (Matsuda et al., 2001). Clinical, phenotypical, and pathological studies of the saposin A knock-out mouse have revealed that the absence of saposin A results in symptoms similar to, but more mild than traditional globoid cell leukodystrophy caused by mutation in galactosylceramidase (Matsuda et al., 2001; Suzuki and Suzuki, 1970). Numerous differences exist between the two types of leukodystrophies, metachromatic and globoid cell leukodystrophy. While in metachromatic leukodystrophy there is pronounced substrate (sulfatide) accumulation in the brain, there is no over accumulation of galactosylceramide in the brain of patients with globoid cell leukodystrophy (Jatzkewitz, 1958; Suzuki, 2003). This difference has been attributed to the early and rapid loss of myelin, the exclusive site of galactosylceramide, in globoid cell leukodystrophy (Miyatake and Suzuki, 1972; Suzuki, 2003). Mouse models of a saposin D knock-out suggest that saposin D deficiency leads to a unique

condition characterized by urine and neural ceramide lipidosis (Matsuda et al., 2004). Other mutations, although rare, affecting the initiation codon of the prosaposin gene result in total prosaposin deficiency. Biochemical analysis of tissue from these patients revealed accumulation of different sphingolipids including glucosylceramide, galactosylceramide, and ceramide. Clinically, total prosaposin deficiency resulted in hyperkinesia, respiratory insufficiency, and hepatosplenomegaly (Bradova et al., 1993; Elleder et al., 2005; Harzer et al., 1989; Hulkova et al., 2001; Paton et al., 1992; Schmid et al., 1992).

LSDs can affect any component involved in lysosomal function or trafficking, not just the activator proteins described above. Mucolipidoses is a group of LSDs that affect hydrolases and proteins essential for lysosomal trafficking. Mucolipidosis type I or sialidosis is caused by mutations in the sialidase gene and can be subdivided into two categories (sialidosis type I and type II). The onset of the first type of sialidosis occurs much later in life than in the more severe sialidosis type 2 which is classified as being of infantile onset. Sialidosis type II is characterized by dysostosis multiplex, short stature, developmental delay, mental retardation, and hepatosplenomegaly; the type I variant is marked by abnormal gait, progressive decline in vision, macular cherry-red spots, and myoclonus syndrome. Deficiency in sialidase causes blockage in the catabolic pathway for degradation of sialylated glycoconjugates leading to accumulation of sialylated oligosaccharides and glycoproteins (Seyrantepe et al., 2003).

The second type of mucolipidosis, also called I-cell disease (ICD), results from mutation of a single gene but causes the mis-sorting of several lysosomal

hydrolases and subsequent accumulation of many lipids and carbohydrates within lysosomes. I-cell disease is an autosomal recessive mutation caused by the absence of UDP-N-acetylglucosamine N-acetylglucosaminyl-1-phosphotransferase. I-cell disease was first identified in 1967 as a LSD and was classified as a mucolipidosis in 1970 since I-cell disease causes symptoms similar to mucopolysaccharidoses and sphingolipidoses (LeRoy, 1967; Spranger and Wiedemann, 1970). ICD is characterized by phase-dense intracytoplasmic inclusions in fibroblasts (inclusion cells) and the presence of a large number of soluble lysosomal hydrolases in extracellular fluids such as serum and urine, and media of cultured fibroblasts (LeRoy, 1967; Leroy and Spranger, 1970). Intriguingly, findings suggest that ICD fibroblasts can internalize and utilize lysosomal enzymes produced by normal cells, whereas normal cells cannot internalize enzymes produced by ICD fibroblasts (Ullrich and von Figura, 1979). This observation led to the biochemical analysis of the differences between enzymes produced by normal cells and those from ICD cells and the discovery of the M6P tag as a lysosomal sorting signal (Vladutiu and Rattazzi, 1979). The absence of functional phosphotransferase in the Golgi of ICD cells results in soluble hydrolases that lack a M6P-tag required for recognition and sorting by the M6PR. Under these conditions, most soluble hydrolases are mis-sorted to the extracellular milieu (Nolan, 1989). However, B-lymphocytes from patients with ICD have near normal lysosomal levels of several soluble lysosomal proteins (Tsuji et al., 1988). A B-lymphoblast cell line derived from patients with ICD was in fact found to appropriately target approximately 45 % of the normal levels of cathepsin D to the lysosomes (Glickman and Kornfeld, 1993). Lysosomal targeting

of SAPs, prosaposin and $G_{M2}AP$ is also unaffected in ICD fibroblasts. These findings resulted in the formulation of the hypothesis that an alternative lysosomal sorting pathway exists that is independent of the M6PR (Rijnboutt et al., 1991a).

UDP-N-acetylglucosamine N-acetylglucosaminyl-1-phosphotransferase is also affected in mucolipidosis type III. Whereas in mucoliopidosis type II/ICD cells have low or completely abrogated phosphotransferase activity, in mucolipidosis type III cells possess the phosphotransferase at higher but still below normal levels. The higher levels of phosphotransferase are suggested to be responsible for the later onset and milder course of mucolipidosis type III compared to that of mucolipidosis type II (Reitman et al., 1981). Clinically, mucolipidosis type III is characterized by short stature, skeletal dysplasia, and mild mental retardation (Kelly et al., 1975).

Mucolipidosis type IV is a rare autosomal recessive disorder with approximately only 100 cases documented worldwide (Gordon and Marchese, 2004). Although the exact cellular cause of mucolipidosis type IV is unknown, it has been speculated to be the result of a deficiency in the transport channel receptor protein, mucolipin-1 (LaPlante et al., 2002). Mucolipidosis type IV is a progressive neurodegenerative disorder clinically characterized by delayed motor development, mental retardation, and corneal opacities (Bach, 2001). At a cellular level, there is an accumulation of phospholipids and gangliosides that is believed to be caused by a defect in the endocytic process (LaPlante et al., 2002).

Several LSDs, such as the Chediak-Highashi syndromes, are associated with defects in lysosomal biogenesis. Chediak-Highashi syndrome is characterized by partial albinism, immune disorders, prolonged bleeding, and progressive neurological

deterioration (Barak and Nir, 1987). At a cellular level, the lysosomes of patients with Chediak-Highashi syndrome appear enlarged but have a full functioning complement of lysosomal proteins. Lysosomal defects appear only in cells possessing secretory lysosomes (ie. azurophilic granules, lytic granules, MHC class II compartments, and melanosomes). The Lyst protein has been demonstrated to be defective in this disorder however its exact role is as of yet unclear. When Lyst is over-expressed in fibroblasts, the result is smaller than normal lysosomes, suggesting a role for Lyst in lysosomal fission (Clark and Griffiths, 2003; Ward et al., 2003).

It is therefore clear from the extensive number of LSDs and their associated phenotypes and pathologies (see Table 1) that lysosomal biogenesis, targeting, and function are important for the maintenance of cellular function and general physical health.

Table 1. Lysosomal Storage Disorders (LSDs). List of various LSDs and the associated faulty proteins. The disorders are categorized according to the type of protein affected: Activators, Soluble Enzymes, Integral Membrane Proteins, Lysosomal Biogenesis, and Lysosomal Trafficking.

Disorder	Deficiency	References
Lysosomal Proteins		
Activators:		
AB-variant of G_{M2} gangliosidosis	$G_{M2}AP$	(Kolter and Sandhoff, 1998)
Variant of metachromatic leukodystrophy	Saposin B	(Stevens et al., 1981)
Variant of Gaucher's	Saposin C	(Christomanou et al., 1986)
Soluble Enzymes:		
B-variant of G_{M2} gangliosidosis / Tay Sachs	β-hexosaminidases A and S	(Kolter and Sandhoff, 1998)
0-varient of G_{M2} gangliosidosis / Sandhoff	β-hexosaminidases A and B	(Kolter and Sandhoff, 1998)
Metachromatic leukodystrophy	Arylsulphatase A	(Gieselmann, 2003)
Gaucher's	Glucosylceramide β-glucosidase	(Beutler, 1991)
Globoid cell leukodystrophy (Krabbe's)	Galactosylceramidase	(Matsuda et al., 2001)
Fabry	α-galactosisidase A	(Levin, 2006)
Glycogen storage disease/ Pompe	acid α-glucosidase	(Raben et al., 2002)
Mucopolysaccharidosis type I/ Hurler	α-L-iduronidase	(Wraith et al., 2005)
Mucopolysaccharidosis type II/ Hunter	Iduronate-2-sulfatase	(Hopwood et al., 1993)
Mucopolysaccharidosis type IIIA/ Sanfilippo	Heparan-N-sulfatase	(Gabrielli et al., 2005)
Mucopolysaccharidosis type IIIB/ Sanfilippo	α-N-acetylglucsaminidase	(Beesley et al., 2005)
Mucopolysaccharidosis type IIID/ Sanfilippo	N-acetylglucosamine-6-sulphatase	(Beesley et al., 2003)
Mucopolysaccharidosis type IVA/ Morquio	N-acetylgalactosamine-6-sulphatase	(Oncag et al., 2006)
Mucopolysaccharidosis type IVB/ Morquio	β-galactosidase	(Bagshaw et al., 2002)
Mucopolysaccharidosis type VI/ Maroteaux-Lamy	N-acetylgalactosamine 4-sulphatase	(Walkley et al., 2005)
Mucopolysaccharidosis type VII/ Sly	β-glucuronidase	(Vogler et al., 2005)
Galactosialidosis	Cathepsin A/ protective protein	(Oheda et al., 2006)
Aspartylglucosaminuria	Aspartylglucosaminidase	(Virta et al., 2006)
Wolman	Acid lipase	(Surve et al., 2005)

Fucosidosis	α-L-fucosidase	(Michalski and Klein, 1999)
GM1 gangliosidosis	β-galactosidase	(Pavlu et al., 2006)
α-Mannosidosis	α-mannosidase	(Pittis et al., 2006)
β-Mannosidosis	β-mannosidase	(Gort et al., 2006)
Neuronal ceroid lipofuscinoses (CNCL)	Cathepsin D	(Ramirez-Montealegre et al., 2006)
Neuronal ceroid lipofuscinoses (CLN1)/ Batten	Palmitoyl protein thioesterase I	(Ramirez-Montealegre et al., 2006)
Neuronal ceroid lipofuscinoses (CLN2)/ Batten	Tripeptidyl peptidase protein I	(Ramirez-Montealegre et al., 2006)
Pycnodysostosis	Cathepsin K	(Helfrich, 2003)
Niemann-Pick types A and B	Acid sphingomyelinase	(Dhami et al., 2006)
Integral Membrane Proteins:		
Mucolipidosis type I (sialidosis)	Sialidase (neuraminidase I)	(Seyrantepe et al., 2003)
Mucopolysaccharidosis type IIIC/ Sanfilippo	Acetyl CoA/N-acetyltransferase	(Ausseil et al., 2006)
Cystinosis	Cystinosin	(Town et al., 1998)
Salla	Sialin	(Verheijen et al., 1999)
Lysosomal Biogenesis		
Chediak-Higashi syndrome	Lyst/ beige	(Clark and Griffiths, 2003)
Lysosomal Trafficking		
Mucolipidosis type II (ICD)	GlcNAc-phosphotransferase	(Reitman et al., 1981)
Mucolipidosis type III	GlcNAc-phosphotransferase	(Reitman et al., 1981)
Mucolipidosis type IV	Mucolipin-1?	(Gordon and Marchese, 2004
Hermansky-Pudlak syndrome type 2	AP-3 β3 subunit	(Bonifacino, 2004b)
Variants of Hermansky-Pudlak syndrome	AP-3 δ (mocha), μ3, σ3 subunits	(Bonifacino, 2004b)

Chapter 3: Materials and Methods

Cell Lines and Cell Culture

To verify and validate our results, experiments were conducted in different cell lines; COS-7, an African Green Monkey kidney fibroblast cell line, TM4, a mouse Sertoli cell line, wild type human foreskin fibroblasts, and fibroblasts obtained from the skin of ICD patients.

COS-7 cells (CRL-1651) were purchased from ATCC (Manassas, VA, USA) and cultured in Dulbecco's modified Eagle's medium (DMEM) (Invitrogen, Burlington, ON, CAN) supplemented with 10 % fetal bovine serum (FBS), 5 % penicillin and streptomycin, and L-glutamine. Cells were maintained at 5 % CO_2 at 37°C.

TM4 cells (CRL-1715) were purchased from ATCC (Manassas, VA, USA) and cultured in DMEM/F12 medium supplemented with 5 % horse serum, 2.5 % FBS, and 5 % antibiotics. Cells were maintained at 5 % CO_2 at 37°C. TM4 Sertoli cells are professional phagocytes and contain large numbers of lysosomes (Hassan et al., 2004).

Wild type human foreskin fibroblasts (CRL-2522) were purchased from ATCC (Manassas, VA, USA) and cultured in Eagle's Minimal Essential medium with Earle's BB and 2 mM L-glutamine (ATCC, Manassas, VA, USA) supplemented with 10 % FBS. Cells were maintained at 5 % CO_2 at 37°C.

Fibroblasts from patients with ICD (FFF0251996) were provided by Dr. M. Filocamo (Diagnosi Pre-Postnatale Malattie Metaboliche-Istitueo G. Gaslini, Italy). The cells were cultured in DMEM supplemented with 20 % fetal bovine serum and maintained in an atmosphere of 5 % CO_2 at 37 °C.

Transfection

DNA

The day prior to transfection, 1.6 X 10^6 cells were seeded in 100 mm plates or 1.0 X 10^5 cells in each of the 24-well plate. The cells were incubated overnight with complete medium to achieve 70-80 % confluency on the day of transfection. Before transfection, the cells were washed with fresh complete medium and a final volume of 7 ml complete medium was added to each 100 mm plate or 0.15 ml of complete medium per well of a 24-well plate. Subsequently in the case of the 100 mm plates, a well-mixed solution of 4.0 µg of DNA, 300 µl of serum/antibiotics-free medium, and 25 µl of Polyfect Transfection Reagent (Qiagen, Mississauga, ON, CAN) was incubated at room temperature for 10 minutes. For the wells of the 24-well plates, 1 µg of DNA, 25 µl of serum/antibiotics-free medium and 4 µl of Polyfect Transfection Reagent were incubated together at room temperature for 10 minutes. After the 10 minute incubation, 1 ml of complete medium was added to the DNA-Polyfect solution, mixed, and added in a drop-wise manner to the 100 mm plates. For cells cultured in the wells of a 24-well plate, 0.2 ml of medium was added to the DNA-Polyfect mixture prior to its transfer onto the cells. The transfected cells were incubated in an atmosphere of 5% CO_2 at 37 °C for 24 hours to allow gene expression.

siRNA

On the day of transfection 1 X 10^5 cells were plated on treated cover slips in a 24-well plate or 4 X 10^6 cells were plated into 100 mm plates. For the short time prior to transfection, cells were incubated under normal growth conditions at 37 °C in 5 %

CO_2. In the meantime siRNA was mixed with serum/antibiotics-free medium and Hiperfect (Qiagen, Mississauga, ON, CAN). For cells cultured in the 24-well plate, 40 ng of short-interfering RNA (siRNA) was incubated for 10 minutes with 100 µl of serum/antibiotics-free medium and 5 µl of Hiperfect. In the case of the 100 mm plates 500 ng of siRNA was incubated for 10 minutes with 150 µl of serum/antibiotics-free medium and 35 µl of Hiperfect. Subsequent to incubation at room temperature, the siRNA-Hiperfect solution was added to the cells in a drop-wise manner. The cells were then cultured under normal growth conditions for 48 – 72 hours to allow for gene silencing.

Plasmids and Constructs

The wild-type sortilin-myc construct was a generous gift from Dr. Claus Petersen (University of Aarhus, DEN). Truncated sortilin-myc is a dominant-negative construct of sortilin that possesses the luminal and transmembrane domains of sortilin, but lacks the cytosolic tail (Figure A). This construct has been previously generated and characterized in our lab (Lefrancois et al., 2003). Mutations Y14A and L17A in the cytosolic tail of sortilin-myc were generated using the QuikChange II XL Mutagenesis kit from Stratagene (La Jolla, CA, USA) according to the manufacturer's protocol. Briefly, PAGE purified mutagenic primers (Table 2) were used in a PCR reaction to introduce point mutations into specific sites of the wild-type construct. The PCR products were digested with Dpn I restriction enzyme to eliminate all parental dsDNA. Subsequently, the Dpn I treated DNA was transformed in XL10-Gold supercompetent cells. Transformation reactions were plated on an ampicillin-

containing agar plates. Several colonies were selected, amplified and purified using High Speed Midi-prep Kit (Qiagen, Mississauga, ON, CAN). Positive clones were verified by sequencing at Bio S&T (Lachine, QC, CAN.

Three chimeric prosaposin-albumin constructs were used (Figure B). The first chimera consisted of albumin, and the D-domain and C-terminus of prosaposin. The remaining constructs consisted of albumin and either the D-domain or the C-terminus of prosaposin. These constructs were generated in the mammalian expression vector pcDNA3.1B, which contains a myc epitope tag before the stop codon. All of the chimeric constructs were previously produced and characterized in our laboratory (Zhao and Morales, 2000). The mutations affecting the D-domain of prosaposin were previously introduced in our lab into the albumin-D-domain-C-terminus chimeric construct using the QuikChange II XL Mutagenesis kit from Stratagene (La Jolla, CA, USA) as described above. The mutations produced were: E463K and E491K.

Antibodies

Primary Antibodies

Endogenous sortilin was detected using a mouse monoclonal antibody purchased from BD Transduction Laboratories (San Jose, CA, USA). Sortilin-myc constructs were detected using a mouse monoclonal anti-myc antibody (9E10) obtained from Santa Cruz Biotechnology, as was the mouse anti-GFP antibody (Santa Cruz, CA, USA). The M6PR was detected using a rabbit polyclonal antibody from Dr M. Sosa (Instituto de Histología y Embriología (IHEM)-CONICET, Universidad Nacional de Cuyo, Mendoza, ARG) and has been previously demonstrated to

recognize the CI-M6PR (Romano et al., 2006). Polyclonal goat antibodies specific for cathepsins D, H, K, and L, as well as anti-flotillin-1 antibody were purchased from Santa Cruz Biotechnology (Santa Cruz, CA, USA). Cathepsin B antibody was a rabbit polyclonal antibody also obtained from Santa Cruz Biotechnology (Santa Cruz, CA, USA). The rabbit polyclonal antibody to prosaposin was produced and characterized in our lab (Zhao and Morales, 2000). Goat anti-$G_{M2}AP$ antibody was a generous gift from Dr. Sandhoff (Kekulé-Institut, Bonn, GER). Rabbit polyclonal anti-LAMP-1 antibody was a generous gift from Dr. J. Mort (Shriner's Hospital, Montreal, QC, CAN). LAMP-1 and Golgin-97 mouse monoclonal antibodies were purchased from Santa Cruz Biotechnology (Santa Cruz, CA, USA). The rabbit polyclonal anti-Vps26 antibody was a kind gift from Dr. J.S. Bonifacino (NIH, Bethesda, MD, USA). The Vps26 antibody was previously described by Haft et al. (Haft et al., 2000). A mouse monoclonal anti-γ-adaptin antibody and rabbit anti-β-actin antibodies were purchased from Sigma-Aldrich (Oakville, ON, CAN).

Secondary Antibodies

Goat anti-rabbit IgG and goat anti-mouse IgG antibodies conjugated to Alexa 488 or Alexa 594 were purchased from Molecular Probes (Burlington, ON, CAN). Donkey anti-goat IgG antibodies conjugated to Alexa 488 or Alexa 594 were also obtained from Molecular Probes (Burlington, ON, CAN).

Detection of primary antibodies by Western blotting was done using goat anti-rabbit IgG and goat anti-mouse IgG antibodies conjugated to horseradish peroxidase (HRP) purchased from Santa Cruz Biotechnology (Santa Cruz, CA, USA). For goat

primary antibodies, a donkey anti-goat IgG conjugated to HRP was used and also acquired from Santa Cruz Biotechnology (Santa Cruz, CA, USA).

RNAi Probes

shRNA

Short hairpin RNA (shRNA) consists of a single-stranded RNA containing two regions of complementary sequences that refold into a double-stranded loop region and a connecting loop stem with a 3' terminal uridine tract. Based on previous results from our laboratory using chemically synthesized siRNA, a sequence with unknown homologies other than to sortilin (AAGGTGGTGTTAACAGCAGAG) was selected for designing the short hairpin RNA (shRNA) targeting sortilin (Lefrancois et al., 2003). This sequence was subcloned into the plasmid-based expression vector pSilencer 3.1 H1-neo that contains a strong H1 RNA pol III promoter (Ambion, Austin, TX, USA). Polyfect transfection reagent (Qiagen, Mississauga, ON, CAN) was utilized as described above to transfect the plasmid into COS-7 cells. Cells constitutively expressing the shRNA were resistant to neomycin, and selected for using Geneticin (GIBCO, Burlington, ON, CAN). The purpose of this strategy was to initiate the production of shRNA in order to trigger cleavage of endogenous sortilin mRNA by the enzyme Dicer and thereby silence sortilin mRNA. As a negative control, a pSilencer 3.1 H1-neo vector containing a sequence with no known homology was purchased from Ambion (Austin, TX, USA).

siRNA

The sequence selected to silence Vps26 expression (retromer) (5'-CTCTATTAAGATGGAAGTG'3') has been previously tested and characterized (Arighi et al., 2004). The 5'-GGCAUCAAGUAUCGGAAGA-3' sequence for μ1A (AP-1) has also been previously examined (Janvier and Bonifacino, 2005). Both of these RNAi sequences were produced with a 3'-Alexa Fluor 488 tag by Qiagen (Mississauga, ON, CAN). A negative control siRNA with no known homologies was also purchased from Qiagen with a 3'-Alexa Fluor 488 tag. These constructs were transfected into cells using the Hiperfect reagent from Qiagen (Mississauga, ON, CAN) as described above.

Analysis of Knockdown Efficiency

Efficiency of the shRNA knockdown was assessed after selecting clones stably expressing the sortilin shRNA. RT-PCR using 2 μg of total RNA was performed after RNA extraction using the RNeasy kit from Qiagen (Mississauga, ON, CAN). First strand cDNA was synthesized by PCR using the OmniScript Reverse Transcriptase kit (Qiagen, Mississauga, ON, CAN) and oligo (dT) primers. For PCR, 2 μg of cDNA was added to a mixture containing 2.5 μg of 10x buffer (20 mM $MgCl_2$), 1 μg dNTP, 0.5 U Taq purchased from Qiagen (Mississauga, ON, CAN), and 1 μg of each primer (sortilin: 5'- CGG TCC GAA TCC ATG AAG AAA TAT GTC TGT GGG GGA AG -3' and 5'- AAT TAT CTC GAG GTC GAC TTC CAA GAG GTC CTC ATC TC -3'; β-actin: 5'- AGA GCC ACC AAT CCA CAC AG -3' and 5'- CTC TCT TCC AGC CTT CTT TC -3') designed in our laboratory and synthesized

by AlphaDNA (Montreal, QC, CAN). The PCR amplification conditions for denaturation were 94°C for 1 minute, 55°C for 1 minute for annealing, and 72°C for 2 minutes extension time. The program was run for 30 cycles followed by a 10 minute final extension at 72°C. The products were electrophoresed in a 1.5% (w/v) agarose gel containing 0.5% ethidium bromide.

Verification of the efficiency in shRNA knockdown of sortilin and siRNA knockdown of Vps26 and μ1A was also verified by Western blotting. COS-7 cells stably expressing sortilin, as well as cells 72 hours post-transfection with Vps26, m1A, or the negative control siRNA were assayed. Cells evaluated were rinsed twice with cold phosphate buffered saline (PBS), and lysed for 30 minutes with 50 μl of lysis buffer containing 50 mM Tris-HCl (pH 6.0), 0.15 M NaCl, 0.5% NP-40 and a protease inhibitor cocktail (Roche, Laval, QC, CAN). The cell extract was then boiled with 10 μl of 6 X SDS-sample buffer. Proteins were separated on a 10 % SDS-PAGE gel and transferred to a 0.45 μm nitrocellulose membrane (BioRad, Hercules, CA, USA). The membrane was blocked in a 5% milk PBS-T (PBS and Tween-20) solution and probed overnight at 4 °C with a mouse monoclonal anti-sortilin antibody at 1:1000, a mouse monoclonal anti-γ-adaptin at 1:2500, or a rabbit polyclonal anti-Vps26 antibody at 1:5000. The blots were washed three times with PBS-T before one hour incubation with secondary antibody. Goat anti-mouse IgG HRP at 1:5000 was used to detect sortilin primary antibody, whereas the same secondary antibody was used at 1:15000 to detect γ-adaptin primary antibody. Goat anti-rabbit IgG HRP was used at 1:15000 to detect Vps26 antibody. Subsequent to incubation with the secondary antibody, three more washes were done with PBS-T, and the membrane

was developed by ECL Plus Western Blotting Detection System (Amersham Biosciences, Piscataway, NJ, USA) and Kodak BioMax Light Film.

Western Blotting: Expression of Sorting Receptors and Lysosomal Proteins

COS-7, ICD, and wild type human fibroblasts cells were rinsed twice with cold PBS, and lysed for 30 minutes with 50 µl of lysis buffer as described above (50 mM Tris-HCl (pH 6.0), 0.15 M NaCl, 0.5% NP-40 and a protease inhibitor cocktail (Roche, Laval, QC, CAN). The cell extracts were then boiled for 10 minutes with 10 µl of 6 X SDS-sample buffer and centrifuged for 5 minutes at 13500 rpm in a small benchtop centrifuge. Proteins were separated on a 10 % SDS-PAGE gel and transferred to a 0.45 µm thick nitrocellulose membrane (BioRad, Hercules, CA, USA). The membranes were blocked in a 5% milk PBS-T solution and probed overnight at 4 ^{o}C with primary antibody. Sortilin was detected using the mouse monoclonal antibody at 1:1000; cathepsins D, H, K, and L and $G_{M2}AP$ were detected using goat polyclonal antibodies at 1:1000; cathepsin B, prosaposin, LAMP-1 and M6PR were rabbit polyclonal antibodies diluted 1:1000. Appropriate secondary antibodies conjugated to HRP were incubated with the membranes for 1 hour at room temperature. After 3 washes with PBS-T, the membranes were developed by ECL Plus Western Blotting Detection System (Amersham Biosciences, Piscataway, NJ, USA) and Kodak BioMax Light Film.

Co-immunoprecipitation I: The Interaction of Soluble Lysosomal Proteins with Sorting Receptors

COS-7, ICD, or wild type human fibroblast cells were used for co-immunoprecipitation (Co-IP) of wild type sortilin, M6PR, and dominant-negative sortilin. Co-IP for the dominant-negative sortilin required transfection with the truncated sortilin-myc construct. Cells were harvested 24 hours post transfection or once they had obtained 100 % confluency in the case of non-transfected cells. The cells were lysed in 1 ml of lysis buffer (50 mM Tris-HCl (pH 6.0), 0.15 M NaCl, 0.5% NP-40 and a protease inhibitor cocktail (Roche, Laval, QC, CAN)) and pre-cleared using 50 µl of protein A or protein G Sepharose beads (Amersham Biosciences, Piscataway, NJ, USA). The supernatants were subsequently incubated with 50 µl of protein A Sepharose beads coupled to either anti-cathepsin B or prosaposin antibody at 4°C overnight. For Co-IP with cathepsins D, H, K, and L, the cell supernatants were incubated overnight at 4°C with 50 µl of protein G Sepharose beads coupled to anti-cathepsin D, H, K, or L antibody. The beads were then washed three times with PBS and boiled in 45 µl of 3 X SDS-PAGE sample buffer. Proteins were separated on a 10 % SDS-PAGE gel, transferred to a nitrocellulose membrane and visualized by immunoblotting with mouse monoclonal anti-myc, anti-sortilin or rabbit polyclonal anti-M6PR antibodies diluted to 1:1000. Protein was detected with the appropriate secondary antibodies coupled to HRP followed by ECL Plus Western Blotting Detection System (Amersham Biosciences, Piscataway, NJ, USA) and Kodak BioMax Light Film.

Confocal Microscopy I: Localization of Sortilin and Soluble Lysosomal Proteins

COS-7, ICD, or wild type human fibroblast cells were seeded onto cover slips 24 hours prior to transfection with wild type or truncated sortilin-myc. Twenty four hours post-transfection the cells were washed twice with 1 X PBS and fixed for 10 minutes in 4 % paraformaldehyde. Another 3 washes with PBS were done before the cells were permeabilized with 0.25 % Triton X-100 for 5 minutes. Blocking was performed for 1 hour in 3 % goat or rabbit serum and 0.1 % Triton X-100. Primary antibody incubation was performed at a 1:150 dilution overnight at 4°C in the case of cathepsins B, D, H, and L. For anti-myc, anti-golgin-97, anti-cathepsin K, and rabbit or mouse anti-LAMP-1 primary antibodies, the concentration used was 1:200 under similar conditions. Anti-prosaposin antibody was used at a concentration of 1:350. After incubation with the primary antibodies, the cells were washed three times for 5 minutes with PBS. Incubation of the cells with the appropriate Alexa-conjugated secondary antibodies (Alexa 488 green or Alexa 594 red) diluted to 1:300 was performed for 1 hour at room temperature. The cells were washed again 3 times for 5 minutes with PBS and treated with 300 µl of 0.007 µg/µl Hoeschst 33342. Subsequently, the cells were washed 3 times with PBS and once with water. The cover slips were mounted onto slides using Geltol (Thermo Electron Corporation, Waltham MA, USA). The immunofluorescent staining was visualized with an LSM 510 confocal microscope (Carl Zeiss, Montreal, QC, CAN). The number of LAMP-1 positive compartments per cell area was assessed quantitatively using AxioVision LE 4.6 (Carl Zeiss, Montreal, QC, CAN). The cell area was measured and expressed as number of pixels within the perimeter of demarcated randomly chosen cells.

The Effect of Sortilin Inhibition on Soluble Lysosomal Proteins

Confocal Microscopy

COS-7 cells stably expressing sortilin shRNA were fixed in 4 % paraformaldehyde and compared to mock transfected cells. These cells were permeabilized, blocked, and stained for prosaposin, cathepsins B, D, H, K, and L as described above. Similarly, lysosomes were visualized using anti-LAMP-1 antibody, followed by secondary antibody conjugated to Alexa 594 (red). The immunofluorescent staining was visualized with an LSM 510 confocal microscope (Carl Zeiss, Montreal, QC, CAN). The number of LAMP-1 positive compartments per cell area was assessed by AxioVision LE 4.6 (Carl Zeiss, Montreal, QC, CAN). The cell area was measured and expressed as number of pixels.

Pulse-Chase Analysis

COS-7 cells stably expressing sortilin shRNA were washed twice with 1 X PBS and starved for 30 minutes in 5 ml of methionine-free, cysteine-free DMEM (Invitrogen, Burlington, ON, CAN) supplemented with 5 % dialyzed FBS. The cells were pulse-labeled for 30 minutes in 4 ml medium supplemented with 1023 μCi/ml [^{35}S] methionine (Amersham Biosciences, Piscataway, NJ, USA). The chase was performed using DMEM containing 10 % FBS, 5 nM unlabeled methionine and 2.5 nM unlabeled cysteine for 0, 30, 60, and 90 minutes. Following this, culture medium was collected, and pre-cleared with 50 μl of protein A or G Sepharose beads (Amersham Biosciences, Piscataway, NJ, USA) by incubation at 4°C for 2 hours. Meanwhile, the cells were washed twice with PBS and collected. They were lysed on

ice for 30 minutes in 500 µl of lysis buffer (50 mM Tris-HCl (pH 6.0), 0.15 M NaCl, 0.5% NP-40 and a protease inhibitor cocktail (Roche, Laval, QC, CAN)). The cell extracts were also pre-cleared with 50 µl of protein A or G Sepharose beads by incubating at 4°C for 2 hours. Both the pre-cleared medium and cellular supernatants were incubated with 50 µl of protein A Sepharose beads coupled to either anti-prosaposin or anti-cathepsin B antibody at 4°C overnight. Protein G Sepharose beads coupled to anti-cathepsins D, H, K, and L were also used for immunoprecipitation. The immuno-complexed beads were washed with PBS and the complex eluted from the protein Sepharose beads with 45 µl of 3 X SDS-PAGE sample buffer. The samples were boiled for 10 minutes at 100°C in a salt bath before being resolved on a 10 % SDS-PAGE gel and transferred to a 0.45 µm nitrocellulose membrane (BioRad, Hercules, CA, USA). The membranes were then analyzed by autoradiography. The experiment was repeated 3 times and results of these were quantified using Quantity One 4.3.1 from BioRad (Hercules, CA, USA).

Isolation of Detergent-Resistant Membranes: Mutational Analysis of Amino Acids Implicated in Localization to Detergent-Resistant Membranes

TM4 Sertoli cells were transfected with wild-type sortilin-myc 24 hours prior to fractionation. COS-7 cells were transfected with: an empty pcDNA3.1 vector, the wild type albumin-D-domain-C-terminus prosaposin chimera, the albumin-D-domain prosaposin chimera, the albumin-C-terminus prosaposin chimera, or the mutant albumin-prosaposin chimeras (E463K, or E491K). Additionally, similar cells were co-transfected with the wild type albumin-D-domain-C-terminus prosaposin chimera

and sortilin shRNA. Ten 100 mm plates of cells were transfected with each type of construct. Twenty four hours post-transfection, when the cells had obtained approximately 90 % confluency, they were washed three times with ice cold 1 X PBS, scraped, and centrifuged for 5 minutes at 1000 rpm at 4 °C. The cellular pellet (approximately 5 mg of cells) was resuspended in 1.33 ml of buffer A (50 mM Tris-HCL, pH 7.5, 150 mM NaCl, and 1 % cold Triton X-100 detergent). The solution was homogenized by 10 strokes in a glass homogenizer and incubated for 60 minutes on ice before being diluted in a 1:1 ratio with 80 % sucrose in a solution of buffer B (50 mM Tris-HCL, pH 7.5 and 150 mM NaCl). The homogenate was loaded into an 8 ml ultra-clear ultracentrifuge tube and overlayed with 2.6 ml of 30 % and 10 % sucrose. This suspension was centrifuged overnight at 4 °C using an SW41 rotor at 100,000 x g (25 000 rpm). The gradients were then aliquoted into 11 equal fractions of 750 µl each from the top of the tube (Figure 25A). The protein concentration of the eleven fractions was normalized by dilution in water. The fractions were analyzed by separation on a 10 % acrylamide gel and subsequently transferred to 0.45 µm nitrocellulose membrane and immunoblotted with the appropriate antibodies. The albumin-prosaposin constructs were detected using anti-myc antibody. The presence of DRMs was determined by detection with anti-flotillin-1 antibody, and was co-localized with anti-sortilin antibody.

Co-immunoprecipitation II: The Interaction of Cytosolic Adaptors with Sortilin

COS-7 cells were transfected with wild type sortilin-myc, Y14A or L17A sortilin-myc constructs, or pcDNA3.1B as a control. Twenty four hours subsequent to

transfection, the cells were washed with 1 X PBS, harvested and lysed for 30 minutes in 1 ml of lysis buffer (50 mM Tris-HCl (pH 6.0), 0.15 M NaCl, 0.5% NP-40 and a protease inhibitor cocktail (Roche, Laval, QC, CAN)). The cell lysate was pre-cleared using 50 µl of protein A Sepharose beads (Amersham Biosciences, Piscataway, NJ, USA). To examine the interaction between the sortilin-myc constructs and Vps26 or γ-adaptin, immunoprecipitation was accomplished by incubating the cellular supernatants with 50 µl of protein A Sepharose beads coupled to anti-myc antibody at 4°C overnight. The resulting complexes were then washed three times with PBS and boiled in 45 µl of 3X SDS-PAGE sample buffer. Proteins were separated on a 10 % SDS-PAGE gel, transferred for 2 hours to a 0.45 µm nitrocellulose membrane and visualized by immunoblotting with either anti-Vps26 diluted to 1:5000 or anti-γ-adaptin antibody diluted to 1:2500. Anti-rabbit and anti-mouse secondary antibodies coupled to HRP were used at a dilution of 1:10000.

Yeast two-hybrid Assay

The sortilin C-terminal tail (residues 779-831) was subcloned into either the pB42AD or pGAD424 vector. Truncation mutations were obtained by inserting a stop codon after residue 789, 799, 809 or 819. Vps26, Vps29 and Vps35 were cloned into the pLexA, pGAD424 or pGBKT7 vectors. The co-transformed yeast strains were plated on synthetic medium plates lacking leucine and tryptophan (GAL4, two-hybrid) or lacking histidine and tryptophan (LexA, two-hybrid). Colonies after 72 hours of growth were re-plated on synthetic medium plates lacking leucine, tryptophan and

histidine (GAL4, two-hybrid) or lacking histidine, tryptophan and leucine (LexA, two-hybrid).

Confocal Microscopy II: Localization of Sortilin Mutant Constructs

Cells were seeded onto cover slips and transfected 24 hours later with wild type sortilin, Y14A or L17A sortilin-myc constructs using Polyfect according to manufacturer's protocol described above (Qiagen, Mississauga, ON, CAN). The cells were incubated for 24 hours before being fixed, permeabilized, and blocked as described above. Primary antibody incubation was performed at 4 °C overnight using anti-myc, antibody at 1:250 and anti-LAMP-1 antibody at 1:200. After incubation with the primary antibodies, the cells were washed three times with PBS and incubated with Alexa-conjugated secondary antibody diluted to 1:300 for 1 hour at room temperature. The cells were then washed three times with PBS and treated with 300 µl of Hoeschst 33342 as previously described. The cover slips were again washed with PBS, double-distilled water, and mounted onto slides using Geltol (Thermo Electron Corporation, Waltham MA, USA). The immunofluorescence staining was visualized with an LSM 510 confocal microscope (Carl Zeiss, Montreal, QC, CAN).

Cycloheximide-Chase: Sortilin Stability

COS-7 cells expressing control, Vps26 or µ1A siRNA were trypsinized 72 hours post-transfection. A cellular suspension of each was incubated for 0, 2, 4, or 6 hours in a solution of complete DMEM, 25 mM HEPES, pH 7.4, and 40 µg/ml cycloheximide. After incubation, the cells were centrifuged at 2000 x g in a benchtop

centrifuge for 10 minutes at 4 °C. Subsequently, the cells were lysed for 30 minutes and prepared in loading buffer as described above. Samples were run on a 10 % acrylamide gel, transferred to a nitrocellulose membrane, and immunoblotted for sortilin as previously described.

Confocal Microscopy III: Localization of Sortilin and its Ligands in the Absence of Cytosolic Adaptors

The effect of Vps26 (retromer) or μ1A (AP-1) inhibition by siRNA on sortilin localization was analyzed by confocal immunomicroscopy and compared to mock transfected cells. Cells were seeded onto cover slips and immediately transfected with the siRNA using Hiperfect according to manufacturer's protocol described above (Qiagen, Mississauga, ON, CAN). 48 hours post-transfection with the siRNA, the cells were transfected with a sortilin-myc construct and washed twenty four hours later with PBS and fixed for 10 minutes in 4 % paraformaldehyde. The cells were then permeabilized with 0.25 % triton X-100 for 5 minutes. Blocking was performed for 1 hour in 3 % goat serum and 0.1 % Triton X-100. Primary antibody incubation was performed at a 1:300 dilution overnight at 4°C for anti-myc, anti-prosaposin, anti-cathepsin B, anti-LAMP1, anti-γ-adaptin and, anti-Vps26p antibodies. After incubation with the primary antibodies, the cells were washed three times with PBS and incubated with Alexa-conjugated secondary antibodies diluted to 1:300 for 1 hour at room temperature. The cells were then washed three times with PBS and treated with 300 μl of 0.007 μg/μl Hoeschst 33342 for 10 minutes. The cells were again washed three times with PBS and once with double-distilled water. The cover slips

were mounted using Geltol (Thermo Electron Corporation, Waltham MA, USA). The immunofluorescence staining was visualized with an LSM 510 confocal microscope (Carl Zeiss, Montreal, QC, CAN).

Pulse-Chase Analysis II: The Effect of Retromer and AP-1 Inhibition on Ligand Secretion

COS-7 cells were transfected with control, Vps26, or μ1A siRNA in 100 mm plates. 72 hours post-transfection, the cells were washed with sterile PBS and subsequently starved for 30 minutes in 4 ml of methionine-free, cysteine-free DMEM (Invitrogen, Burlington, ON, CAN) supplemented with 5 % dialyzed fetal bovine serum. The cells were pulse-labeled for 30 minutes in 4 ml medium supplemented with 1023 μCi/ml [^{35}S] methionine (Amersham Biosciences, Piscataway, NJ, USA). The chase was carried out using DMEM with 10 % fetal bovine serum, 5 nM unlabeled methionine and 2.5 nM unlabeled cysteine for 0, 30, 60, and 90 minutes. The culture medium was subsequently collected into new tubes and pre-cleared with 50 μl of protein A Sepharose beads at 4°C for 1 hour. The media was then incubated with 50 μl of protein A Sepharose beads coupled to antibody. Immunoprecipitation was performed using anti-prosaposin or anti-cathepsin B antibody at 4°C overnight. The beads were then washed three times with PBS and the proteins eluted from the immuno-complexed beads with 45 μl of 3X SDS-PAGE sample buffer. The samples were boiled for 10 minutes at 100°C and subjected to reducing SDS-PAGE to be analyzed by autoradiography. This procedure was repeated 3 times and the results

were averaged and quantified using the Quantity One program from BioRad (Hercules, CA, USA).

Table 2. Sortilin Mutant Construct Primers. List of the primers employed to generate the Y14A, L17A, and FLV-807-809-AAA sortilin mutant constructs using the QuikChange kit from Stratagene.

Y14A	5'- TTC CTG GTG CAT CGA GCC TCT GTG CT -3'
L17A	5'- ATC GAT ACT CTG TGG CGC AGC AGC AT -3'
FLV-807-809-AAA	5'- GAA ATA TGT CTG TGG GGG AAG GGC CGC GGC GCA TCG ATA CTC TGT GCT GCA G -3'

Figure A. Sortilin and Truncated Sortilin Constructs. Schematic diagram of wild type sortilin in the trans-Golgi (TGN) membrane (A). Sortilin interacts with the VHS domain of the monomeric GGA adaptor proteins via an acidic cluster dileucine signal in its cytosolic tail. GGA adaptor proteins are subsequently responsible for the recruitment of clathrin and accessory proteins implicated in clathrin-coated vesicle formation and trafficking. A sortilin construct that lacks its cytosolic domain is unable to interact with GGA adaptors and is therefore retained in the TGN (B). The truncated sortilin construct possesses a myc tag (B). Modified from Current Opinion in Cell Biology (Robinson et al., 2001).

A)

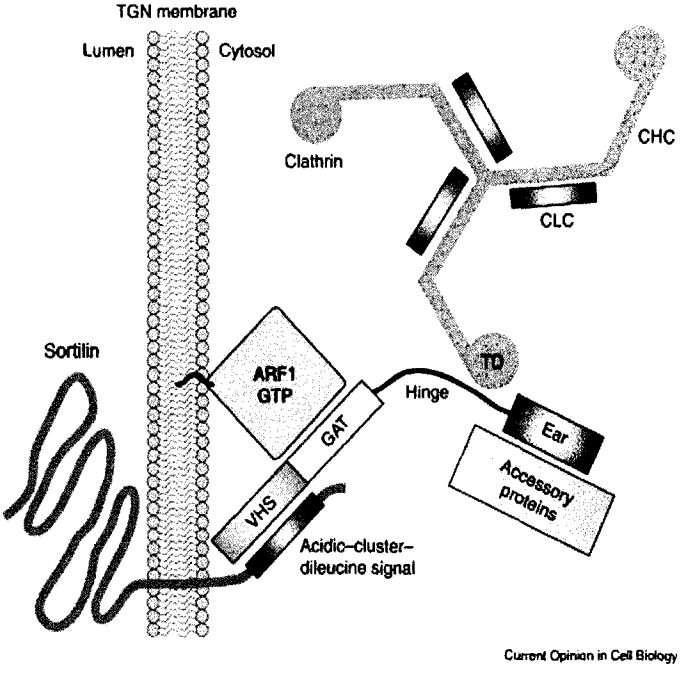
TGN membrane
Lumen
Cytosol
Clathrin
CHC
CLC
TD
Sortilin
ARF1
GTP
GAT
Hinge
Ear
Accessory proteins
VHS
Acidic–cluster–dileucine signal
Current Opinion in Cell Biology

B)

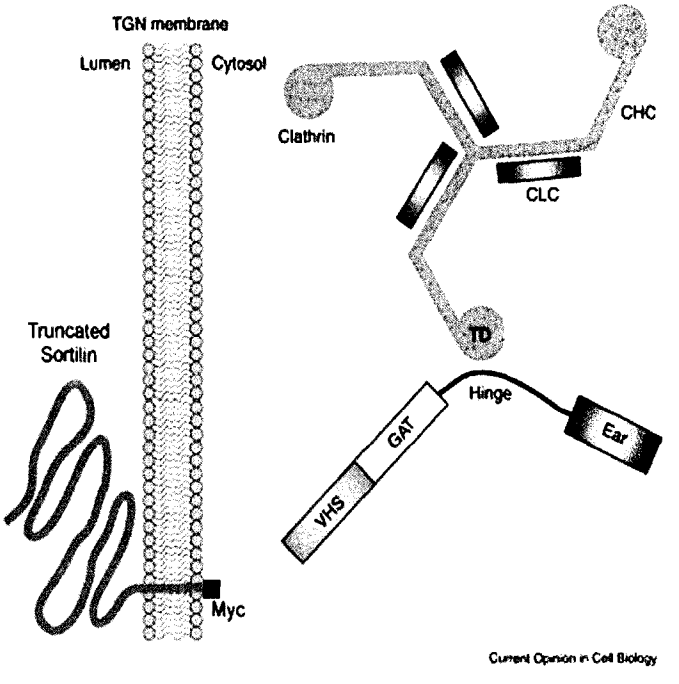
TGN membrane
Lumen
Cytosol
Clathrin
CHC
CLC
TD
Truncated Sortilin
Hinge
GAT
Ear
VHS
Myc
Current Opinion in Cell Biology

Figure B. Chimeric Albumin-Prosaposin Constructs. Schematic representation of albumin linked to the prosaposin D-domain as well as the prosaposin C-terminus (Alb/D/C-term) (A). Chimeric constructs consisting of albumin and only the C-terminus of prosaposin (B) or the D-domain of prosaposin (C) were utilized to examine which domain of prosaposin is important for its association with detergent-resistant membranes (DRMs).

A)

B)

C)

Chapter 4: Results Part 1

Luminal Ligands of Sortilin (Cargo Proteins)

Expression of Sorting Receptors and Lysosomal Proteins

Rationale: To verify the expression of endogenous lysosomal proteins and sorting receptors within COS-7, ICD, and wild type human fibroblasts Western blot analysis was conducted. Cathepsins are synthesized as pre-pro-enzymes in the ER, processed to pro-enzymes which are transported through the Golgi, and are finally cleaved into mature enzymes within the lysosomal compartment (Hasilik, 1992). It is therefore important to validate the ability of the antibodies used in this investigation to detect the appropriate form of the cathepsins (ie. the pro-forms that bind sorting receptors in the TGN).

Experimental Results: Lysates from COS-7, ICD, and wild type human fibroblasts were boiled in 6 X sample buffer and resolved on a 10 % acrylamide gel prior to being transferred to nitrocellulose membrane. The sorting receptors, sortilin and M6PR, were detected with anti-sortilin and anti-M6PR antibodies producing bands at 100 kDa and 300 kDa respectively in all three cell lines (Figure 1A and 1B). LAMP-1, a frequently utilized marker of lysosomes, was also present in all three cell types as a single 70 kDa band (Figure 1C). SAPs, prosaposin and $G_{M2}AP$, were detected in all cell lines in 2 different forms: prosaposin as both its intracellularly destined 68 kDa form and as its 70 kDa secretory form and $G_{M2}AP$ as 27 kDa immature and 22 kDa mature forms (Figure 1D and 1E). Anti-Cathepsins D and H antibodies also produced bands representative of their immature and mature lysosomal forms in COS-7, ICD, and wild type human fibroblasts (Figure 1G and 1H). Cathepsin B was identified in its 37 kDa immature form in all three cell types but only in its 25 kDa mature form in COS-7 and wild type human fibroblasts (Figure 1F).

However, while all three cells lines possessed the immature forms of cathepsins K and L (39 kDa and 37 kDa respectively), only wild type human fibroblasts contained mature cathepsin K (27 kDa) whereas mature cathepsin L (27 kDa) was found exclusively in COS-7 cells (Figure 1I and 1J). These results confirm the presence of the sorting receptors and lysosomal proteins in their appropriate forms in the cell lines of interest in this study.

The Interaction of Soluble Lysosomal Proteins and Sorting Receptors

Rationale: It is well established that the transport of cathepsin B from the TGN to the lysosomes is dependent on the M6PR (Lobel et al., 1989). The transport of other cathepsins, including cathepsins D, H, K, and L, remains in question. While, the trafficking of cathepsin D is in part dependent on the M6PR, the transport of cathepsin H appears to be independent of this sorting receptor (Rijnboutt et al., 1991b; Tanaka et al., 2000). Similarly, the ability of cathepsins K and L to interact with and traffic to the lysosomes by the M6PR has been questioned (Claveau and Riendeau, 2001; Gottesman, 1978). To investigate whether or not sortilin or the M6PR bind the cathepsins in question, co-immunoprecipitation assays were performed using the lysates of COS-7, wild type human fibroblasts, or ICD cells. Cathepsin B, a well known ligand of the M6PR, was used as a negative control. Prosaposin, a SAP and established ligand of sortilin, was examined as a positive control (Lefrancois et al., 2003).

Experimental Results: The binding of cathepsins to the sorting receptors was initially examined in COS-7 and wild type human fibroblasts. In these cell lines, as

expected, when anti-prosaposin antibody was conjugated to protein A Sepharose beads, it was capable of immunoprecipitating sortilin, but not the M6PR (Figures 2A and 3A). Contrary to this, the negative control, anti-cathepsin B antibody coupled to protein A Sepharose beads, was capable of immunoprecipitating the M6PR, but not sortilin (Figures 2B and 3B). When examined by Co-IP, both cathepsins D (Figures 2C and 3C) and H (Figures 2D and 3D) were capable of interacting with sortilin and pulling it out of the cell lysate. However, cathepsin D (Figures 2C and 3C) also immunoprecipitated the M6PR, producing a band at 300 kDa whereas cathepsin H (Figures 2D and 3D) was incapable of binding the M6PR in these Co-IP assays. Cathepsins K (Figures 2E and 3E) and L (Figures 2F and 3F), like cathepsin B, were seen here to bind to the M6PR but not the sortilin sorting receptor.

In ICD fibroblasts the phosphotransferase implicated in the addition of M6P tags to ligands of the M6PR is mutated. Consequently, ligands of the M6PR fail to recognize and bind to this sorting receptor (Reitman et al., 1981). When Co-IP was performed using ICD fibroblasts, none of the soluble lysosomal proteins examined were found to bind the M6PR (Figure 4A-4F). However, prosaposin, as well as cathepsins D and H were found to interact with sortilin as in COS-7 and wild type human fibroblasts (Figure 4A, 4C, and 4D).

Similar experiments were conducted in all three cells transfected with a truncated sortilin-myc construct. This dominant-negative construct of sortilin lacks its cytosolic domain which contains an acidic-cluster dileucine signal that has previously been demonstrated to be essential in the interaction of sortilin with the GGA adaptor proteins and in turn for lysosomal targeting (Lefrancois et al., 2003; Nielsen et al.,

2001). When the Co-IP of truncated sortilin-myc was performed using anti-prosaposin (Figures 2A, 3A, and 4A) or anti-cathepsin B (Figures 2B, 3B, and 4B), D (Figures 2C, 3C, and 4C), H (Figures 2D, 3D, and 4D), K (Figures 2E, 3E, and 4E), or L (Figures 2F, 3F, and 4F) antibodies, the results obtained were similar to those for wild type sortilin. Co-IP with prosaposin (Figures 2A, 3A, and 4A) and cathepsins D (Figures 2C, 3C, and 4C) and H (Figures 2D, 3D, and 4D) produced bands at 95 kDa. Thus, the deletion of the cytosolic domain of sortilin did not disturb the interaction with its ligands.

Effect of Truncated Sortilin on the Transport of Soluble Lysosomal Proteins

Rationale: To investigate if sortilin is implicated in the lysosomal targeting of cathepsins D, H, K or L, COS-7 and wild type human fibroblasts were transfected with the myc-tagged truncated sortilin construct. The effect of transfection on the transport of the lysosomal proteins was analyzed by confocal microscopy. Typically sortilin is localized to both the perinuclear Golgi region and punctate lysosomal structures (Figure 5A, and 5C). Without its cytosolic tail sortilin can not bind GGA adaptor proteins but retains its ability to bind ligands via its luminal domain (Lefrancois et al., 2003). Thus, truncated sortilin and its ligands have been shown to remain in the Golgi apparatus (Figure 5B, and 5D) (Lefrancois et al., 2003).

Experimental Results: COS-7 and human skin fibroblast cells expressing the truncated sortilin construct were compared to untransfected cells for the distribution of prosaposin and cathepsins B, D, H, K, and L (Figures 6, 7, 8, 9, 10 and 11). In order to examine the lysosomal localization of the soluble lysosomal proteins in question,

their distribution was compared to that of LAMP-1, an integral membrane protein localized to lysosomes, and the truncated sortilin-myc construct. Prosaposin (green) was found in the perinuclear region of untransfected cells, as well as in punctate lysosomal structures labeled in red with LAMP-1 (Figure 6A, and 6D). Truncated sortilin-myc abolished the presence of prosaposin in the lysosomes of both cell lines (Figure 6C and 6F) and caused retention of prosaposin in the TGN along with truncated sortilin-myc (Figure 6B and 6E). Cathepsin B (green) was unaffected by the truncated sortilin-myc construct as is seen by its presence in compartments labeled in red with LAMP-1 of both untransfected and transfected cells (Figures 7A-7F).

Transfected and untransfected cells were also stained for cathepsins D (Figure 10), H (Figure 11), K (Figure 8), or L (Figure 9) and then incubated with secondary antibody conjugated to Alexa 488 (green). Similar to cathepsin B, the lysosomal localization of cathepsins K (Figure 8) and L (Figure 9) in transfected cells was not altered as compared to untransfected cells (Figures 8 and 9). Untransfected cells stained with anti-cathepsin D (Figure 10A, and 10D), or anti-cathepsin H (Figure 11A, and 11D) antibodies revealed the presence of cathepsins D and H in punctate lysosomal structures that overlapped with LAMP-1 (red). On the other hand, anti-cathepsin D (Figure 10C, and 10F) and anti-cathepsin H (Figure 11C, and 11F) antibodies did not yield a granular staining in cells expressing truncated sortilin but yielded a green fluorescence in the perinuclear region that overlapped with truncated sortilin-myc (Figures 10B, 10F, 11B, and 11F). However, while expression of truncated sortilin entirely abolished the presence of cathepsins D and H in LAMP-1 positive compartments, it did not significantly affect the overall number of lysosomes

labeled with LAMP-1 as was seen by immunofluorescence. The number of LAMP-1 positive compartments per cell area, expressed as number of pixels, was similar between untransfected (0.14 ± 0.03) and transfected cells (0.14 ± 0.02).

Assessment of Sortilin shRNA Knockdown

Rationale: To investigate the fate of sortilin ligands in the absence of the sortilin sorting receptor, shRNA specific to sortilin was generated. Based on previous results from chemically synthesized siRNA, a sequence with no known homologies other than to sortilin (AAGGTGGTGTTAACAGCAGAG) was selected for the shRNA (Lefrancois et al., 2003). This sequence was subcloned into the pSilencer 3.1 H1-neo vector and stably expressed in COS-7 cells by selection with neomycin. In order to assess the efficiency of this shRNA knockdown of sortilin, RT-PCR and Western blot analysis were performed.

Experimental Results: Efficiency of the shRNA knockdown was first assessed by RT-PCR. The products of RT-PCR were electrophoresed in a 1.5% (w/v) agarose gel containing 0.5% ethidium bromide. While the mock transfected cells expressed sortilin mRNA (200 bp), cells expressing sortilin shRNA did not express sortilin mRNA or protein (Figure 12A). In both instances the levels of β-actin (270 bp) remained constant (Figure 12A). Subsequently, the lysate of COS-7 of similar cells was resolved on a 10 % acrylamide gel and transferred to nitrocellulose membrane. Blotting with an anti-sortilin antibody yielded a 100 kDa band in the mock transfected cells but none in cells expressing sortilin shRNA (Figure 12B). However, the levels of β-actin remained the same in both mock and shRNA transfected cells (Figure 12B).

Thus, the sortilin shRNA specifically inhibited expression of sortilin mRNA and protein.

Effect of Sortilin Inhibition on the Transport of Soluble Lysosomal Proteins

Rationale: To determine the effect of sortilin inactivation on the lysosomal transport of cathepsins D, H, K and L, COS-7 cells stably transfected with sortilin shRNA were examined both by confocal microscopy and pulse-chase. The objective of these experiments was to test the hypothesis that in absence of sortilin, soluble lysosomal proteins whose sole means of lysosomal transport is sortilin would be secreted from the cells. Therefore by confocal microscopy, it is predicted that the staining of sortilin's ligands will be abolished. Alternatively, we hypothesized that sortilin's ligands will be found in increased amounts in the extracellular milieu by pulse-chase analysis. Prosaposin, a known sortilin ligand, was used as a positive control. Cathepsin B, a known M6PR ligand, was used as a negative control.

Experimental Results: For confocal analysis, cells were fixed with 4 % paraformaldehyde and immunostained with anti-LAMP-1 antibody to visualize the lysosomes, as well as with anti-cathepsins B, D, H, K or L antibodies or with anti-prosaposin antibody followed by incubation with secondary antibody conjugated to Alexa 488 or 594 in the case of LAMP-1 (Figures 13, 15, 16, 17, and 18). The typical granular and perinuclear staining of prosaposin and cathepsin H in mock transfected cells (Figures 13A and 16A) was absent in COS-7 cells stably transfected with sortilin shRNA (Figures 13B and 16B). The granular cytoplasmic staining of anti-cathepsins B, D, K, and L antibodies was unaffected by the absence of sortilin (Figures 13C,

13D, 15A, 15B, 17A, 17B, 18A and 18B). In these experiments, the number of lysosomes labeled with LAMP-1 per cell area, expressed as number of pixels, did not vary between mock (0.13 ± 0.04) and sortilin shRNA (0.15 ± 0.03) transfected cells.

Similar cells also stably expressing shRNA were pulsed with [^{35}S] methionine-cysteine and chased with DMEM. Immunoprecipitation of both the cell lysates and culture medium was done at 0, 30, 60, and 90 minutes using anti-prosaposin (Figure 14A), or anti-cathepsins B, D, H, K, or L antibodies (Figures 14B, 15C, 16C, 17C, and 18C). The resulting immunoprecipitates were resolved on 10 % SDS-PAGE gels and visualized by autoradiography. The results were compared to immunoprecipitations of cell lysates and medium from cells that were mock transfected. Ablation of sortilin resulted in increased secretion of prosaposin in its secretory form (70 kDa), as well as induction of secretion of its cellular form (68 kDa) (Figure 14A). Similar results were obtained for cathepsin H (Figure 16C), but no significant effect on the secretion of cathepsins B, D, K, or L (Figures 14B, 15C, 17C, and 18C) was observed when quantified using Quantity One 4.3.1 from BioRad.

Effect of Dominant-Negative Truncated Sortilin in ICD Cells

Rationale: To better understand the role of sortilin and the M6PR in the trafficking of soluble lysosomal proteins, cells in which both the sortilin and the M6PR pathways are blocked were examined here. Fibroblasts from ICD patients have an impaired M6PR pathway, leading to the secretion of many soluble lysosomal hydrolases, such as cathepsin B, into the extracellular milieu. In these experiments,

ICD fibroblasts were transfected with the truncated sortilin-myc construct in order to inhibit the sortilin sorting pathway (Figure 5E, and 5F).

Experimental Results: ICD cells transfected with truncated sortilin-myc were fixed 24 hours post-transfection and compared to untransfected cells. Cells were stained with anti-prosaposin and anti-cathepsins B, D, H, K and L antibodies (green) (Figures 19, 20, 21, 22, 23, and 24). Lysosomes were visualized using anti-LAMP-1 antibody (red). Prosaposin was observed in the perinuclear region and in punctate LAMP-1 positive structures of untransfected cells (Figure 19A). Conversely, prosaposin was exclusively localized in the perinuclear region of cells expressing truncated sortilin-myc (Figure 19B and 19C). On the other hand, in both transfected and untransfected ICD fibroblasts, cathepsin B staining (green) was diffuse and presented no punctate lysosomal structures (Figure 20).

When cathepsins K and L were examined, it was found that cathepsins K (Figure 21) and L (Figure 22) both localized to structures stained with LAMP-1 in untransfected (Figures 21A and 22A) and transfected ICD cells (Figures 21B, 21C, 22B and 22C). However, as with prosaposin, cathepsin D (Figure 23) and H (Figure 24) staining was found in LAMP-1 positive compartments in untransfected ICD cells (Figures 23A and 24A) but excluded from these structures in cells transfected with truncated sortilin (Figures 23C and 24C). In cells expressing truncated sortilin, cathepsins D and H were retained in the perinuclear region along with the truncated sortilin-myc construct (Figure 23B and 24B). Again in these experiments, the total number of LAMP-1 positive compartments per cell area, expressed as number of

pixels, contained within the boundaries of demarcated cells, was similar in untransfected (0.10 ± 0.02) and truncated sortilin-myc transfected cells (0.09 ± 0.01).

Mutational Analysis of Amino Acids Implicated in Localization to Detergent-Resistant Membranes (DRMs)

Rationale: Sphingomyelin synthesis is catalyzed by sphingomyelin-synthase, an enzyme on the luminal leaflet of Golgi membranes that transfers phosphorylcholine to ceramide. Prosaposin, a SAP, not only requires the presence of sortilin, but also of sphingomyelin for its translocation to the lysosomal compartment (Lefrancois et al., 2002). Depletion of sphingomyelin with D-609, a substance that binds to sphingomyelin synthase and interferes with the conversion of ceramide to sphingomyelin, resulted in the inhibition of the lysosomal transport of prosaposin (Lefrancois et al., 1999). Since sphingomyelin is found in DRM microdomains, this experiment was designed to test the hypothesis that sortilin and its ligands reside in DRM domains in COS-7 cells. Flotillin-1 was used as a marker for DRMs.

Furthermore, in an attempt to identify the regions and specific amino acids implicated in the localization of prosaposin to sphingomyelin-rich microdomains, chimeric prosaposin constructs were also examined by fractionation of DRMs. Previous results from our laboratory have linked the delivery of prosaposin to the lysosomes, not only to an interaction with sphingomyelin, but to its D-domain and C-terminus regions (Lefrancois et al., 1999; Zhao and Morales, 2000). Therefore chimeric constructs consisting of albumin and the D-domain of prosaposin alone or in conjunction to the C-terminus were examined along with an albumin-C-terminus

construct. These constructs were used to determine conclusively which domain of prosaposin mediates its interaction with DRMs.

Finally, specific negatively-charged amino acids in the D-domain of a chimeric construct consisting of albumin and both the D-domain and C-terminus of prosaposin were mutated (E463K and E491K) and examined by DRM fractionation. This was done to test the hypothesis that negatively-charged amino acids in prosaposin mediate the interaction of prosaposin with the positively-charged head-groups of sphingomyelin in DRMs. Hypothetically this interaction would bring prosaposin into proximity of sortilin allowing the binding of prosaposin to its sorting receptor. Previous analysis of the ability of E463K and E491K mutant constructs to interact with sortilin revealed that their binding was unaffected, although mutant construct E463K showed defective lysosomal sorting (unpublished results). Here we examine whether the defective lysosomal sorting observed with prosaposin mutant E463K is due to an inability to interact with DRMs.

Experimental Results: To investigate the subcellular localization of sortilin and its newly identified ligands, a DRM isolation assay was done using TM4 Sertoli cells transfected with wild-type sortilin-myc. The choice of TM4 cells for this experiment was based on the morphological presence of a robust Golgi apparatus and a large number of lysosomes. Fractions 1 - 8 (10 % - 30 % sucrose gradient) contained the insoluble detergent membrane fractions. Lipid-rafts are generally concentrated around fractions 4 and 5. Fraction 9-10 (40 % sucrose gradient) represented the soluble protein fraction. Fraction 11 was the cell pellet which typically contains insoluble cell debris and cytoskeletal elements (Figure 25A). The

fractions were resolved on a 4-12 % Bis-Tris gradient gel, transferred to a nitrocellulose filter, and subsequently immunoblotted with anti-cathepsin B, D, and H, anti-prosaposin, anti-sortilin, and anti-M6PR antibodies (Figure 25B). As a marker for lipid-rafts, the fractions were also blotted with anti-flotillin-1 antibody (Figure 25B). Flotillin-1 (47 kDa) was found to be concentrated in fractions 4 and 5. Bands were detected in lipid raft fractions 3, 4, 5, and 6 when anti-sortilin (100 kDa), anti-prosaposin (68 kDa), anti-cathepsin D (47 kDa) antibodies were used. Anti-cathepsin H (37 kDa) antibody yielded bands in DRM fractions 4 and 5. The M6PR (300 kDa) and its ligands, cathepsin B (37 kDa), were both found in soluble protein fraction 9.

A similar technique was employed with COS-7 cells to identify the domains within prosaposin that mediate its association with DRMs. COS-7 cells were transfected with the chimeric albumin-prosaposin constructs (Figure 26B, 26C, and 26D) and compared to cells transfected with only pcDNA3.1 (Figure 26A). The positive control was a chimeric construct consisting of albumin and both the D-domain and C-terminus of prosaposin. This construct was detected using anti-myc antibody and found to be present in fractions 6 to 11 as bands of approximately 80 kDa (Figure 26B), whereas no bands were detected with the anti-myc antibody in cells transfected with pcDNA3.1 (Figure 26A). Interestingly, the construct consisting of albumin and only the D-domain of prosaposin demonstrated very little localization to DRMs and was found in only fractions 9 through 11 as a 70 kDa band (Figure 26C). The albumin-C-terminus construct was present in DRM fractions 6-11 as a 70 kDa band (Figure 26D). In all of the above instances, sortilin was found between fractions 7 to 11 at 100 kDa, and flotillin-1 in fractions 5 through 7 at 47 kDa (Figure 26).

Thus, the albumin chimeric constructs containing the C-terminus of prosaposin (Figure 26B and 26D) were localized in DRMs, whereas the constructs lacking the C-terminus (Figure 26A and 26C) were excluded from DRMs.

The above technique was also exploited to examine the distribution of the prosaposin mutant constructs, E463K and E491K, in DRM fractions. The E463K mutant construct was found as an 80 kDa band in fractions 5-11, whereas E491K was present in fractions 6-11 as similarly sized bands (Figure 27A and 27B). Similarly, COS-7 cells transfected with E463K and E491K mutant constructs were found to have sortilin present in the same fractions as the mutant constructs, as well as flotillin-1 in fractions 3 and 4 (Figure 27A and 27B). Consequently our experiments showed that the E463K and E491K mutations had no effect on the distribution the chimeric constructs to DRMs and implied that the D-domain of prosaposin is not essential in mediating the localization of prosaposin to DRMs. This was confirmed by examining the distribution of the un-mutated chimeric construct that contained both the D-domain and C-terminus of prosaposin when the cells were depleted of sortilin using shRNA (Figure 27C). In cells in which sortilin expression was abolished, the chimeric construct was present in fractions 9-11 (Figure 27C). This result suggests that without sortilin, the localization of prosaposin to DRMs is hindered.

Figure 1. Expression of Lysosomal Sorting Receptors and Proteins. Lysates from COS-7, wild-type human skin fibroblasts, and ICD fibroblasts were probed for expression of sorting receptors and lysosomal proteins by Western blotting. In all three cell lines tested, sortilin was detected as a 100 kDa band, whereas the M6PR was observed at 300 kDa (A and B). An anti-LAMP-1 antibody produced bands at 70 kDa in COS-7, wild-type human skin fibroblasts, and ICD fibroblasts (C). Prosaposin was observed in its 68 kDa intracellular and 70 kDa secretory forms (D). Anti-$G_{M2}AP$ antibody detected both an immature 27 kDa form and 22 kDa mature form of $G_{M2}AP$ (E). Anti-cathepsin B antibody produced bands at both 37 and 25 kDa in COS-7 and wild-type human skin fibroblasts, but only a 37 kDa band in ICD fibroblasts (F). Cathepsins D and H were found in all three cell lines tested in their immature (Cathepsin D: 47 kDa, Cathepsin H: 37 kDa) and processed forms (Cathepsin D: 31 kDa, Cathepsin H: 27 kDa) (G and H). An antibody specific for cathepsin K detected the immature form (39 kDa) of cathepsin K in all three cell lines, but the mature form (27 kDa) was only seen in wild-type human skin fibroblasts (I). Cathepsin L was observed in its 37 kDa form in of the cell lines examined but only in its 27 kDa processed form in COS-7 cells (J).

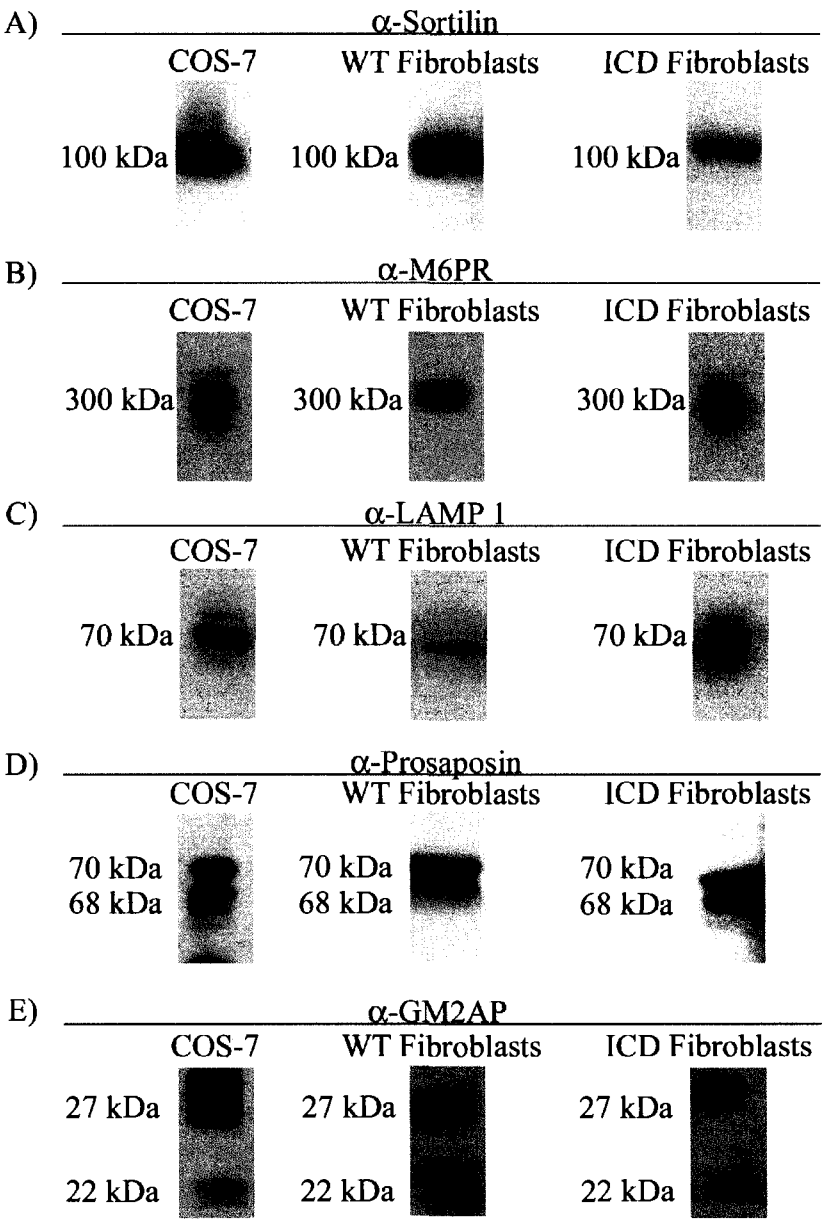
A)
α-Sortilin
COS-7
WT Fibroblasts
ICD Fibroblasts
100 kDa
100 kDa
100 kDa
B)
α-M6PR
COS-7
WT Fibroblasts
ICD Fibroblasts
300 kDa
300 kDa
300 kDa
C)
α-LAMP 1
COS-7
WT Fibroblasts
ICD Fibroblasts
70 kDa
70 kDa
70 kDa
D)
α-Prosaposin
COS-7
WT Fibroblasts
ICD Fibroblasts
70 kDa
68 kDa
70 kDa
68 kDa
70 kDa
68 kDa
E)
α-GM2AP
COS-7
WT Fibroblasts
ICD Fibroblasts
27 kDa
22 kDa
27 kDa
22 kDa
27 kDa
22 kDa

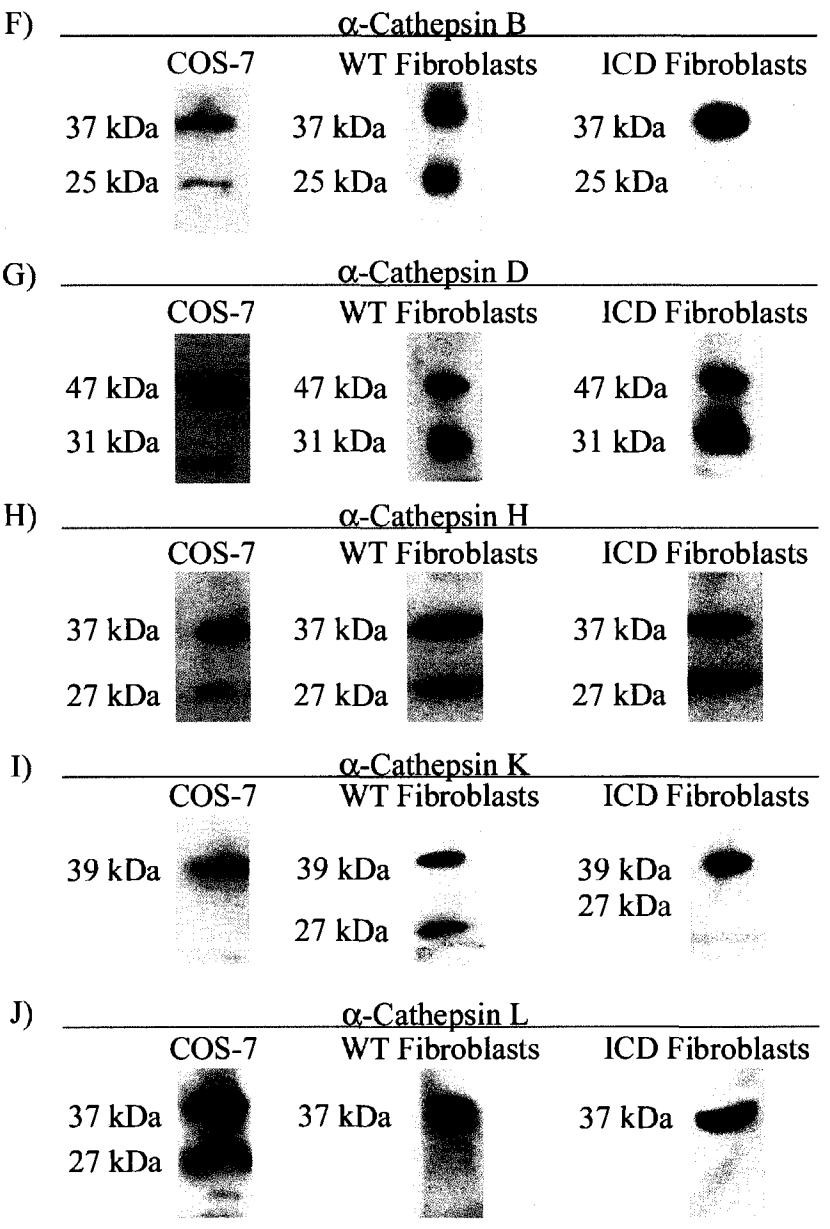
F)
α-Cathepsin B
COS-7
WT Fibroblasts
ICD Fibroblasts
37 kDa
25 kDa
37 kDa
25 kDa
37 kDa
25 kDa
G)
α-Cathepsin D
COS-7
WT Fibroblasts
ICD Fibroblasts
47 kDa
31 kDa
47 kDa
31 kDa
47 kDa
31 kDa
H)
α-Cathepsin H
COS-7
WT Fibroblasts
ICD Fibroblasts
37 kDa
27 kDa
37 kDa
27 kDa
37 kDa
27 kDa
I)
α-Cathepsin K
COS-7
WT Fibroblasts
ICD Fibroblasts
39 kDa
39 kDa
27 kDa
39 kDa
27 kDa
J)
α-Cathepsin L
COS-7
WT Fibroblasts
ICD Fibroblasts
37 kDa
27 kDa
37 kDa
37 kDa

Figure 2. The Interaction of Soluble Lysosomal Proteins with Sorting Receptors in COS-7. To identify the sorting receptor of cathepsins D, H, K, and L, co-immunoprecipitation assays were performed. It was found that the M6P-Rc was precipitated by cathepsins B, D, K, and L (B, C, E, and F) producing a band at 300 kDa. Prosaposin and cathepsin H were not capable of co-immunoprecipitating the M6PR, but rather the receptor was found to remain in the cell lysate (A and D). The interaction of prosaposin and cathepsins B, D, H, K, and L with sortilin was examined in untransfected cells and in COS-7 cells expressing a truncated sortilin-myc construct. When anti-prosaposin or anti-cathepsin D, or H antibody was used to co-immunoprecipitate endogenous sortilin, prosaposin as well as cathepsins D and H interacted with sortilin, producing bands at 100 kDa (A, C, and D). When a similar experiment was conducted using cells expressing the truncated sortilin-myc construct, comparable results were found. Truncated sortilin was immunoprecipitated by prosaposin as well as cathepsins D and H, yielding bands at 95 kDa (A, C, and D). Endogenous and truncated sortilin both remained in the cell lysate when immunoprecipitation was conducted using anti-cathepsin B, K, or L antibody (B, E, and F).

A)

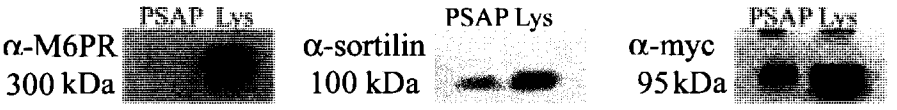
PSAP Lys
α-M6PR
300 kDa
PSAP Lys
α-sortilin
100 kDa
PSAP Lys
α-myc
95 kDa

B)

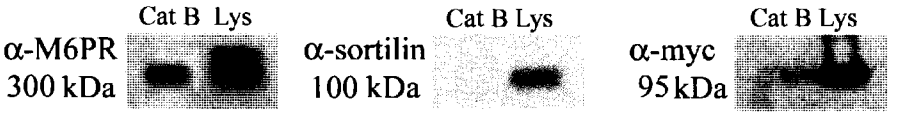
Cat B Lys
α-M6PR
300 kDa
Cat B Lys
α-sortilin
100 kDa
Cat B Lys
α-myc
95 kDa

C)

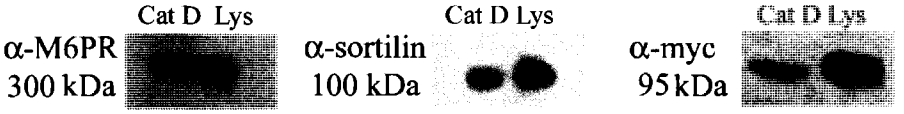
Cat D Lys
α-M6PR
300 kDa
Cat D Lys
α-sortilin
100 kDa
Cat D Lys
α-myc
95 kDa

D)

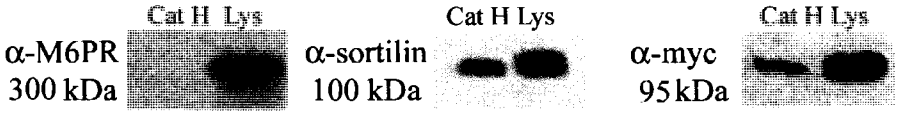
Cat H Lys
α-M6PR
300 kDa
Cat H Lys
α-sortilin
100 kDa
Cat H Lys
α-myc
95 kDa

E)


Cat K Lys
α-M6PR
300 kDa
Cat K Lys
α-sortilin
100 kDa
Cat K Lys
α-myc
95 kDa

F)

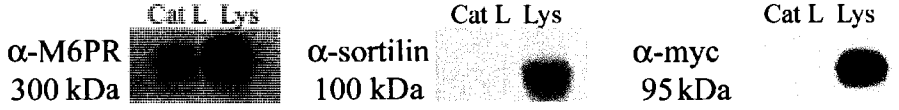
Cat L Lys
α-M6PR
300 kDa
Cat L Lys
α-sortilin
100 kDa
Cat L Lys
α-myc
95 kDa

Figure 3. The Interaction of Soluble Lysosomal Proteins with Sorting Receptors in Wild-Type Human Skin Fibroblasts. To confirm the results obtained in COS-7 cells, co-immunoprecipitation assays were performed in wild-type human fibroblasts. As in COS-7, it was found that the M6PR was precipitated by cathepsins B, D, K, and L (B, C, E, and F). Prosaposin and cathepsin H were not capable of co-immunoprecipitating the M6PR, but rather the receptor was found to remain in the cell lysate (A and D). The interaction of prosaposin and cathepsins B, D, H, K, and L with sortilin was examined in untransfected cells and in cells expressing a truncated sortilin-myc construct. When anti-prosaposin or anti-cathepsin D, or H antibody was used, prosaposin as well as cathepsins D and H interacted with sortilin, producing bands at 100 kDa for endogenous sortilin and 95 kDa for truncated sortilin (A, C, and D). Endogenous and truncated sortilin were not precipitated from the cell lysate when immunoprecipitation was conducted using anti-cathepsin B, K, or L antibody (B, E, and F).

A)


PSAP Lys
α-M6PR
300 kDa
α-sortilin
100 kDa
PSAP Lys
α-myc
95kDa
PSAP Lys

B)

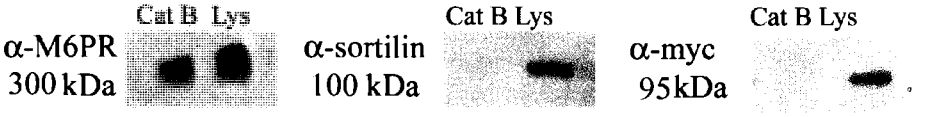
Cat B Lys
α-M6PR
300 kDa
α-sortilin
100 kDa
Cat B Lys
α-myc
95kDa
Cat B Lys

C)

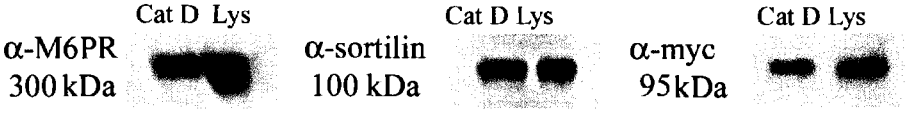
Cat D Lys
α-M6PR
300 kDa
α-sortilin
100 kDa
Cat D Lys
α-myc
95kDa
Cat D Lys

D)

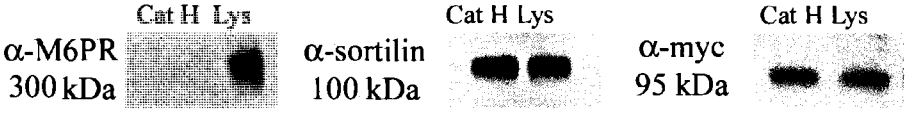
Cat H Lys
α-M6PR
300 kDa
α-sortilin
100 kDa
Cat H Lys
α-myc
95 kDa
Cat H Lys

E)

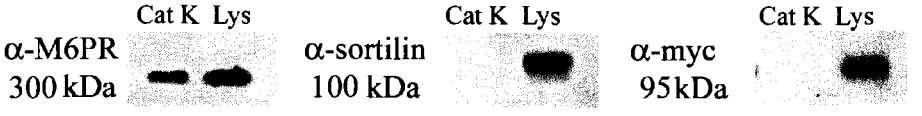
Cat K Lys
α-M6PR
300 kDa
α-sortilin
100 kDa
Cat K Lys
α-myc
95kDa
Cat K Lys

F)


Cat L Lys
α-M6PR
300 kDa
α-sortilin
100 kDa
Cat L Lys
α-myc
95kDa
Cat L Lys

Figure 4. The Interaction of Soluble Lysosomal Proteins with Sorting Receptors in ICD Fibroblasts. To confirm the results obtained in COS-7 and wild-type human fibroblast cells, co-immunoprecipitation assays were performed in ICD fibroblasts. Unlike in COS-7 and wild-type human fibroblasts, the M6PR was not precipitated by anti-prosaposin or anti-cathepsins B, D, H, K, or L antibodies (A, B, C, D, E, and F). The interaction of prosaposin and cathepsins B, D, H, K, and L with sortilin was examined in untransfected cells and in cells expressing a truncated sortilin-myc construct. When anti-prosaposin or anti-cathepsin D, or H antibody was used, prosaposin as well as cathepsins D and H interacted with sortilin, producing bands at 100 kDa for endogenous sortilin and 95 kDa for truncated sortilin (A, C, and D). Endogenous and truncated sortilin were not precipitated from the cell lysate when immunoprecipitation was conducted using anti-cathepsin B, K, or L antibody (B, E, and F).

A)


PSAP Lys
α-M6PR
300 kDa
PSAP Lys
α-sortilin
100 kDa
PSAP Lys
α-myc
95 kDa

B)

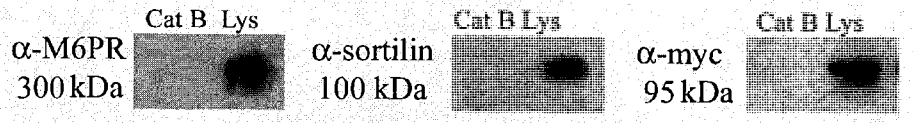
Cat B Lys
α-M6PR
300 kDa
Cat B Lys
α-sortilin
100 kDa
Cat B Lys
α-myc
95 kDa

C)

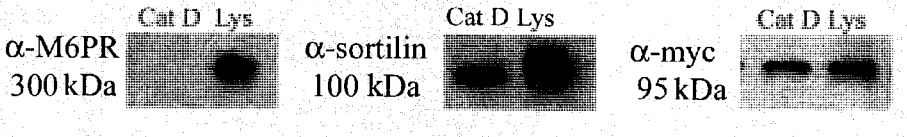
Cat D Lys
α-M6PR
300 kDa
Cat D Lys
α-sortilin
100 kDa
Cat D Lys
α-myc
95 kDa

D)

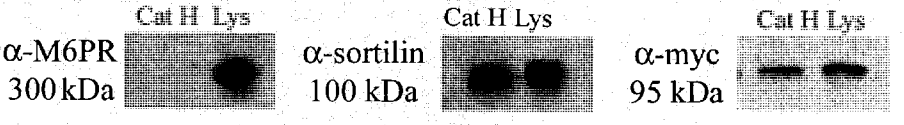
Cat H Lys
α-M6PR
300 kDa
Cat H Lys
α-sortilin
100 kDa
Cat H Lys
α-myc
95 kDa

E)

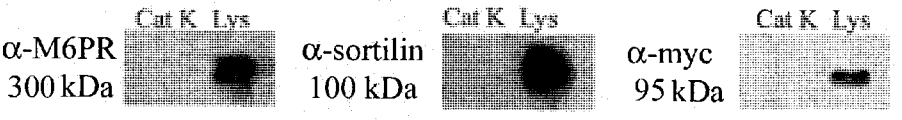
Cat K Lys
α-M6PR
300 kDa
Cat K Lys
α-sortilin
100 kDa
Cat K Lys
α-myc
95 kDa

F)

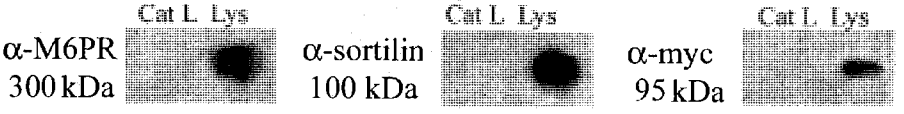
Cat L Lys
α-M6PR
300 kDa
Cat L Lys
α-sortilin
100 kDa
Cat L Lys
α-myc
95 kDa

Figure 5. Localization of Truncated Sortilin-myc. The localization of wild-type sortilin and truncated sortilin-myc was examined by confocal microscopy in COS-7 (A and B), in wild-type human skin fibroblasts (C and D), and in ICD fibroblasts (E and F). Wild-type sortilin-myc (green) was distributed to both the perinuclear Golgi region and punctate lysosomal structures labeled with LAMP-1 (red) (A, C, and E). Without its cytosolic tail, sortilin-myc (green) is still present in the perinuclear region of all three cell lines examined, but absent from LAMP-1 positive structures (red) (B, D, and F). The scale bars shown equal 8 μm and apply to all panels.

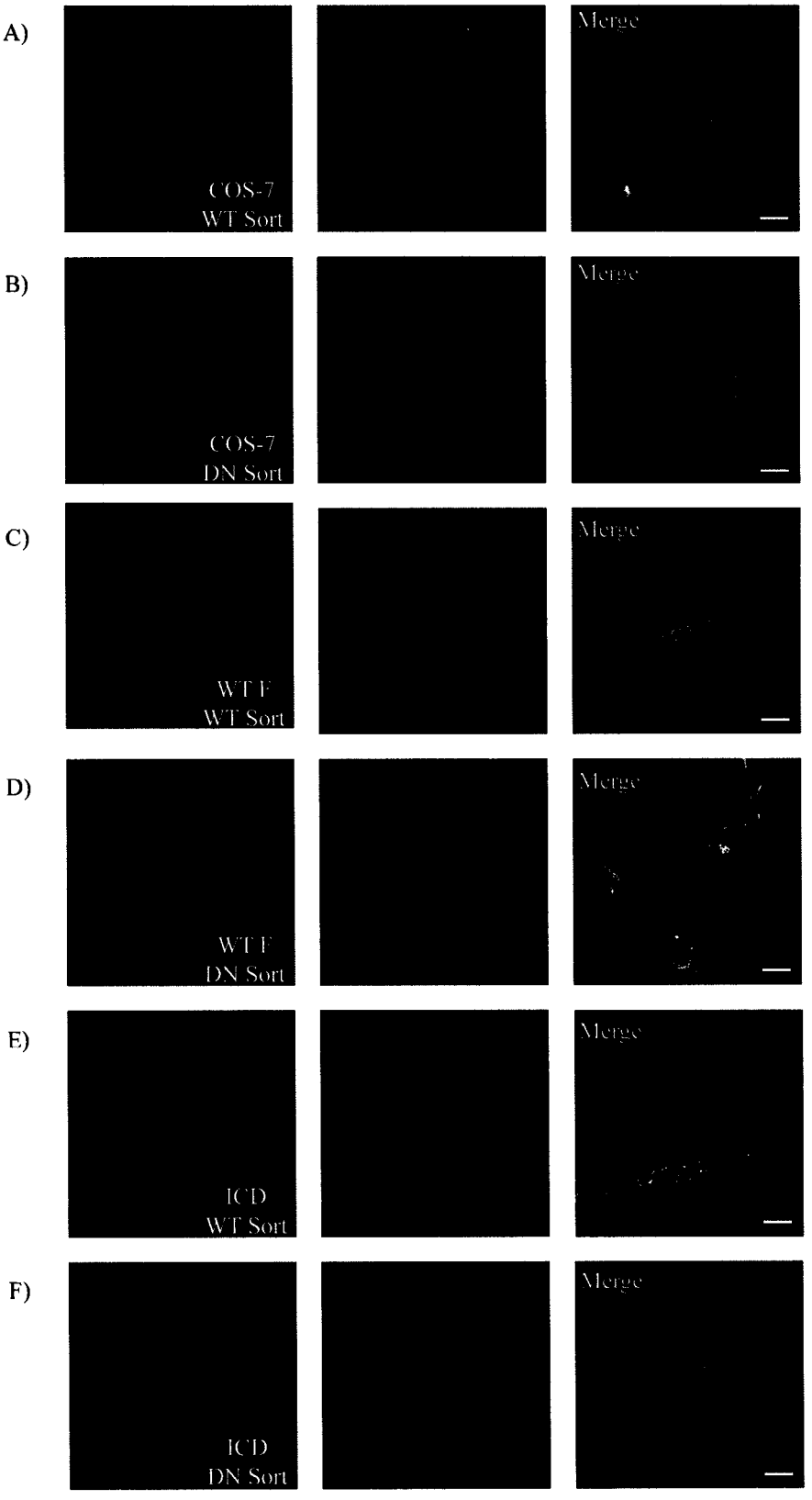
A)
COS-7
WT Sort
Merge
B)
COS-7
DN Sort
Merge
C)
WT F
WT Sort
Merge
D)
WT F
DN Sort
Merge
E)
ICD
WT Sort
Merge
F)
ICD
DN Sort
Merge

Figure 6. Lysosomal Targeting of Prosaposin. COS-7 (A-C) and wild-type human skin fibroblast cells (D-F) were either untransfected or transfected with truncated sortilin prior to fixation in 4 % paraformaldehyde. The cells were then stained with anti-prosaposin and anti-myc or anti-LAMP-1 antibodies. In untransfected cells, prosaposin (green fluorescence) localized in both the perinuclear region as well as in punctate lysosomes labelled with LAMP-1 (red fluorescence) (A and D). Alternatively, in cells transfected with dominant-negative truncated sortilin-myc, prosaposin staining (green fluorescence) in punctate lysosomal structures was abolished (B, C, E, and F). Rather prosaposin was found to colocalize (yellow) with the truncated sortilin-myc construct in the perinuclear region (B and E). However the LAMP-1 positive granules (red fluorescence) were present and unaffected in transfected cells (C and F). In all panels the nuclei are stained with Hoechst 33342 (blue). The scale bars shown equal 8 μm and apply to all panels.

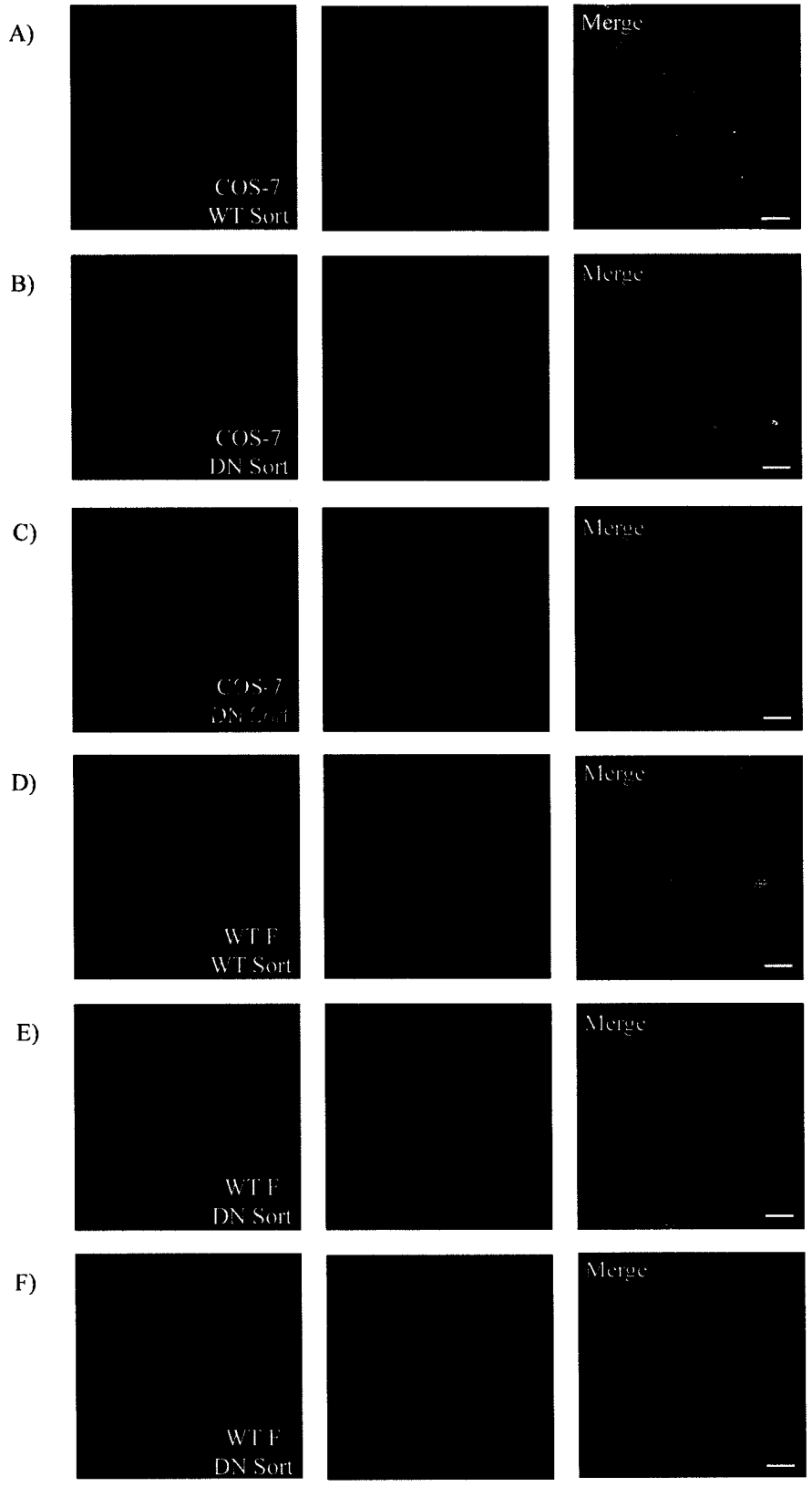
A)
COS-7
WT Sort
Merge
B)
COS-7
DN Sort
Merge
C)
COS-7
DN Sort
Merge
D)
WT F
WT Sort
Merge
E)
WT F
DN Sort
Merge
F)
WT F
DN Sort
Merge

Figure 7. Lysosomal Targeting of Cathepsin B. Untransfected and truncated-sortilin-myc transfected COS-7 (A-C) and wild-type human skin fibroblast cells (D-F) were fixed in 4 % paraformaldehyde and stained with anti-cathepsin B and anti-myc or anti-LAMP-1 antibodies. In untransfected cells, cathepsin B (green) was found to localize to the perinuclear Golgi region as well as to punctate structures that stained with LAMP-1 (red) (A and D). The staining pattern of cathepsin B (green) was unaltered in cells expressing truncated sortilin (red) (B and E). Additionally the staining pattern and number of LAMP-1 positively-labeled compartments (red) was unaffected in transfected cells (C and F). Nuclei are stained with Hoechst 33342 and are seen in blue. The scale bars shown equal 8 μm and apply to all panels.

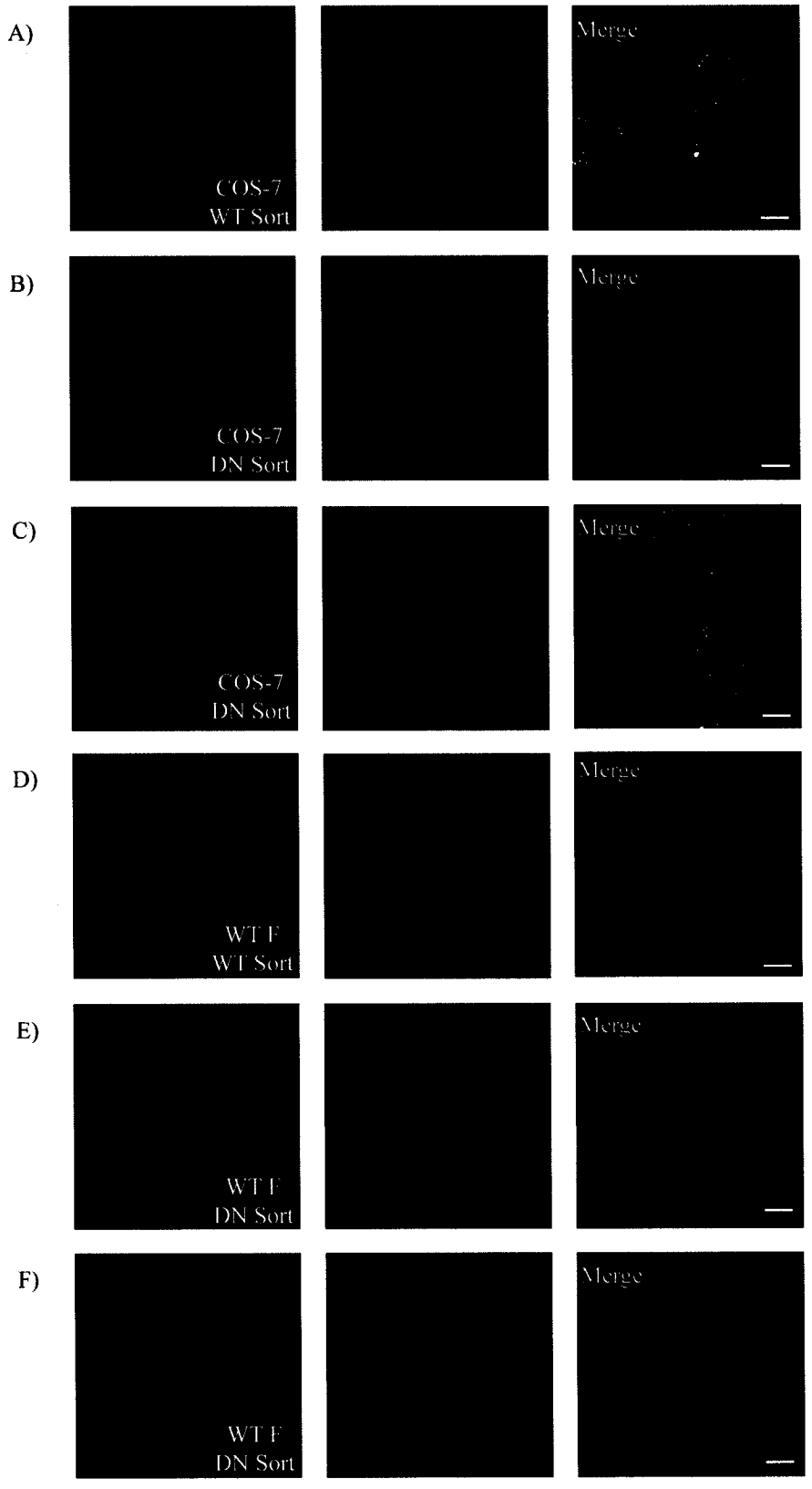
A)
COS-7
WT Sort
Merge
B)
COS-7
DN Sort
Merge
C)
COS-7
DN Sort
Merge
D)
WT F
WT Sort
Merge
E)
WT F
DN Sort
Merge
F)
WT F
DN Sort
Merge

Figure 8. Lysosomal Targeting of Cathepsin K. Untransfected and truncated-sortilin-myc transfected COS-7 (A-C) and wild-type human skin fibroblast cells (D-F) were fixed in 4 % paraformaldehyde and stained with anti-cathepsin K and anti-myc or anti-LAMP-1 antibodies. In untransfected cells, cathepsin K (green) was found to localize to punctate structures that stained with LAMP-1 (red) (A and D). The pattern of cathepsin K staining (green) was unaltered in cells expressing truncated sortilin (red) (B and E). Similarly the staining pattern of LAMP-1 positively-labeled compartments (red) was unaffected in transfected cells (C and F). Nuclei are stained with Hoechst 33342 and are seen in blue. The scale bars shown equal 8 μm and apply to all panels.

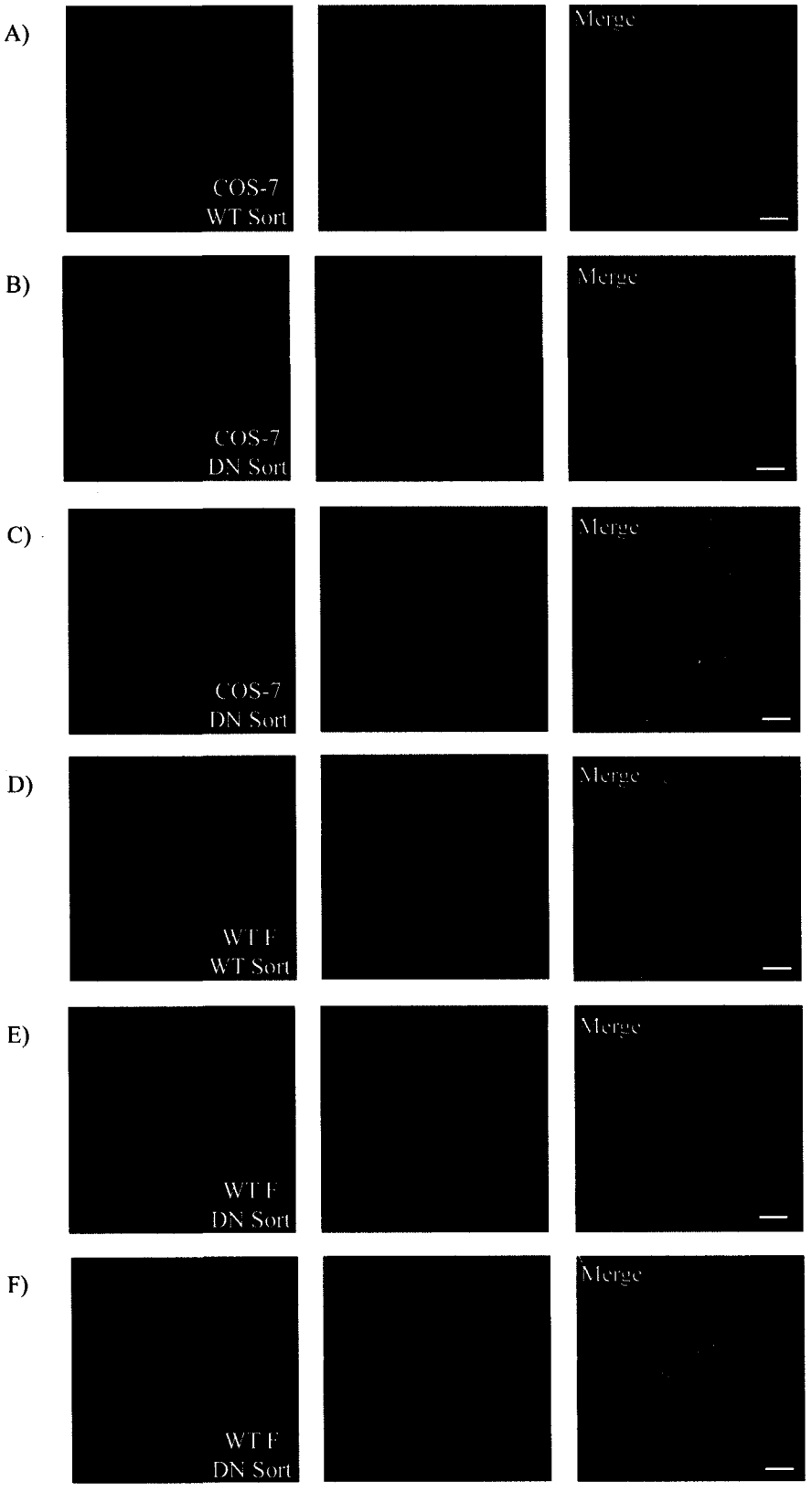
A)
COS-7
WT Sort
Merge
B)
COS-7
DN Sort
Merge
C)
COS-7
DN Sort
Merge
D)
WT F
WT Sort
Merge
E)
WT F
DN Sort
Merge
F)
WT F
DN Sort
Merge

Figure 9. Lysosomal Targeting of Cathepsin L. Untransfected and truncated-sortilin-myc transfected COS-7 (A-C) and wild-type human skin fibroblast cells (D-F) were fixed in 4 % paraformaldehyde and stained with anti-cathepsin L and anti-myc or anti-LAMP-1 antibodies. In untransfected cells, cathepsin L (green) was found to localize to the perinuclear Golgi region as well as to punctate structures that stained with LAMP-1 (red) (A and D). The distribution of cathepsin L (green) was unaltered in cells expressing truncated sortilin (red) (B and E). The staining pattern and number of LAMP-1 positively-labeled compartments (red) was unaffected in transfected cells (C and F). Nuclei are stained with Hoechst 33342 and are seen in blue. The scale bars shown equal 8 μm and apply to all panels.

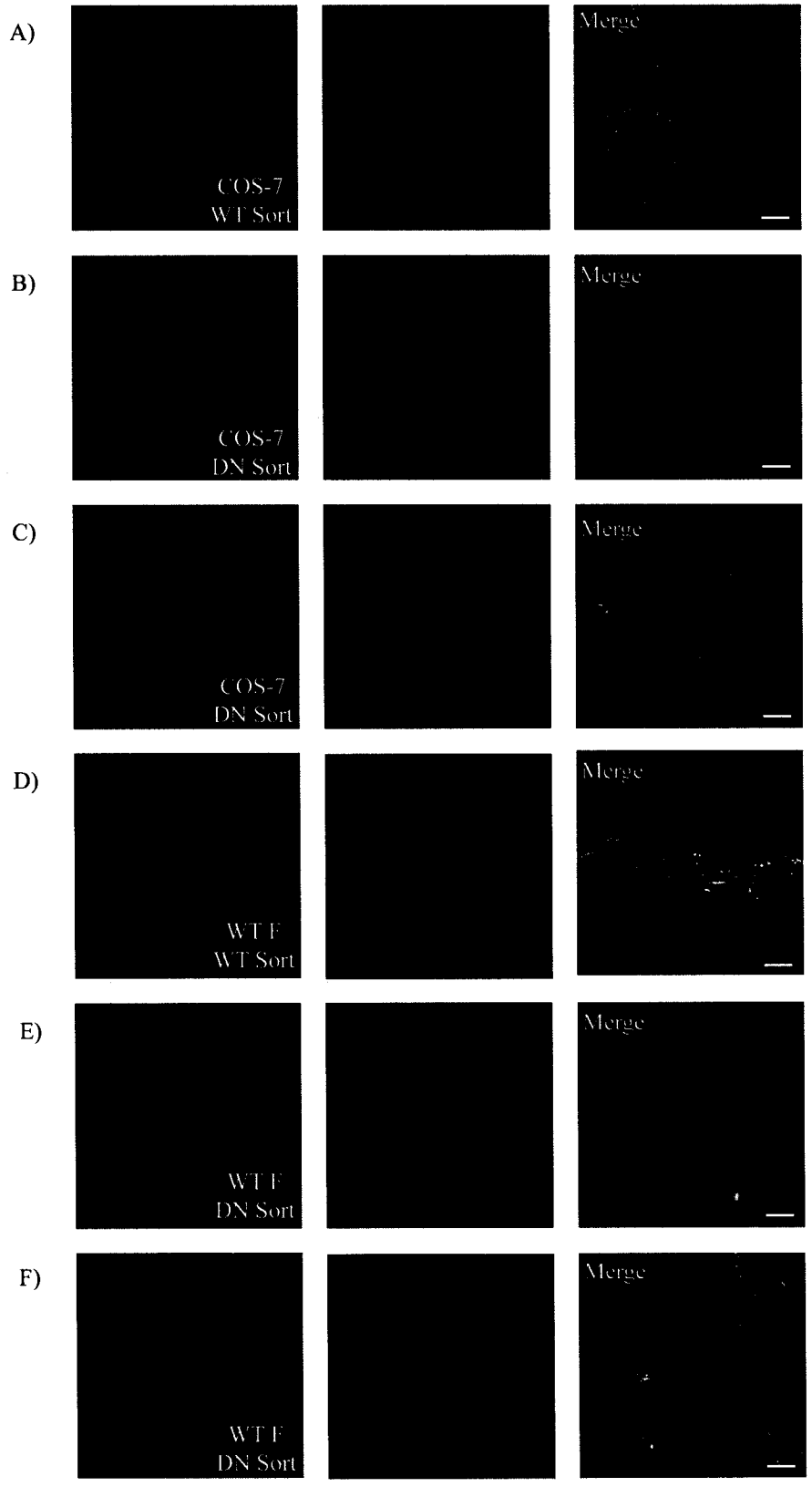
A)
COS-7
WT Sort
Merge
B)
COS-7
DN Sort
Merge
C)
COS-7
DN Sort
Merge
D)
WT F
WT Sort
Merge
E)
WT F
DN Sort
Merge
F)
WT F
DN Sort
Merge

Figure 10. Lysosomal Targeting of Cathepsin D. COS-7 (A-C) and wild-type human skin fibroblast cells (D-F) that were untransfected, or expressing truncated sortilin-myc were fixed and stained with anti-cathepsin D and anti-myc or anti-LAMP-1 antibody. In untransfected cells cathepsin D antibody (green) labels punctate lysosomal structures labeled with LAMP-1 (red) (A and D). Figures B, C, E, and F illustrate cells expressing truncated sortilin. Note that in these transfected cells, anti-cathepsin D (green) antibody staining is only observed in the Golgi region and colocalizes (yellow) with anti-myc staining (red) (B and E). The LAMP-1 (red) positive granules of the cell are still present in transfected cells (C and F). Nuclei are stained with Hoechst 33342 and are seen in blue. The scale bars shown equal 8 μm and apply to all panels.

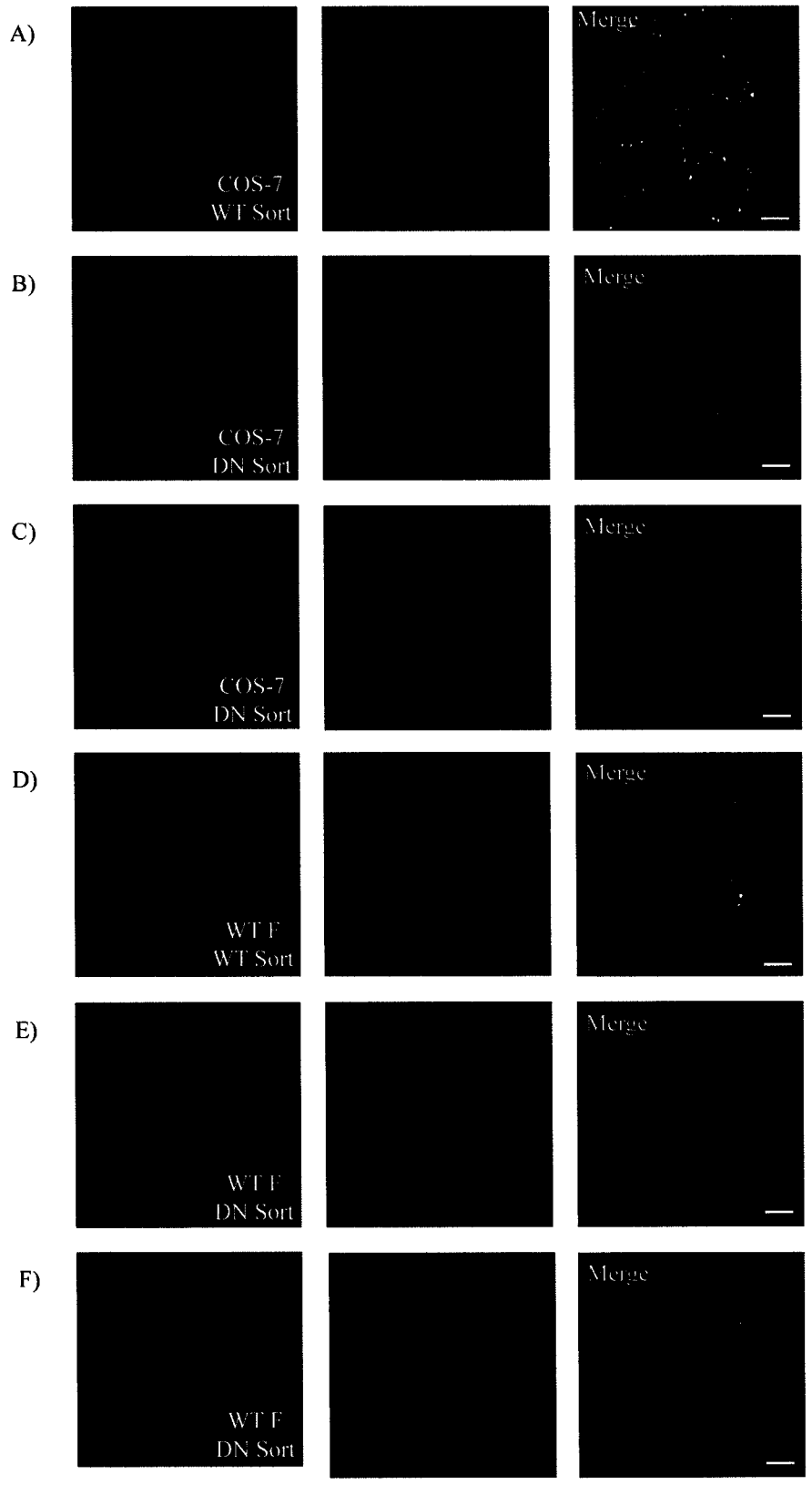
A)
COS-7
WT Sort
Merge
B)
COS-7
DN Sort
Merge
C)
COS-7
DN Sort
Merge
D)
WT F
WT Sort
Merge
E)
WT F
DN Sort
Merge
F)
WT F
DN Sort
Merge

Figure 11. Lysosomal Targeting of Cathepsin H. COS-7 (A-C) and wild-type human skin fibroblast cells (D-F) were either transfected with a truncated sortilin-myc construct or fixed directly. Cathepsin H was examined using an anti-cathepsin H antibody detected by an Alexa 488 coupled secondary antibody (green), whereas anti-myc and anti-LAMP-1 antibodies were visualized with Alexa 594 coupled secondary antibodies (red). In untransfected cells (A and D), cathepsin H (green) was found in punctate lysosomal structures labeled with LAMP-1 (red). Figures B, C, E, and F illustrate cells expressing truncated sortilin. Note that anti-cathepsin H antibody (green) stained the Golgi region only and colocalized (yellow) with anti-myc antibody (red) (B and E). Figures C and F show that the transfected cells presented normal punctate cytoplasmic granular structures labeled with LAMP-1 (red). Nuclei are stained with Hoechst 33342 and are seen in blue. The scale bars shown equal 8 μm and apply to all panels.

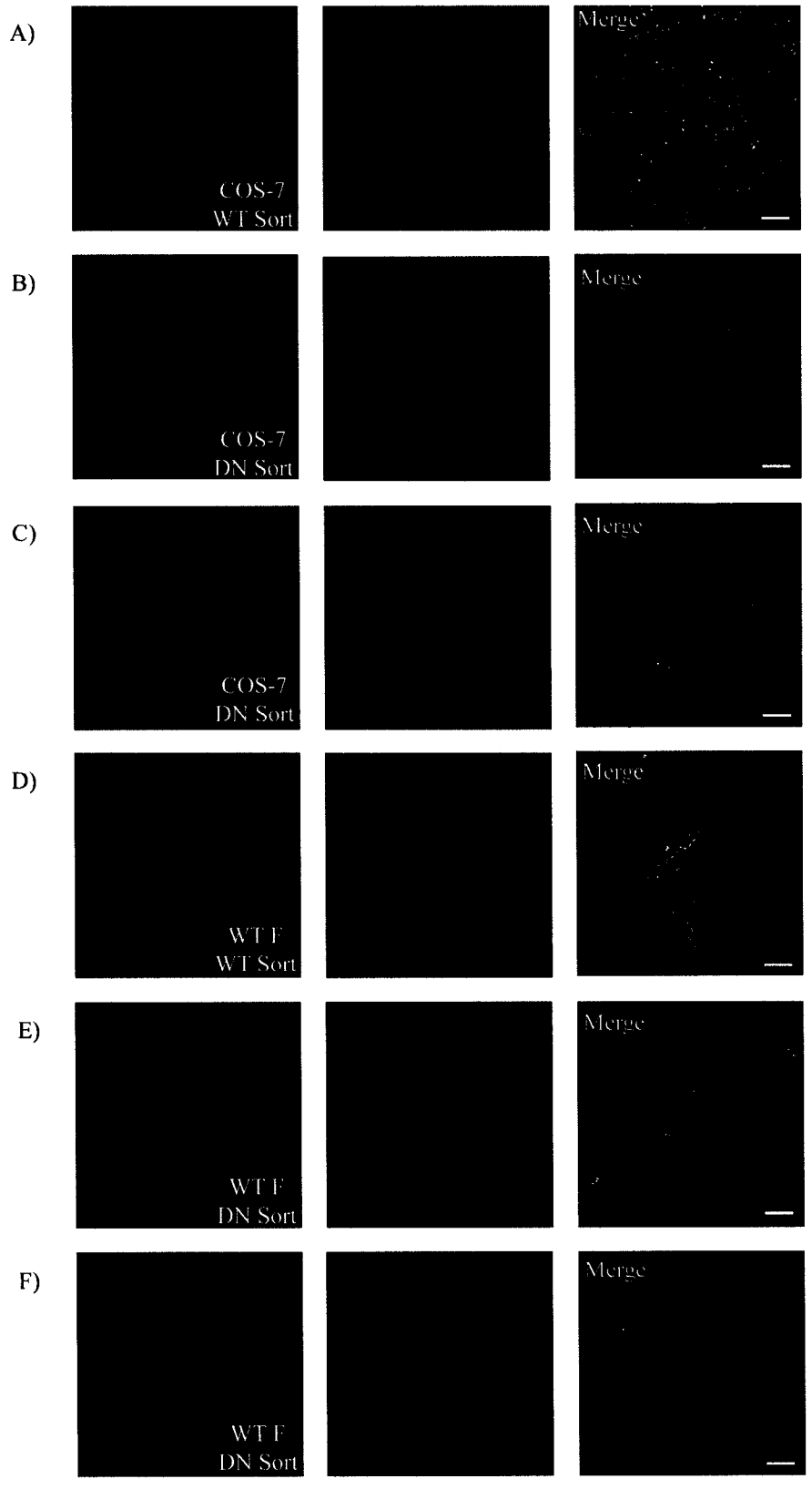
A)
COS-7
WT Sort
Merge
B)
COS-7
DN Sort
Merge
C)
COS-7
DN Sort
Merge
D)
WT F
WT Sort
Merge
E)
WT F
DN Sort
Merge
F)
WT F
DN Sort
Merge

Figure 12. Efficiency of Sortilin shRNA Knockdown. COS-7 cells were stably transfected with either mock or sortilin targeted shRNA. To assess the efficiency of the knockdown of sortilin, RT-PCR was performed subsequent to RNA extraction. The RT-PCR products were resolved on a 1.5% (w/v) agarose gel containing 0.5% ethidium bromide. Mock transfected cells possessed sortilin mRNA, whereas those expressing sortilin shRNA did not (A). Both mock transfected and sortilin shRNA expressing cells contained comparable levels of β-actin (A). The efficiency of knockdown of sortilin was also examined by Western blotting (B). Cells transfected with mock siRNA retained sortilin expression, but those with sortilin siRNA did not (B).

A)

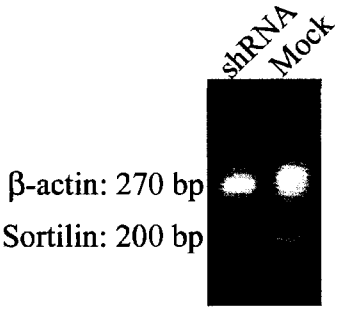
shRNA
Mock
β-actin: 270 bp
Sortilin: 200 bp

B)

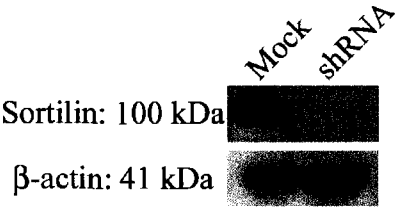
Mock
shRNA
Sortilin: 100 kDa
β-actin: 41 kDa

Figure 13. The Effect of Sortilin Inhibition on Prosaposin and Cathepsin B. Confocal Microscopy Analysis. COS-7 cells stably expressing sortilin specific shRNA (C and D) were compared to mock transfected cells (A and C) for the distribution of prosaposin (A and B) and cathepsin B (C and D). The distribution of prosaposin and cathepsin B (green) was compared to LAMP-1 (red). In mock transfected cells, both prosaposin and cathepsin B staining was present in the perinuclear region and punctate lysosomal structures labeled with LAMP-1 (A and C). In cells expressing sortilin shRNA, prosaposin staining was abolished (B), but cathepsin B staining was unaffected (D). Nuclei are stained with Hoechst 33342 and are seen in blue. The scale bars shown equal 8 μm and apply to all panels.

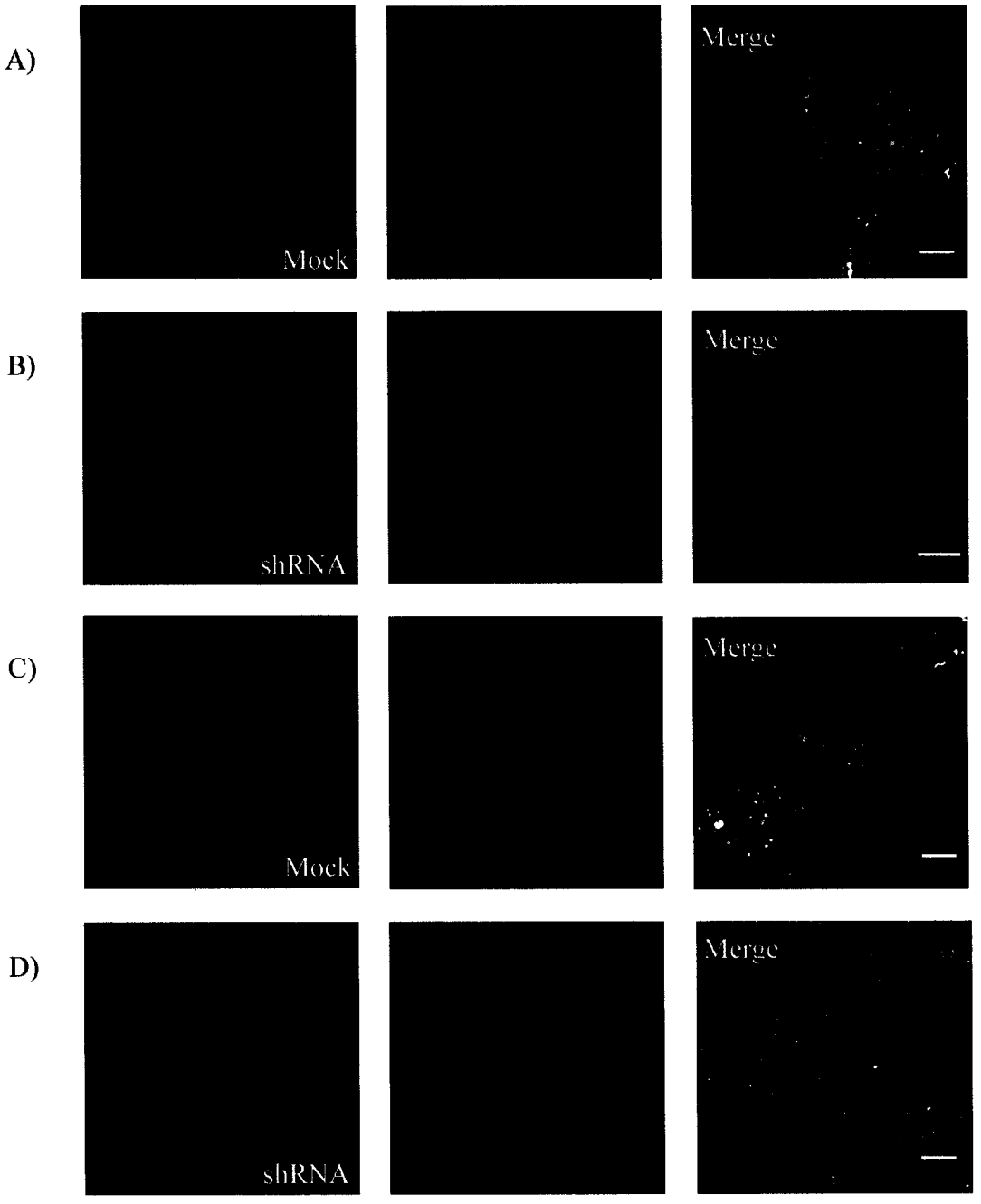
A)
Mock
Merge
B)
shRNA
Merge
C)
Mock
Merge
D)
shRNA
Merge

Figure 14. The Effect of Sortilin Inhibition on Prosaposin and Cathepsin B. Pulse-Chase Analysis. Mock transfected COS-7 cells or cells stably expressing sortilin shRNA were examined for secretion of prosaposin and cathepsin B by pulse-chase. Cells were labeled with [^{35}S] methionine for 30 minutes and chased for 0, 30, 60, and 90 minutes. Both the cells and the culture media were collected and utilized for immunoprecipitation with anti-prosaposin (A) and anti-cathepsin B (B). Prosaposin (A) increased in quantity in the culture media at earlier time points in sortilin shRNA expressing cells, whereas cathepsin B (B) secretion was unchanged. Quantification of the amount of protein secreted is shown for each experiment.

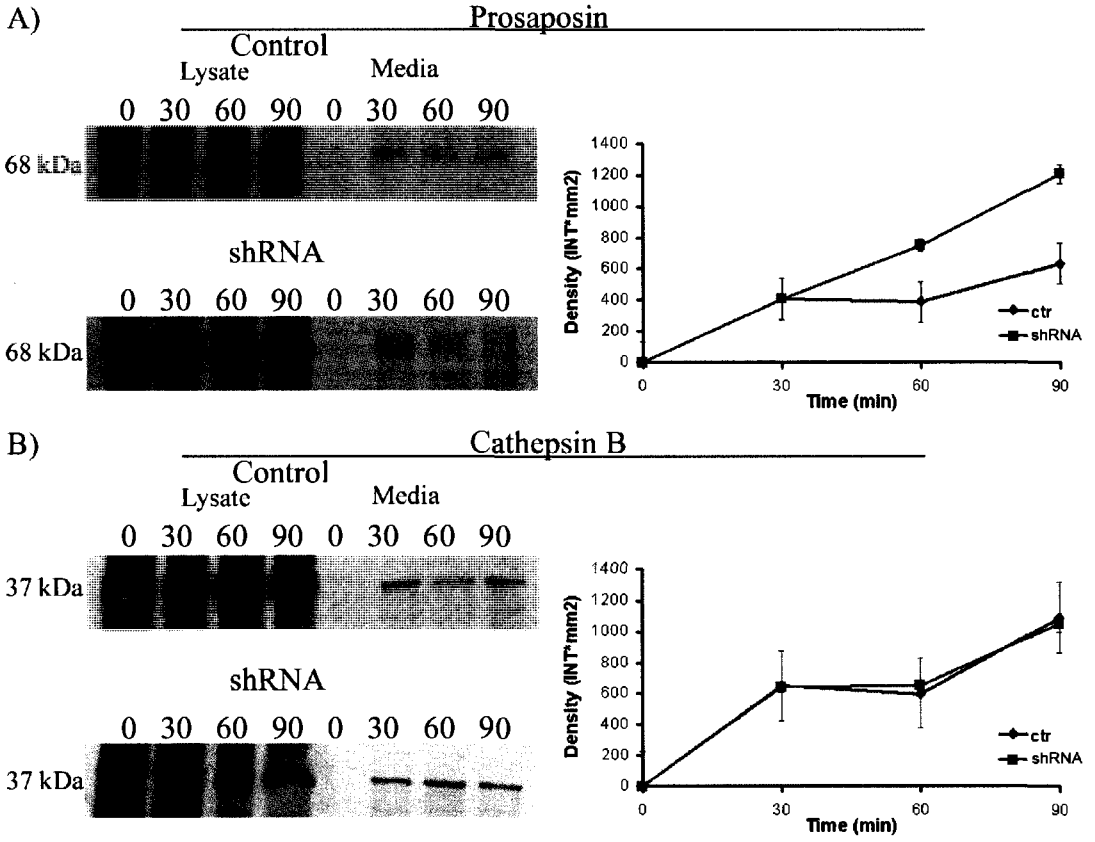
A)
Prosaposin
Control
Lysate
Media
0 30 60 90 0 30 60 90
68 kDa
shRNA
0 30 60 90 0 30 60 90
68 kDa
Density (INT*mm2)
1400
1200
1000
800
600
400
200
0
0
30
60
90
Time (min)
ctr
shRNA
B)
Cathepsin B
Control
Lysate
Media
0 30 60 90 0 30 60 90
37 kDa
shRNA
0 30 60 90 0 30 60 90
37 kDa
Density (INT*mm2)
1400
1200
1000
800
600
400
200
0
0
30
60
90
Time (min)
ctr
shRNA

Figure 15. The Effect of Sortilin Inhibition on Cathepsin D. COS-7 cells stably expressing sortilin specific shRNA (B) were compared to mock transfected cells (A) by confocal microscopy for the distribution of cathepsin D. Cathepsin D (green) staining was compared to LAMP-1 (red). In mock transfected cells (A) and shRNA expressing cells (B); anti-cathepsin D antibody dyed punctate lysosomal structures that were labeled with LAMP-1. Nuclei are stained with Hoechst 33342 and are seen in blue. The scale bars shown equal 8 μm and apply to all panels. Similar cells were examined by pulse-chase analysis for secretion of cathepsin D (C). Cells were labeled with [^{35}S] methionine for 30 minutes and chased for 0, 30, 60, and 90 minutes. The cells and the culture media were collected and incubated with anti-cathepsin D antibody bound to protein A Sepharose beads for immunoprecipitation (C). Cathepsin D secretion was observed here to be unchanged in shRNA expressing cells when contrasted with mock transfected cells (C). Quantification of the amount of protein secreted is shown.

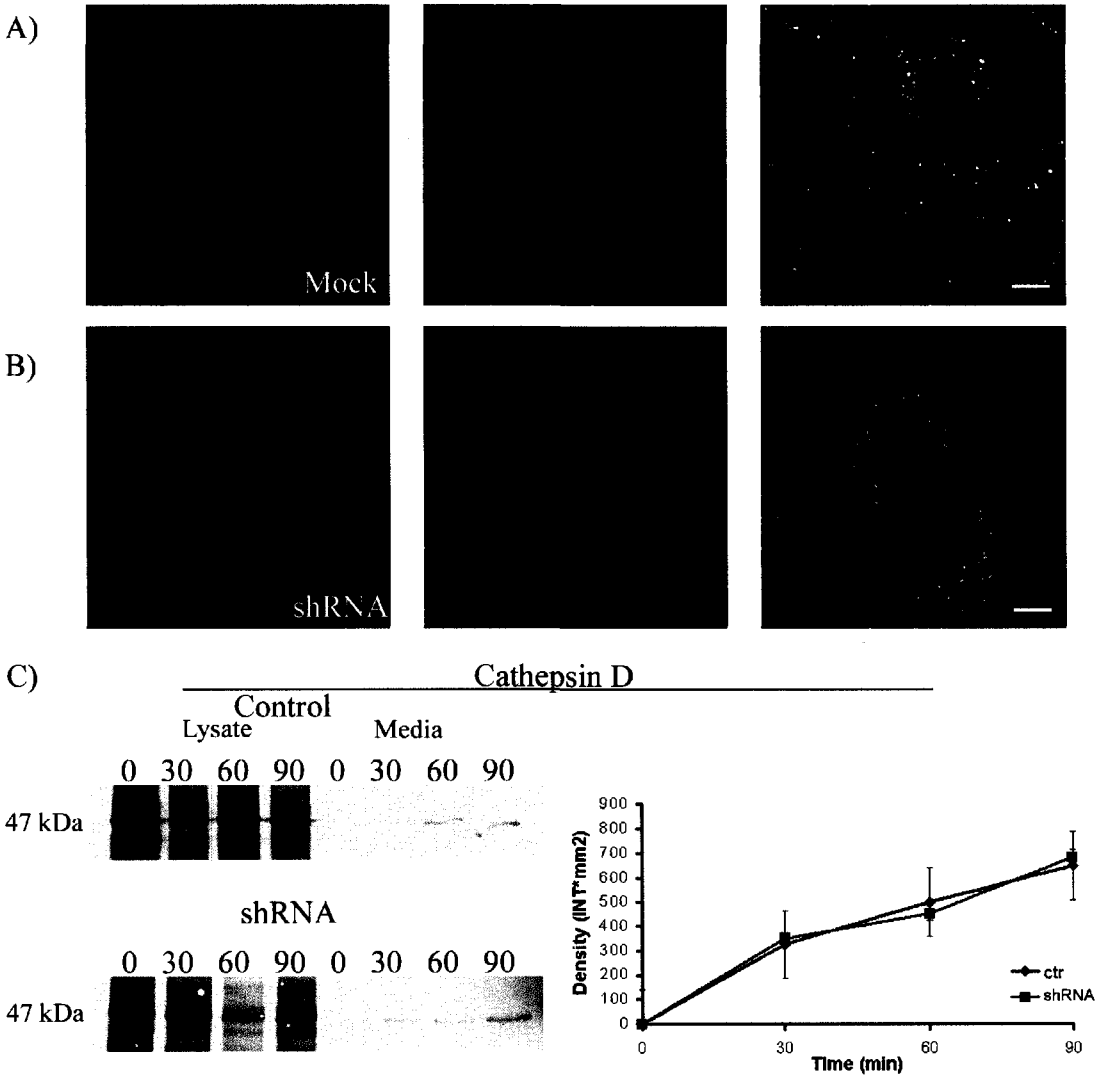
A)
Mock
B)
shRNA
C)
Cathepsin D
Control
Lysate
Media
0 30 60 90 0 30 60 90
47 kDa
shRNA
0 30 60 90 0 30 60 90
47 kDa
Density (INT*mm2)
900
800
700
600
500
400
300
200
100
0
0
30
60
90
Time (min)
ctr
shRNA

Figure 16. The Effect of Sortilin Inhibition on Cathepsin H. COS-7 cells stably expressing sortilin specific shRNA (A) were compared by confocal microscopy to mock transfected cells (B) for the distribution of cathepsin H. The distribution of cathepsin H (green) was compared to LAMP-1 (red). In mock transfected cells, cathepsin H staining was present in punctate lysosomal structures labeled with LAMP-1 (A). However, in cells expressing sortilin shRNA, cathepsin H staining was abrogated (B). Nuclei are stained with Hoechst 33342 and are seen in blue. The scale bars shown equal 8 μm and apply to all panels. Similarly, mock transfected COS-7 cells or cells stably expressing sortilin shRNA were examined for secretion of cathepsin H by pulse-chase (C). Cells were labeled with [^{35}S] methionine for 30 minutes and chased for 0, 30, 60, and 90 minutes. Both the cells and the culture media were collected and utilized for immunoprecipitation with anti-cathepsin H antibody (C). The quantity of cathepsin H secreted into the culture medium was greater and occurred earlier in shRNA expressing cells as compared to mock transfected cells. Quantification of the amount of protein secreted is shown.

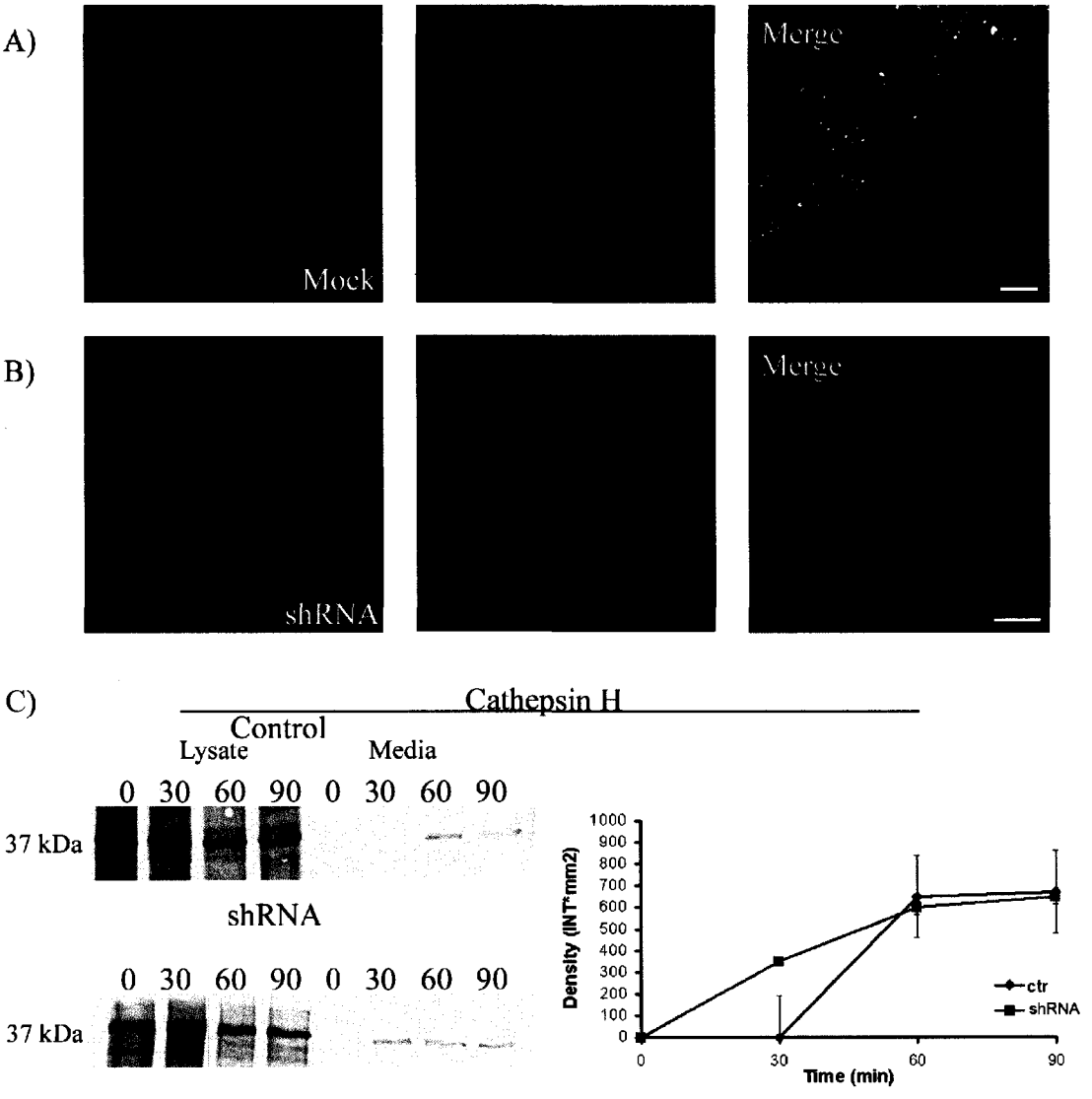
A)
Merge
Mock
B)
Merge
shRNA
C)
Cathepsin H
Control
Lysate
Media
0 30 60 90 0 30 60 90
37 kDa
shRNA
0 30 60 90 0 30 60 90
37 kDa
Density (INT*mm2)
1000
900
800
700
600
500
400
300
200
100
0
0
30
60
90
Time (min)
ctr
shRNA

Figure 17. The Effect of Sortilin Inhibition on Cathepsin K. COS-7 cells stably expressing sortilin specific shRNA (B) were compared to mock transfected cells (A) by confocal microscopy for the distribution of cathepsin K. The distribution of cathepsin K (green) was compared to LAMP-1 (red). In both mock transfected cells (A) and shRNA expressing cells (B), cathepsin K staining was present in punctate lysosomal structures labeled with LAMP-1. Nuclei are stained with Hoechst 33342 and are seen in blue. The scale bars shown equal 8 μm and apply to all panels. Similar cells were examined by pulse-chase analysis for secretion of cathepsin K (C). Cells were labeled with [^{35}S] methionine for 30 minutes and chased for 0, 30, 60, and 90 minutes. The cells and the culture media were collected and utilized for immunoprecipitation with anti-cathepsin K antibody (C). Cathepsin K secretion was unchanged in shRNA expressing cells as compared to mock transfected cells (C). Quantification of the amount of protein secreted is shown.

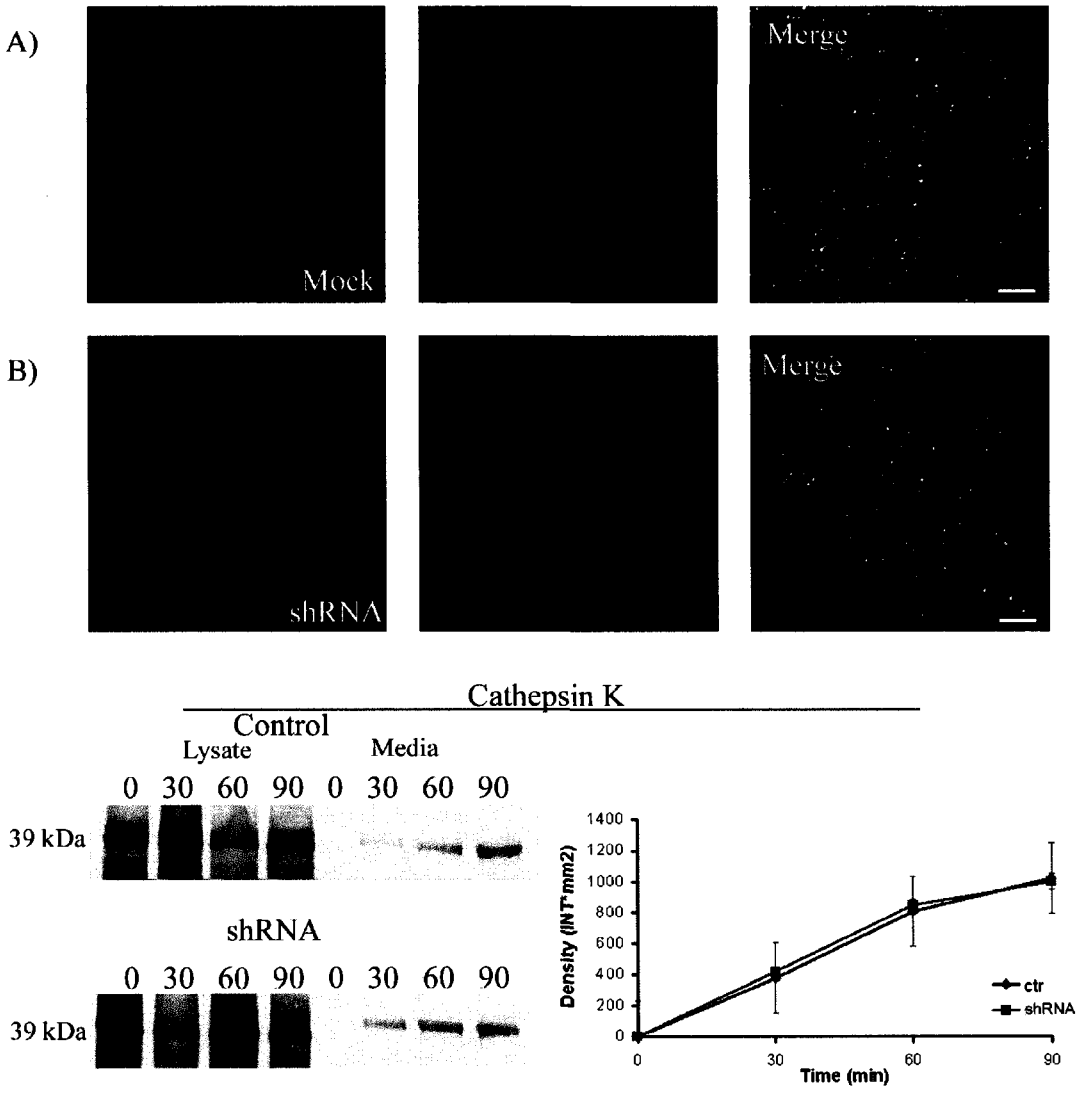
A)
Mock
Merge
B)
shRNA
Merge
Cathepsin K
Control
Lysate
Media
0 30 60 90 0 30 60 90
39 kDa
shRNA
0 30 60 90 0 30 60 90
39 kDa
Density (INT*mm2)
1400
1200
1000
800
600
400
200
0
0
30
60
90
Time (min)
ctr
shRNA

Figure 18. The Effect of Sortilin Inhibition on Cathepsin L. COS-7 cells stably expressing sortilin shRNA (B) were compared to mock transfected cells (A) by confocal microscopy for the distribution of cathepsin L. Cathepsin L (green) staining was compared to anti-LAMP-1 staining (red). In both mock transfected cells (A) and shRNA cells (B), cathepsin L was present in LAMP-1 positive structures. Nuclei are stained with Hoechst 33342 and are seen in blue. The scale bars shown equal 8 μm and apply to all panels. Similar cells were examined by pulse-chase analysis for secretion of cathepsin L (C). Cells were labeled with [^{35}S] methionine for 30 minutes and chased for 0, 30, 60, and 90 minutes. The cells and the culture media were collected and utilized for immunoprecipitation with anti-cathepsin L antibody (C). Cathepsin L secretion was unchanged in shRNA expressing cells relative to mock transfected cells (C). Quantification of the amount of protein secreted is shown.

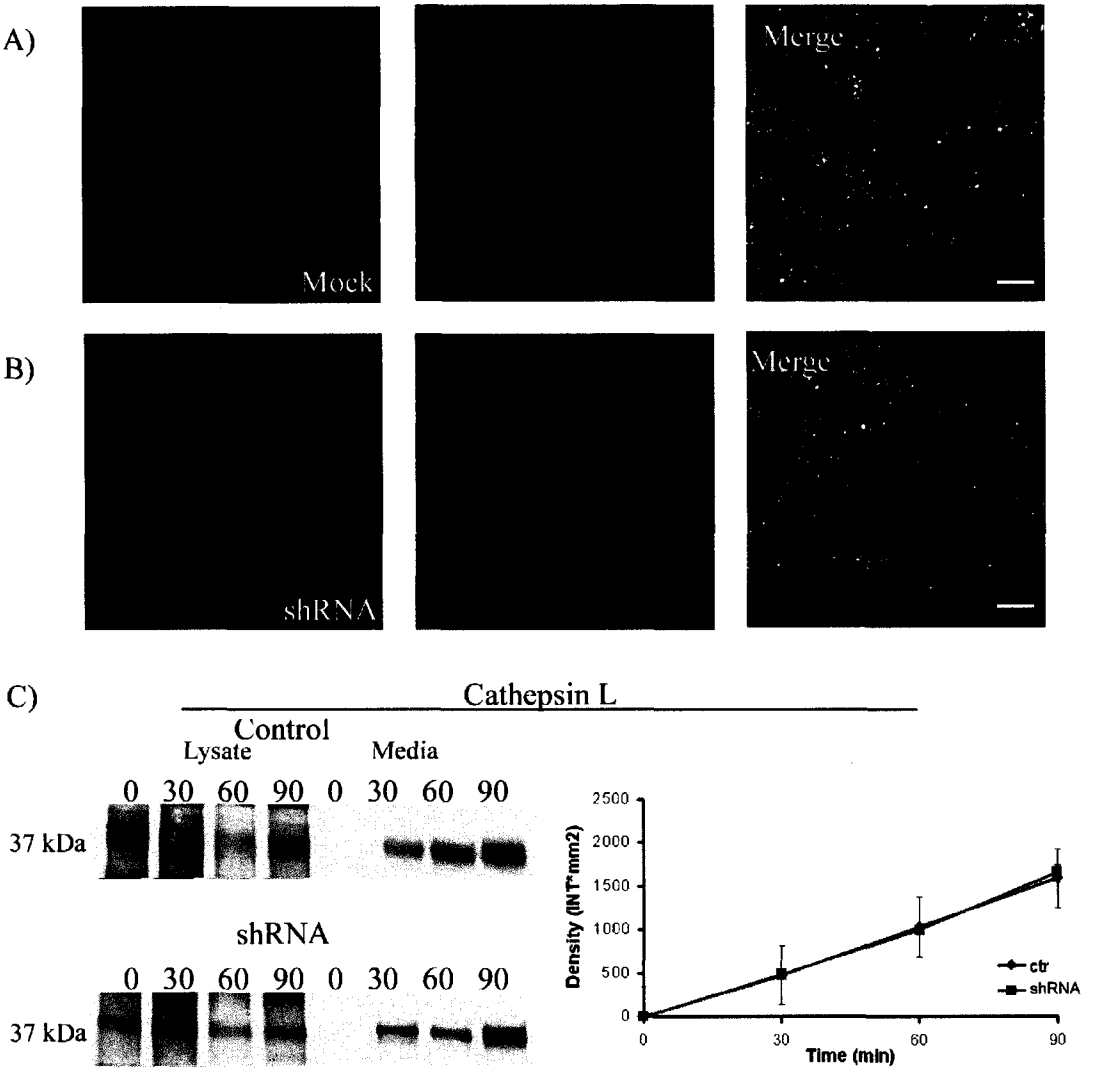
A)
Mock
Merge
B)
shRNA
Merge
C)
Cathepsin L
Control
Lysate
Media
0 30 60 90 0 30 60 90
37 kDa
shRNA
0 30 60 90 0 30 60 90
37 kDa
Density (INT*mm2)
2500
2000
1500
1000
500
0
0
30
60
90
Time (min)
ctr
shRNA

Figure 19. Lysosomal Targeting of Prosaposin in the Absence of Sortilin and the M6PR Pathways. Untransfected ICD fibroblasts were compared to ICD fibroblasts transfected with the truncated sortilin-myc construct. All cells were stained with LAMP-1 or myc (red), as well as with anti-prosaposin (green). Prosaposin (green) was distributed in punctate structures stained with LAMP-1 (red) of untransfected cells (A), but absent from these same structures in cells expressing truncated sortilin-myc (B and C). In transfected cells, prosaposin colocalized with anti-myc (red) (B), but not with LAMP-1 (red) (C). Nuclei are stained with Hoechst 33342 and are seen in blue. The scale bars shown equal 8 μm and apply to all panels.

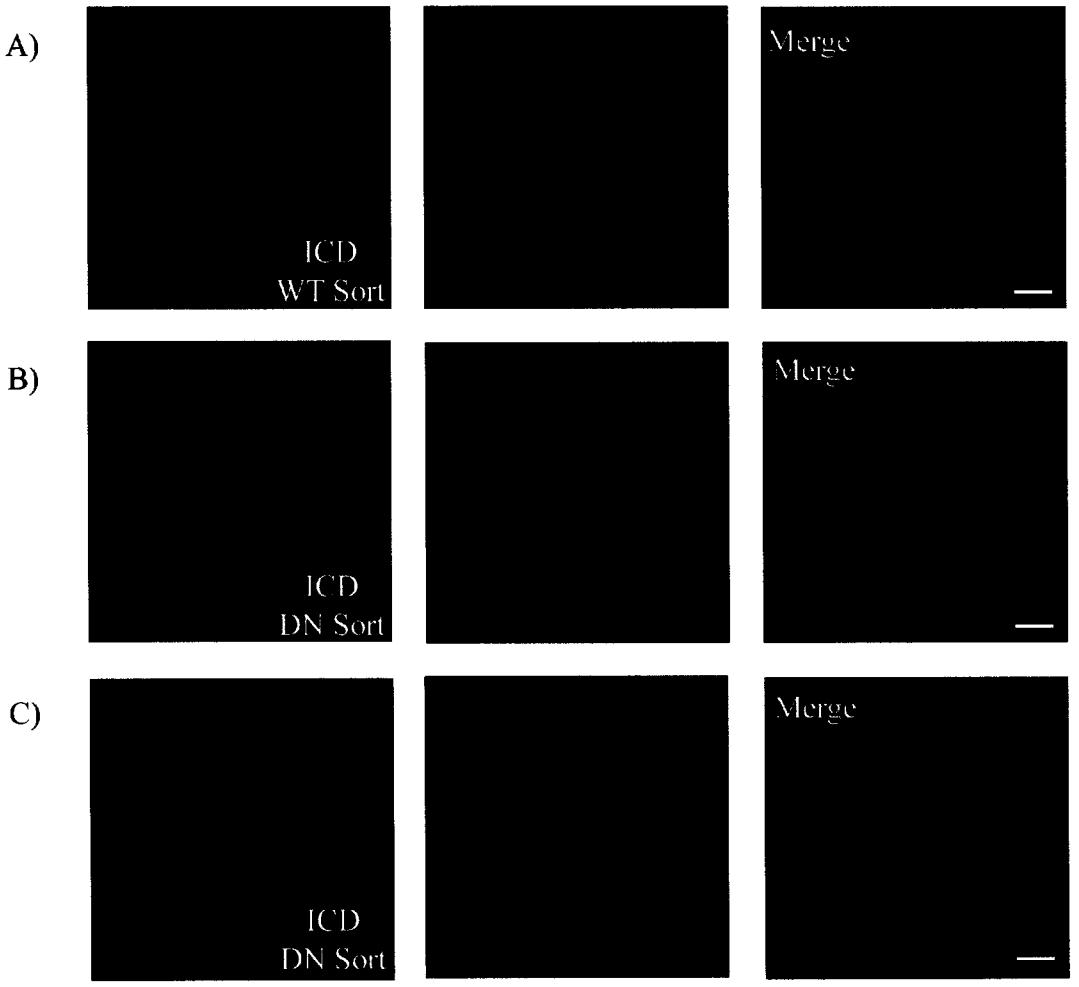
A)
ICD
WT Sort
Merge
B)
ICD
DN Sort
Merge
C)
ICD
DN Sort
Merge

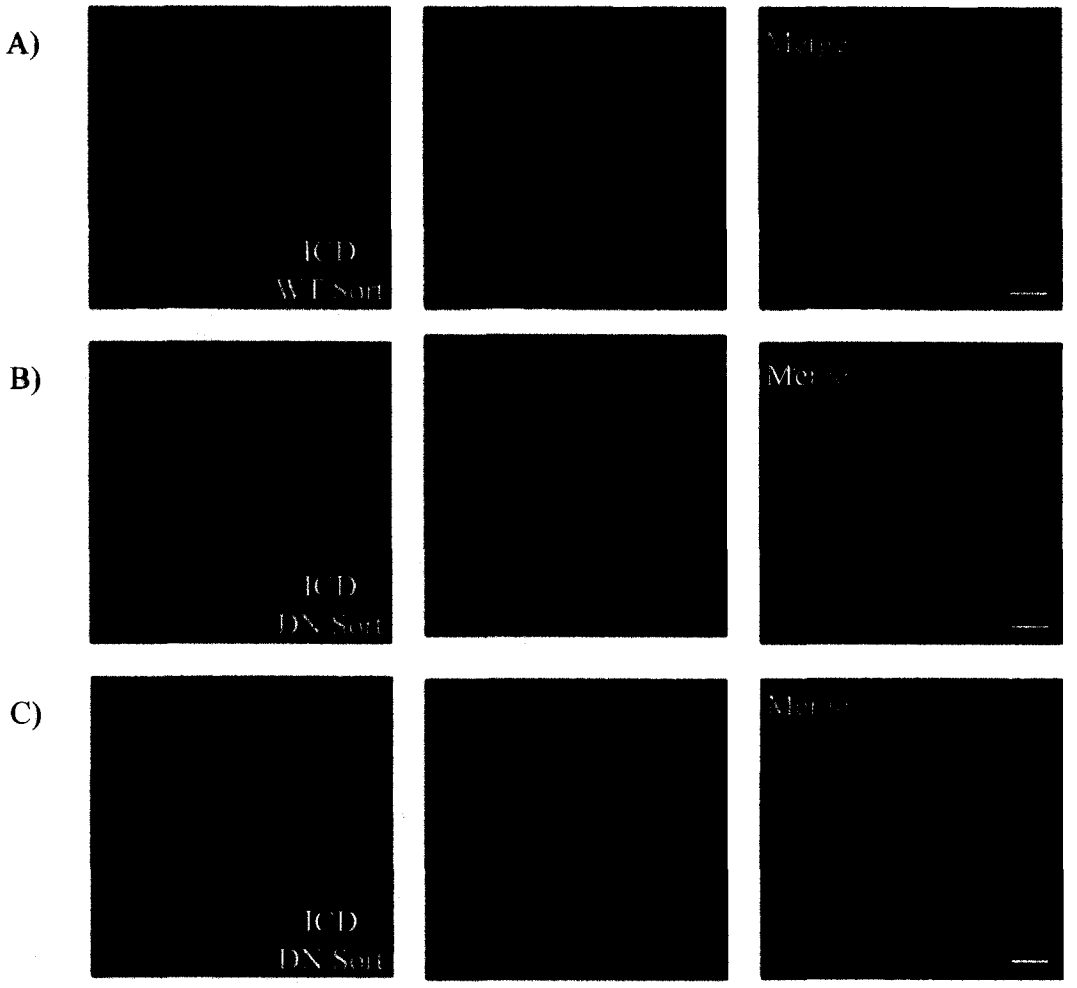
A)
ICD
WT Sort
B)
ICD
DN Sort
C)
ICD
DN Sort

Figure 20. Lysosomal Targeting of Cathepsin B in the Absence of Sortilin and the M6PR Pathways. Untransfected ICD fibroblasts were compared to ICD fibroblasts transfected with truncated sortilin-myc. The cells were stained with cathepsin B (green) and anti-myc (B) or anti-LAMP-1 (red) antibodies (A and C). Untransfected (A) or transfected cells (B and C) stained with anti-cathepsin B antibody showed no co-localization of cathepsin B with LAMP-1 in lysosomal structures (A and C). Nuclei are stained with Hoechst 33342 and are seen in blue. The scale bars shown equal 8 μm and apply to all panels.

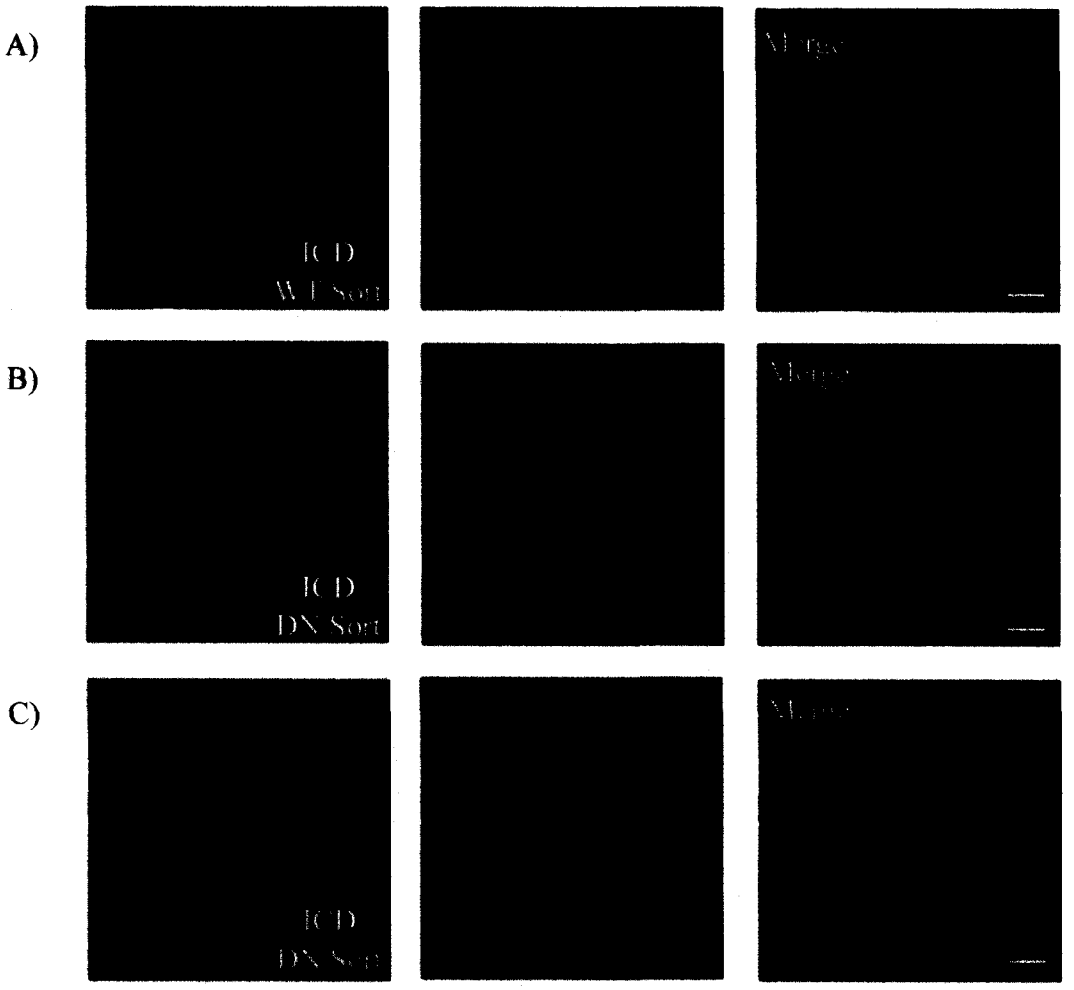
A)
B)
C)

Figure 21. Lysosomal Targeting of Cathepsin K in the Absence of Sortilin and the M6PR Pathways. Untransfected ICD fibroblasts were compared to ICD fibroblasts transfected with truncated sortilin-myc. The cells were stained with cathepsin K (green) and anti-myc (B) or anti-LAMP-1 (red) antibodies (A and C). Untransfected (A) and transfected cells (B and C) stained with anti-cathepsin K antibody showed colocalization (yellow) of cathepsin K with LAMP-1 in lysosomal granules (A and C). Nuclei are stained with Hoechst 33342 and are seen in blue. The scale bars shown equal 8 μm and apply to all panels.

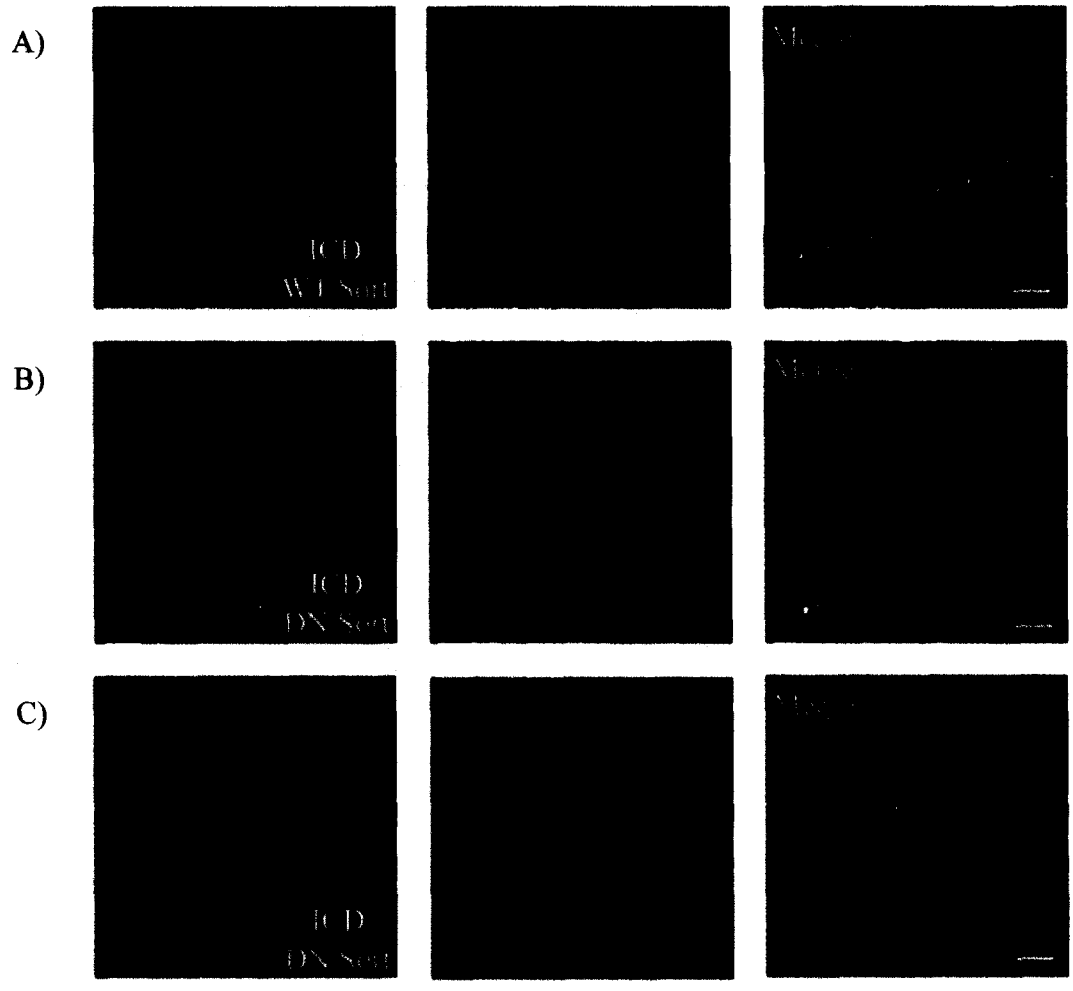
A)
B)
C)

Figure 22. Lysosomal Targeting of Cathepsin L in the Absence of Sortilin and the M6PR Pathways. Untransfected ICD fibroblasts were compared to ICD fibroblasts transfected with truncated sortilin-myc. The cells were labeled with anti-cathepsin L antibody (green) and anti-myc (B) or anti-LAMP-1 (red) antibodies (A and C). Untransfected (A) and truncated sortilin-myc transfected cells (B and C) both had colocalization (yellow) of cathepsin L with LAMP-1 in lysosomal structures (A and C). Nuclei are stained with Hoechst 33342 and are seen in blue. The scale bars shown equal 8 μm and apply to all panels.

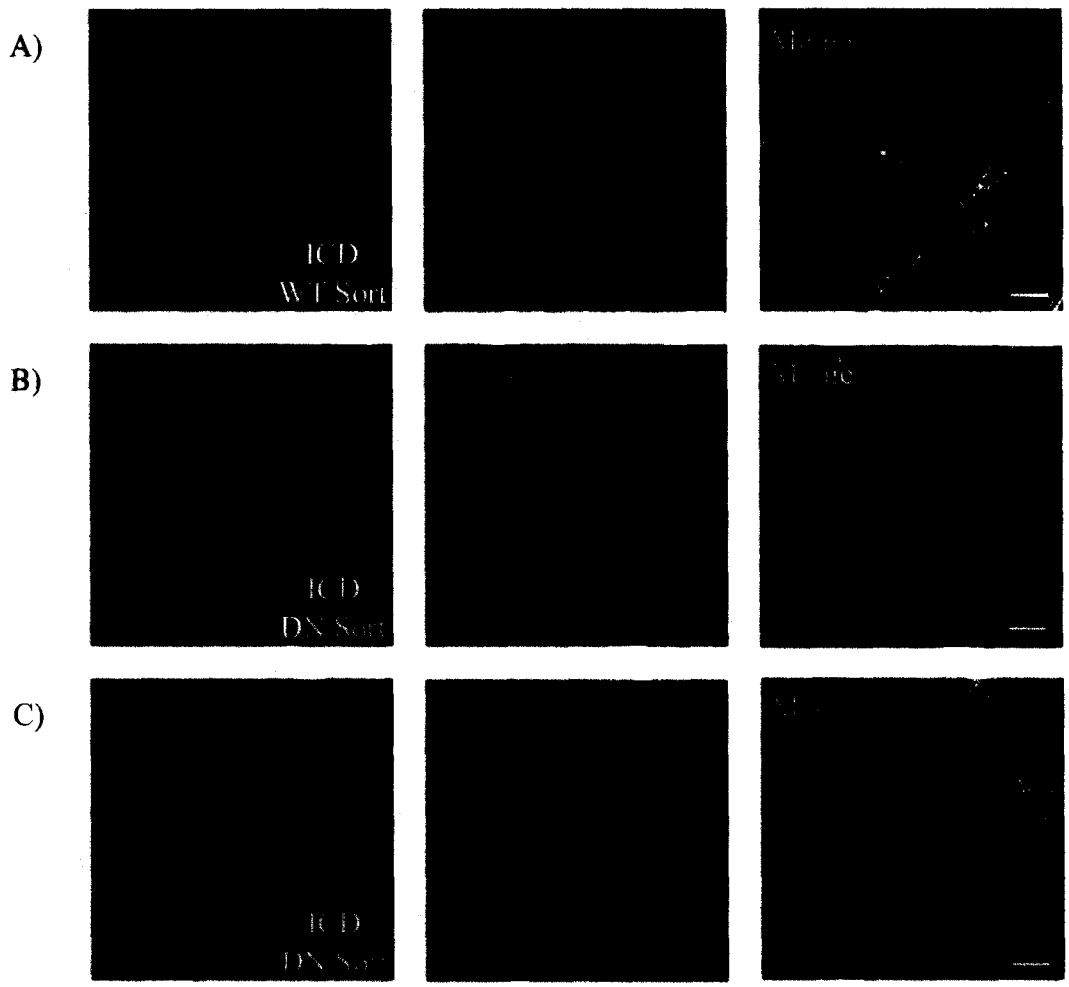
A)
ICD
WT Sort
B)
ICD
C)
ICD

Figure 23. Lysosomal Targeting of Cathepsin D in the Absence of Sortilin and the M6PR Pathways. Untransfected ICD fibroblasts were compared to ICD fibroblasts transfected with the truncated sortilin-myc construct. All cells were stained with LAMP-1 (A and C) or myc (B) (red) as well as with anti-cathepsin D (green). Cathepsin D was found to localize to LAMP-1 positive granules in untransfected cells (A), but this punctate staining was abolished in truncated sortilin transfected cells (B and C). In transfected cells, cathepsin D colocalized (yellow) with anti-myc in the perinuclear Golgi region (B). Nuclei are stained with Hoechst 33342 and are seen in blue. The scale bars shown equal 8 μm and apply to all panels.

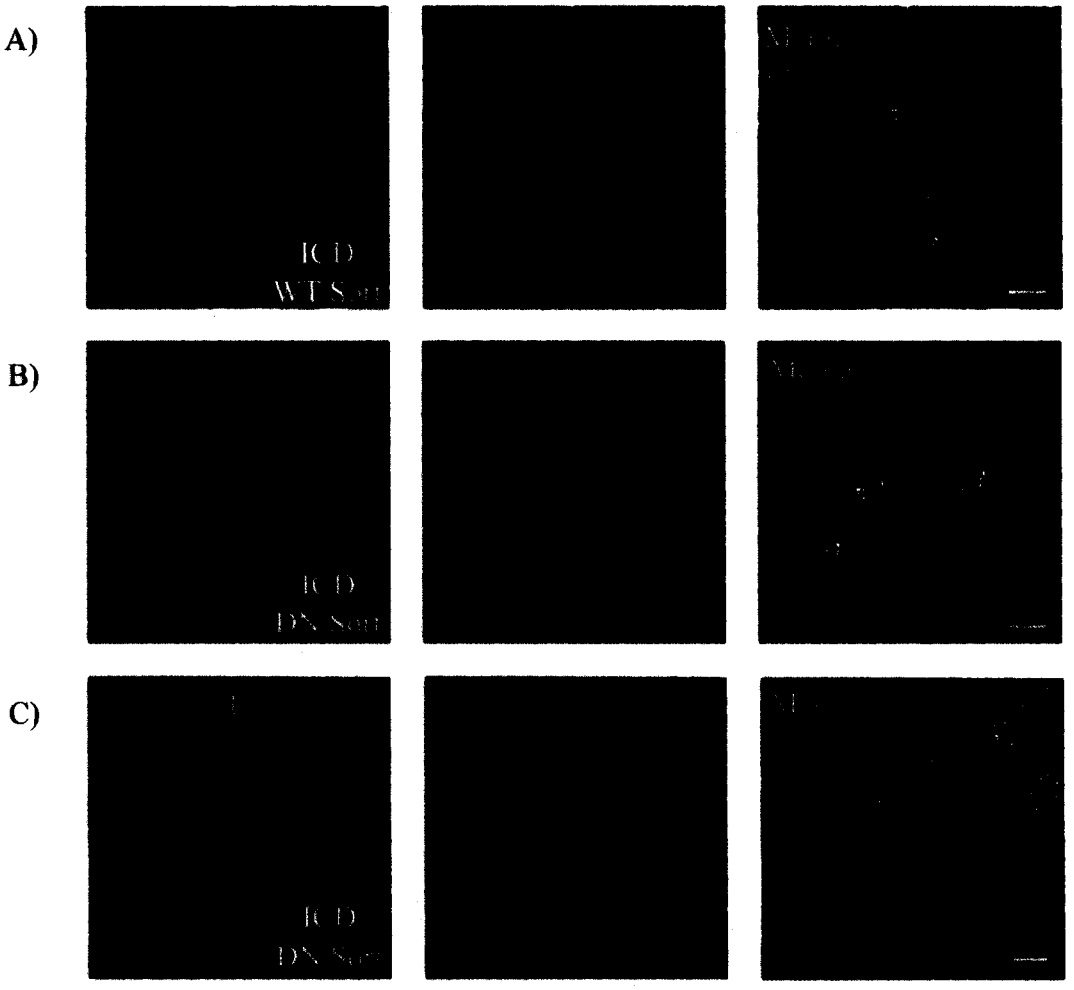
A)
B)
C)

Figure 24. Lysosomal Targeting of Cathepsin H in the Absence of Sortilin and the M6PR Pathways. Untransfected ICD fibroblasts were compared to ICD fibroblasts transfected with the truncated sortilin-myc construct. All cells were stained with LAMP-1 or myc (red) as well as with anti-cathepsin H (green). Cathepsin H (green) was present in LAMP-1 (red) labeled structures of untransfected cells (A). Transfection with truncated sortilin-myc completely inhibited the granular localization of cathepsin H (B and C) that was observed in untransfected cells (A). In transfected cells, cathepsin H colocalized with anti-myc (red) (B), but not with LAMP-1 (red) (C). Nuclei are stained with Hoechst 33342 and are seen in blue. The scale bars shown equal 8 μm and apply to all panels.

A)

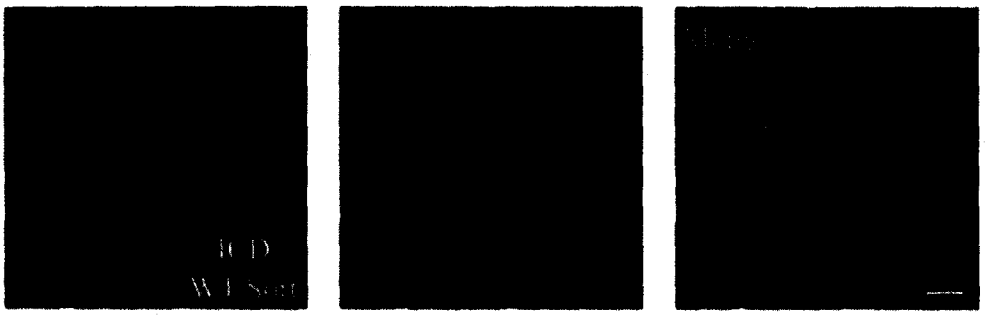

B)

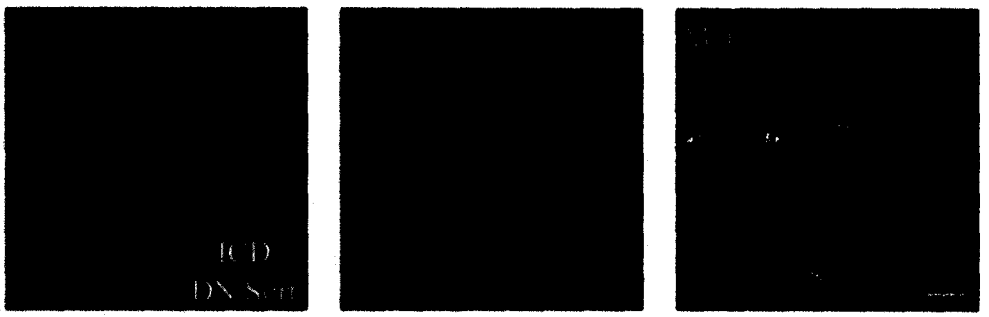

C)

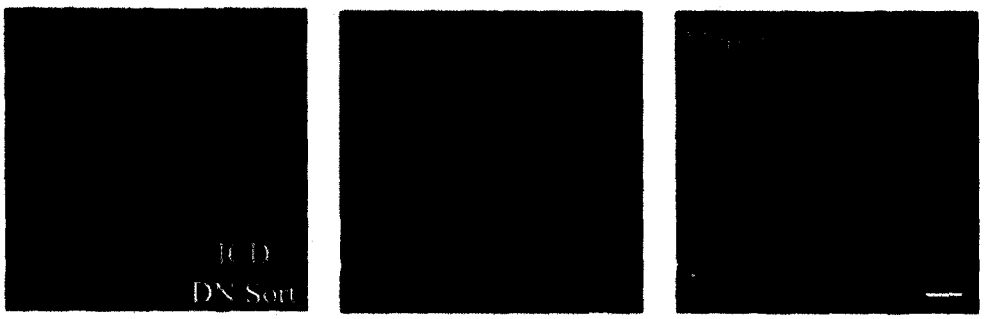

Figure 25. Distribution of Sortilin and its Ligands in Detergent Resistant Membrane (DRM) Fractions. DRMs were isolated by fractionation on a sucrose gradient (A). Fractions 1-8 (10% - 30% sucrose gradient) are insoluble detergent membrane fractions. Generally, lipid rafts are found among fractions 3-6 and concentrated in fractions 4-5. Fraction 9 is the soluble protein fraction and fraction 11 is the pellet containing insoluble cell debris and cytoskeletal elements (A). Immunoblotting of the fractions with anti-flotillin-1 (47 kDa) revealed that this protein is found in fractions 4 and 5 (B). Bands were also detected in lipid raft fractions 3-6 with anti-sortilin (100 kDa), anti-prosaposin (68 kDa), anti-cathepsin D (47 kDa), and anti-cathepsin H (37 kDa) antibodies (B). The anti-M6PR (300 kDa) and anti-cathepsin B (37 kDa), antibodies identified bands in fraction 9 only (B).

A)

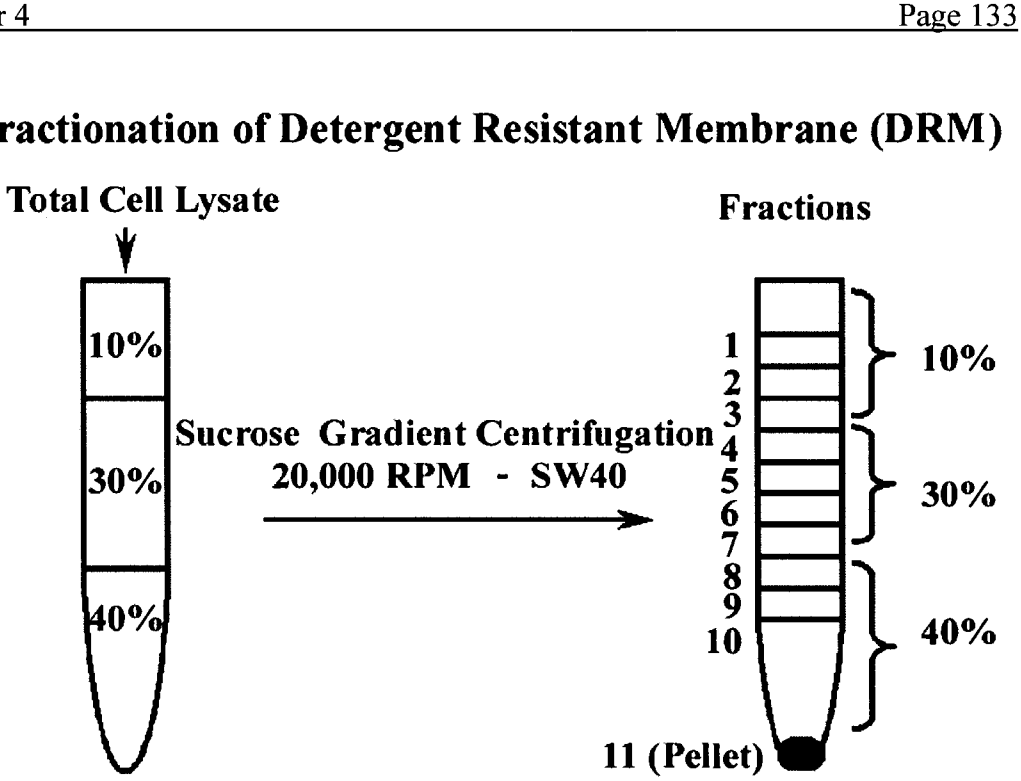
Fractionation of Detergent Resistant Membrane (DRM)
Total Cell Lysate
Fractions
10%
30%
40%
Sucrose Gradient Centrifugation
20,000 RPM - SW40
1
2
3
4
5
6
7
8
9
10
11 (Pellet)
10%
30%
40%

B)

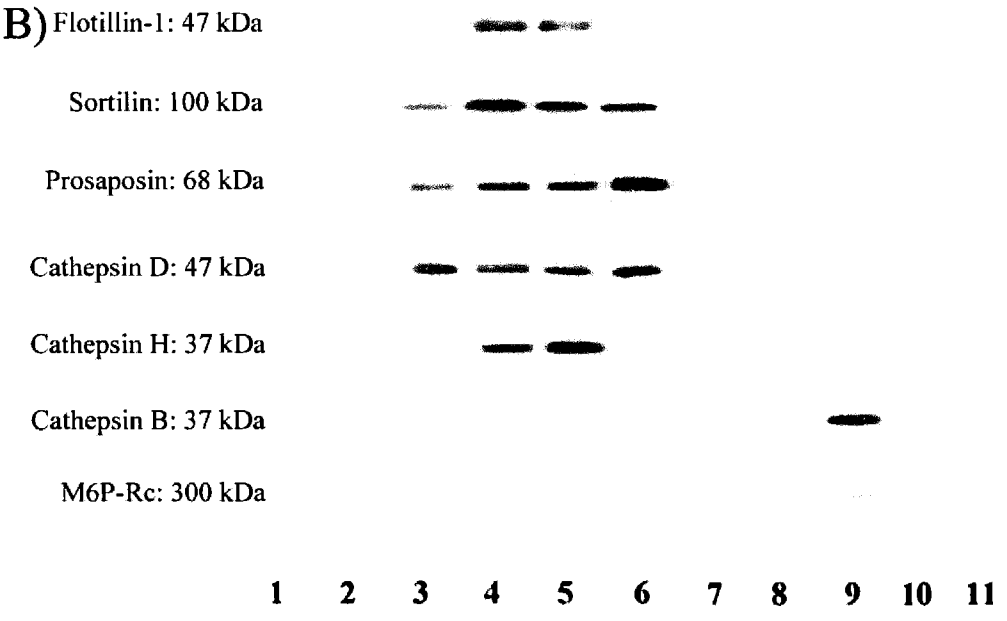
Flotillin-1: 47 kDa
Sortilin: 100 kDa
Prosaposin: 68 kDa
Cathepsin D: 47 kDa
Cathepsin H: 37 kDa
Cathepsin B: 37 kDa
M6P-Rc: 300 kDa
1 2 3 4 5 6 7 8 9 10 11

Figure 26. Distribution of Chimeric Prosaposin Constructs in DRM Fractions. To analyze the distribution of chimeric prosaposin constructs to DRMs, fractionation was done using sucrose gradients. COS-7 cells transfected with pcDNA3.1 (A), Albumin-D-domain-C-terminus (B), Albumin-D-domain (C), or Albumin-C-terminus (D) myc-tagged chimeric constructs were collected, homogenized, and fractionated. The fractions collected were resolved on 10 % acrylamide gels and blotted with anti-sortilin, anti-myc, and anti-flotillin-1 antibodies. Fractions from cells transfected with pcDNA3.1 showed bands for sortilin at 100 kDa in fractions 8-11, flotillin-1 at 47 kDa in fractions 5 and 6, but no bands with anti-myc antibody (A). The Albumin-D-domain-C-terminus construct was detected as 80 kDa bands in fractions 6-11 along with sortilin (B) in fractions 7-11. The Albumin-D-domain chimeric construct was (C) present in fractions 9, 10, and 11 whereas the Albumin-C-terminus construct was detected by anti-myc antibody as a 70 kDa band in fractions 6-11 (D). Fractions from cells expressing the Albumin-D-domain or Albumin-C-terminus constructs had bands for sortilin present in fractions 8 to 11 and flotillin-1 in fractions 5 and 6 (C and D).

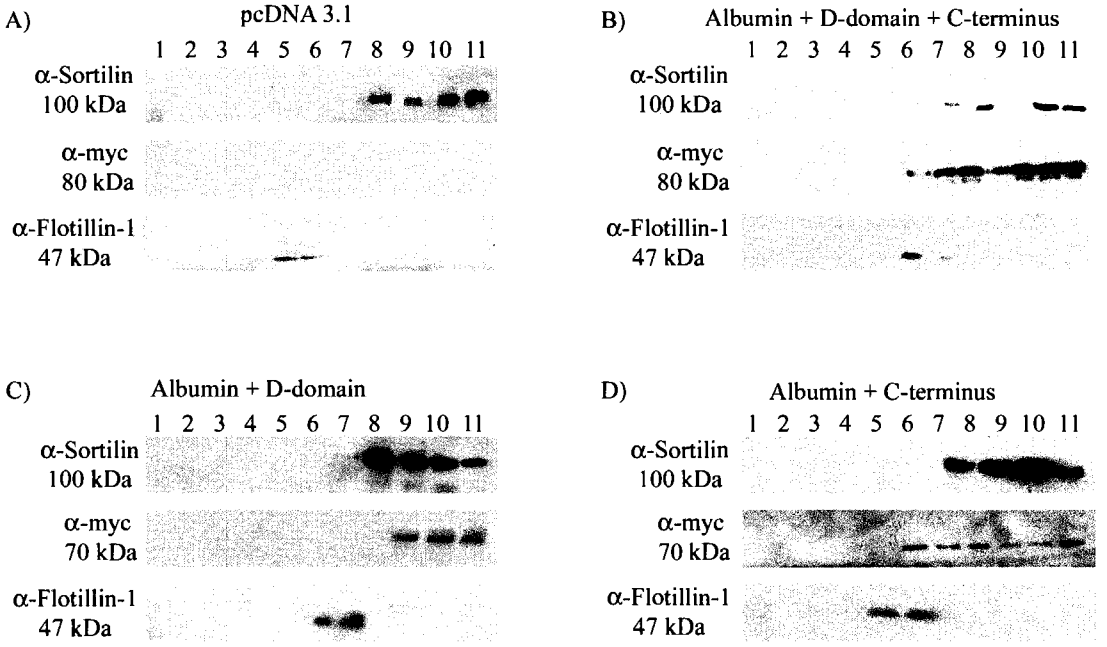
A)
pcDNA 3.1
1 2 3 4 5 6 7 8 9 10 11
α-Sortilin
100 kDa
α-myc
80 kDa
α-Flotillin-1
47 kDa
B)
Albumin + D-domain + C-terminus
1 2 3 4 5 6 7 8 9 10 11
α-Sortilin
100 kDa
α-myc
80 kDa
α-Flotillin-1
47 kDa
C)
Albumin + D-domain
1 2 3 4 5 6 7 8 9 10 11
α-Sortilin
100 kDa
α-myc
70 kDa
α-Flotillin-1
47 kDa
D)
Albumin + C-terminus
1 2 3 4 5 6 7 8 9 10 11
α-Sortilin
100 kDa
α-myc
70 kDa
α-Flotillin-1
47 kDa

Figure 27. Distribution of E463K and E491K Prosaposin Mutant Constructs in DRM Fractions. To analyze the distribution of the E463K and E491K mutant chimeric constructs to DRMs, fractionation was done using sucrose gradients. COS-7 cells transfected with either the E463K (A) or E491K (B) constructs were collected, homogenized, and fractionated. The fractions collected were resolved on 10 % acrylamide gels and blotted with anti-sortilin, anti-myc, and anti-flotillin-1 antibodies. Both mutant constructs produced bands of 80 kDa with E463K in fractions 5-11 and E491K in fractions 6-11 (A and B). Sortilin was found at 100 kDa in similar fractions as the E463K (A) and E491K (B) mutant constructs. Flotillin-1 was observed in fractions 3 and 4 (A and B). An un-mutated chimeric construct containing both the D-domain and C-terminus of prosaposin was found only in fractions 9-11 when sortilin expression was abrogated using shRNA (C). Flotillin-1 distribution was unaffected by sortilin shRNA as is seen by bands present in fractions 3 and 4 (C).

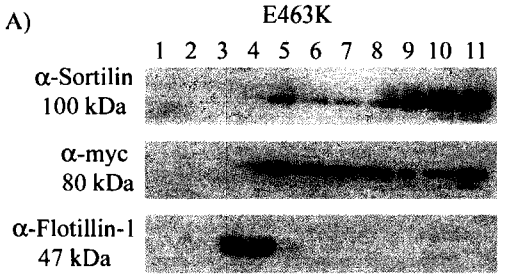
A)
E463K
1 2 3 4 5 6 7 8 9 10 11
α-Sortilin
100 kDa
α-myc
80 kDa
α-Flotillin-1
47 kDa

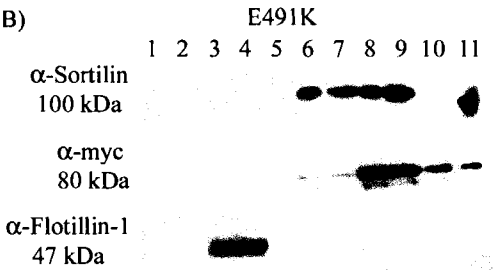
B)
E491K
1 2 3 4 5 6 7 8 9 10 11
α-Sortilin
100 kDa
α-myc
80 kDa
α-Flotillin-1
47 kDa

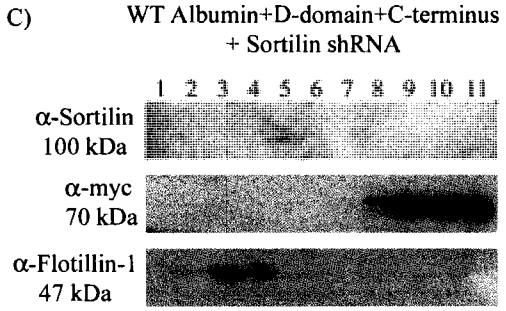
C)
WT Albumin+D-domain+C-terminus
+ Sortilin shRNA
1 2 3 4 5 6 7 8 9 10 11
α-Sortilin
100 kDa
α-myc
70 kDa
α-Flotillin-1
47 kDa

Chapter 5: Results Part 2

Cytosolic Ligands of Sortilin (Adaptor Proteins and Complexes)

The Interaction of Cytosolic Adaptors with Sortilin

Rationale: It has been established that the M6P receptor interacts with the retromer complex via its cytoplasmic tail to be recycled from the endosome to the Golgi compartment (Arighi et al., 2004). Given that the cytosolic tail of sortilin possesses a high degree of structural and functional similarities to the cytosolic tail of the M6P receptor, we hypothesized that sortilin may share an evolutionary conserved mechanism. Results using a chimeric construct consisting of CD8 and the cytosolic tail of sortilin suggested that this hypothesis may be correct (Seaman, 2007). However, due to the chimeric nature of the probe we decided to test this hypothesis with full-length sortilin. Thus, we employed a co-immunoprecipitation assay to examine if full-length sortilin interacts with the retromer complex. Since AP-1 has been shown to bind to the cytosolic tail of the cation independent M6P receptor (CI-MPR) and the CD8-sortilin chimera (Le Borgne et al., 1993), we also tested the interaction of sortilin with AP-1 using a similar co-immunoprecipitation approach.

Additionally, to characterize the regions in the cytosolic tail of sortilin that interact with retromer or AP-1, a Yeast Two-Hybrid approach was employed. To identify the residues involved in this interaction we designed and tested various C-terminal deletion constructs of sortilin. The sortilin deletion constructs used were residues: 779-789, 779-799, 779-809, and 779-819.

Experimental Results: To this end, COS-7 cells were transfected with either a sortilin-myc construct, or pcDNA3.1B (empty vector) as a control. The cells were lysed and subsequently immunoprecipitated using an anti-myc antibody conjugated to protein A Sepharose beads. The resulting complexes were resolved on a 10 %

acrylamide gel, transferred to a nitrocellulose membrane, and immunoblotted for either Vps26 or γ-adaptin (Figure 28A). Given that sortilin co-immunoprecipitates with retromer, via an interaction with Vps35, Vsp26 being a known component of the retromer complex should be present in the immunoprecipitate. Our results showed that sortilin-myc was capable of immunoprecipitating both the Vps26 domain of retromer and the γ-adaptin subdomain of AP-1, producing bands at 35 kDa and 90 kDa respectively (Figure 28A). These results demonstrate that full length sortilin interacts with both retromer and AP-1.

In addition, sortilin C-terminal deletion constructs were investigated by Yeast Two-Hybrid for their ability to interact with the various subunits of retromer and AP-1. Using the Gal4 Yeast Two-Hybrid system we were unable to detect an interaction between sortilin and any of the retromer components (results not shown). Because retromer is not an abundant protein we decided to use a more sensitive approach, i.e., the LexA system. When the entire cytoplasmic tail of sortilin (residues 779-831) was tested, a specific interaction with Vps35 was observed, as sortilin did not interact with either Vps26 or Vps29 (Figure 28B). We found that residues 789-799 were required for this interaction with Vps35 (Figure 28B).

Using the Gal4 system, we demonstrated that the recruitment of the AP-1 complex to the cytoplasmic tail of sortilin is mediated by the medium subunit of AP-1, μ1 (Figure 28C). To determine which residues of the sortilin cytoplasmic tail were important for this interaction we used the same c-terminal truncations of sortilin as described above (Figure 28C). Interestingly, residues 789-799 also were required to mediate the interaction with the medium subunit of AP-1, μ1 (Figure 28C).

Mutational Analysis of the Sortilin- Retromer or AP-1 Interaction

Rationale: While the initial results obtained with a CD8 chimeric sortilin construct suggest a role for an FLV motif found in the cytosolic tail of sortilin (Seaman, 2007), a more common sorting motif is found between residues 789-799, namely a tyrosine motif (YXXΦ). The YXXΦ sequence is of interest since it has been previously implicated in the trafficking of sorting receptors and in the recruitment of accessory proteins (Cooper and Stevens, 1996; Nielsen et al., 2001). Significantly, the YXXΦ sequence has been shown to be essential for the retrograde traffic of Vps10p in yeast (Cooper and Stevens, 1996; Nielsen et al., 2001). Therefore, to further characterize the interaction between full-length sortilin and both retromer and AP-1, the cytosolic tail of sortilin was mutated within the 10 amino acid stretch identified above. Two mutations, Y14A and L17A, were made to target the YSVL consensus sequence in sortilin. The sequence of the cytosolic tail of sortilin is shown in Figure 29A and important sorting motifs are highlighted in pink

Experimental Results: The interaction between Y14A or L17A mutated sortilin with both Vps26 (retromer) and γ-adaptin (AP-1) was tested in COS-7. Protein A Sepharose beads conjugated to anti-myc antibody were incubated with the cell lysate. The resulting immunoprecipitated complexes were run on a 10 % acrylamide gel, transferred to a nitrocellulose membrane and immunoblotted with anti-Vps26 or anti-γ-adaptin antibody (Figure 29B, 29C, and 29D). In this experiment we used the anti-Vps26 antibody since Vps26 is a component of retromer and should immunoprecipitate sortilin bound to Vps35. The results showed that while mutating either Y14A or L17A in the cytosolic tail of sortilin inhibited its interaction with

Vps35/Vps26, the interaction with γ-adaptin was unaffected, producing bands at 90 kDa (Figure 29C and 29D).

Localization of Sortilin Mutant Constructs

Rationale: To determine the effect of the Y14A and L17A mutations on the trafficking of sortilin in COS-7 cells, immunofluorescence microscopy was employed. The subcellular localization of the Y14A and L17A constructs was compared to LAMP-1 which traffics to lysosomes independently of sortilin.

Experimental Results: Briefly, cells transfected with the mutant sortilin constructs were fixed in 4 % paraformaldehyde prior to staining with both anti-myc and anti-LAMP-1 antibodies and compared to cells expressing wild-type sortilin-myc. Secondary antibodies conjugated to either Alexa 488 or Alexa 594 were used to specifically detect myc (green) and LAMP-1 (red) antibodies. While wild-type sortilin-myc was detected in the perinuclear region and punctate lysosomal structures labeled with LAMP-1 (Figure 30A), the presence of the Y14A sortilin mutant construct was decreased in LAMP-1 positive structures (Figure 30B). Similar results were observed with the L17 sortilin mutant construct (Figure 30C). These results suggest that Y14 and L17 may be essential for the interaction of sortilin with retromer.

Inhibition of Retromer and AP-1

Rationale: To characterize the roles of both the retromer complex and AP-1 in the trafficking of full-length sortilin, two siRNA constructs were designed. The siRNA sequences selected to target the Vps26 domain of retromer and the μ1 subunit

of AP-1 have been previously described (Arighi et al., 2004; Janvier and Bonifacino, 2005). The efficiency of the siRNA knockdown in COS-7 cells was assessed by both Western blotting and immunofluorescent microscopy and compared to cells transfected with a negative control siRNA with no known sequence homologies.

To test the hypothesis that abrogation of AP-1 and/or retromer expression decreases the stability of sortilin, a cycloheximide chase experiment was performed. Treatment of cells with cycloheximide inhibits *de novo* protein synthesis thereby allowing for examination of the fate of existing proteins.

Experimental Results: When the 3'-Alexa Fluor 488 tagged siRNA constructs were expressed in COS-7 cells, there was complete inhibition of retromer and AP-1 expression as detected by Western Blot analysis using antibodies against Vps26 and γ-adaptin respectively (Figure 31A and 31B). However the levels of β-actin remained similar in cells transfected with Vps26, μ1, or the negative control siRNA (Figure 31A and 31B). To further confirm this inhibition, immunofluorescence microscopy was performed on negative control siRNA and retromer or AP-1 specific siRNA transfected cells. After fixation, cells were treated with either anti-Vps26 or anti-γ-adaptin antibody followed by incubation with secondary antibody labeled with Alexa 594 (red). Green staining within the cells suggested siRNA expression in negative control as well as Vps26 and μ1 siRNA treated cells (Figure 31). In cells transfected with the retromer or AP-1 specific siRNA, staining of Vps26 and γ-adaptin was abolished entirely (Figure 31A and 31B). These results suggest that the siRNA constructs specifically inhibited retromer and AP-1 expression.

To examine sortilin's stability in the absence of the retromer complex or AP-1, COS-7 cells were treated with cycloheximide and collected after 0, 2, 4, or 6 hours. The lysates of the treated cells were probed for sortilin expression and the results are shown here (Figure 31C). During the time periods examined, the μ1 siRNA did not greatly alter the expression of sortilin while the Vps26 siRNA caused dramatic reduction in the expression of sortilin (Figure 31C). These results suggests that without retromer sortilin's stability is reduced, leading to the decreased expression of this receptor.

The Effect of Retromer and AP-1 Inhibition on Sortilin and its Ligands

Rationale: The consequence of inhibition of Vps26 and μ1-adaptin by RNAi on the transport of full-length sortilin and its cargo was studied by confocal immunomicroscopy. Cells expressing either Vps26 or μ1 Alexa 488 fluorescently tagged RNAi were further transfected with sortilin-myc and compared to untransfected cells. Given that the lysosomal sorting and recycling of the M6PR has been demonstrated to require both AP-1 and retromer (Arighi et al., 2004; Meyer et al., 2000; Seaman, 2007), cathepsin B, an M6PR ligand, was examined as a positive control. LAMP-1 was used here as a negative control.

Experimental Results: After fixation in 4 % paraformaldehyde, cells were incubated with anti-myc (Figure 32A), anti-cathepsin B (Figure 32B), anti-prosaposin (Figure 32C), or anti-LAMP-1 antibody (Figure 32D). A specific secondary antibody labeled with Alexa 594 was utilized to detect the various antibodies.

When cells expressing Vps26 siRNA were stained for sortilin-myc expression, there was a notable absence of sortilin staining in the perinuclear Golgi region and increased expression in punctate endosomal and/or lysosomal structures (Figure 32A). Therefore, expression of Vps26 siRNA resulted in the re-localization of sortilin from the Golgi apparatus to the endosomal system (Figure 32A). In contrast to inhibition of Vps26, inhibition of μ1 by siRNA resulted in retention of sortilin in the Golgi apparatus (Figure 32A). Interestingly, prosaposin, a well characterized sortilin ligand, was absent from cells transfected with either Vps26 or μ1 siRNA (Figure 32C).

The localization of cathepsin B, a M6P receptor ligand, was also affected in siRNA expressing cells (Figure 32B). Under conditions of retromer and AP-1 abrogation, cathepsin B staining was abolished whereas in control cells, cathepsin B staining was found in punctate endosome/lysosome structures (Figure 32B). Using the same approach, LAMP-1 localization was examined as a negative control. Our results showed that LAMP-1 lysosomal immunostaining was unaffected by either Vps26 or μ1 siRNA expression (Figure 32D).

Metabolic Labeling of Retromer and AP-1 Depleted Cells

Rationale: The lack of prosaposin staining in COS-7 cells deficient in Vps26 or AP-1, suggested that in the absence of functional retromer and AP-1 pathways, ligands of sortilin are secreted from the cell into culture media. To determine the fate of prosaposin in the absence of functional retromer and AP-1 pathways, pulse-chase analysis was performed subsequent to Vps26 or μ1 siRNA expression. Similarly, given that retromer has been implicated in the retrograde transport of the M6P

receptor, the fate of cathepsin B, a ligand of the M6P receptor, was also investigated (Arighi et al., 2004).

Experimental Results: Cells expressing siRNA were pulsed with [^{35}S] methionine-cysteine and chased with DMEM. Immunoprecipitation of the culture medium was done at 0, 30, 60, and 90 minutes using anti-cathepsin B, or anti-prosaposin, antibodies (Figure 33A and 33B). The resulting immunoprecipitates were resolved on 10 % SDS-PAGE gels and visualized by autoradiography. Ablation of Vps26 expression increased the release of both cathepsin B and prosaposin into the culture media (Figure 33A and 33B). Comparable results were obtained for cathepsin B and prosaposin when expression of the μ1 subunit of AP-1 was inhibited by siRNA (Figure 33A and 33B).

Figure 28. Sortilin Interactions with Retromer and AP-1. The interaction of sortilin with the retromer and AP-1 complexes was tested in COS-7 cells using anti-Vps26 and anti-γ-adaptin antibodies respectively (A). Immunoprecipitation was done using anti-myc antibody and the immunoprecipitate was resolved on a 10 % acrylamide gel, transferred to nitrocellulose membrane and blotted with either anti-Vps26 or anti-γ-adaptin antibodies. Lane 1 shows that the lysate from cells transfected with an empty vector, did not immunoprecipitate either Vps26 or γ-adaptin (A). Lane 2 shows that sortilin-myc construct immunoprecipitated both Vps26 and γ-adaptin through interactions with retromer and AP-1 complexes and generate bands at 35 and 90 kDa respectively (A). Lane 3 shows the cell lysate (A). Yeast were co-transformed with the retromer subunits and sortilin c-terminal fragments and tested for interaction using the LexA system (B). The interaction of the μ1 subunit of AP-1 was tested for interaction with sortilin c-terminal fragments. p53 and LT are used as controls for yeast growth (C).

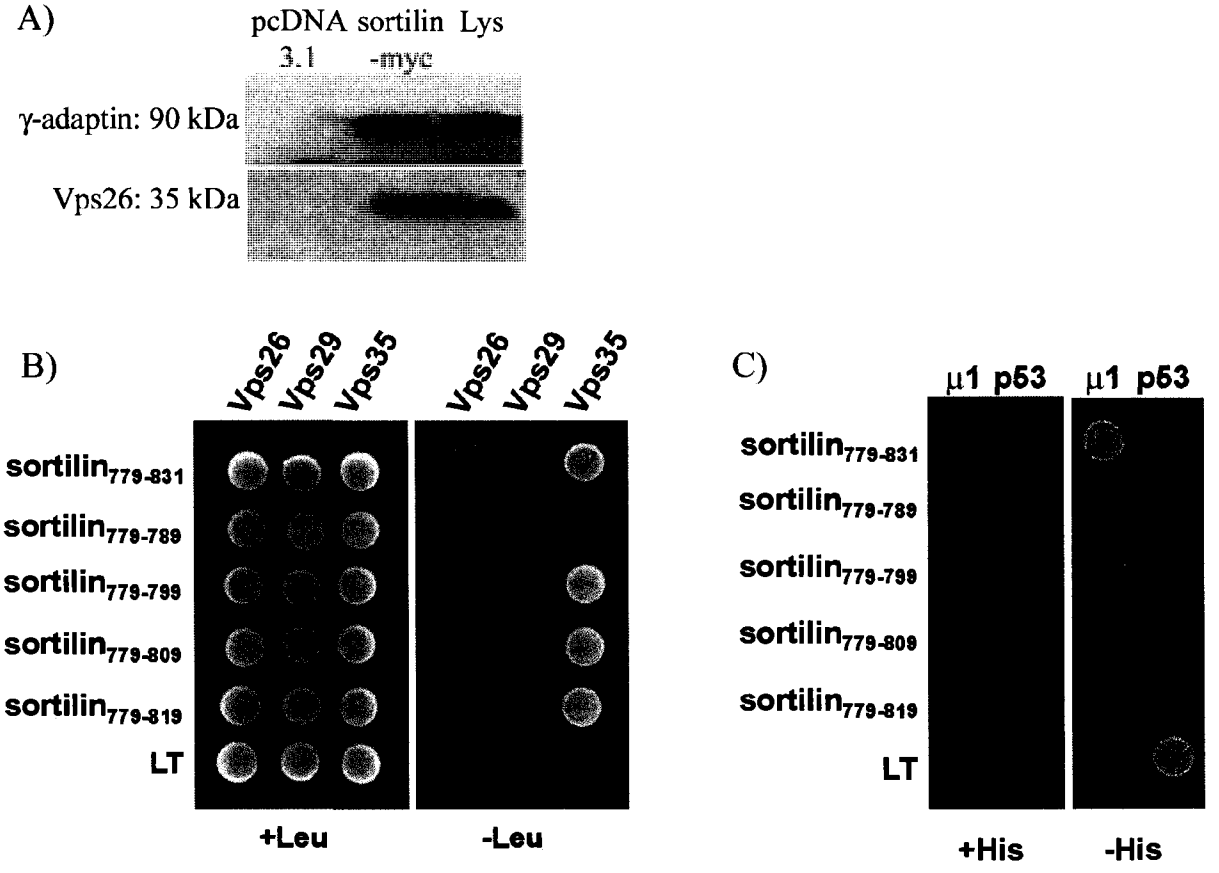
A)
pcDNA 3.1
sortilin -myc
Lys
γ-adaptin: 90 kDa
Vps26: 35 kDa
B)
Vps26
Vps29
Vps35
Vps26
Vps29
Vps35
sortilin779-831
sortilin779-789
sortilin779-799
sortilin779-809
sortilin779-819
LT
+Leu
-Leu
C)
μ1 p53
μ1 p53
sortilin779-831
sortilin779-789
sortilin779-799
sortilin779-809
sortilin779-819
LT
+His
-His

Figure 29. Mutational Analysis of the Sortilin- Retromer and AP-1 Interaction. The binding between sortilin and retromer or AP-1 was studied using sortilin-myc constructs with Y14A and L17A mutations in the cytoplasmic tail of sortilin. Panel A depicts schematically the sortilin receptor and the sequence of its 53 amino acid cytosolic tail. Sortilin consists of a luminal domain that possesses a single Vps10 domain, a TM domain, and a short cytosolic tail (A). Known sorting motifs in the cytosolic tail are shown in pink (A). COS-7 cells were transfected with these constructs as well as with wild type sortilin-myc to verify expression (B). Mutant constructs, Y14A and L17A, were both expressed in COS-7 cells, producing bands at 100 kDa, as verified using anti-myc antibody (B). The interaction of Y14A and L17A sortilin constructs with Vps26/Vps35 (retromer) and γ-adaptin (AP-1) was then examined by co-immunoprecipitation with anti-myc antibody (C and D). Both mutant sortilin constructs were unable to interact with Vps26 via the retromer complex, while the binding of wild type sortilin-myc was unaffected, producing a band at 35 kDa (C). In contrast, Y14A and L17A mutations of sortilin had no effect on binding to γ-adaptin via the AP-1 complex, and bands were visible at 90 kDa for mutants, as well as wild type sortilin-myc (D).

A)

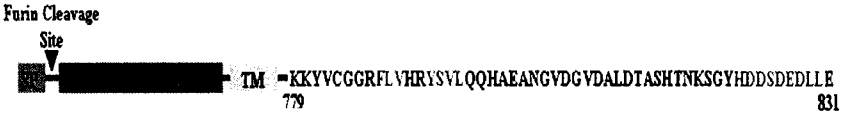

B)

Sortilin-myc Expression

C)

Sortilin-myc Co-IP of Vps26

D)

Sortilin-myc Co-IP of γ-adaptin

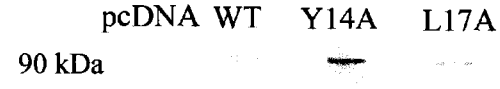

Figure 30. Subcellular Distribution of Y14A and L17A Sortilin Constructs. COS-7 cells expressing either the Y14A (B) or L17A (C) mutant sortilin constructs were fixed in 4 % paraformaldehyde, prepared for immunofluorescent confocal microscopy, and compared to similar cells expressing wild-type sortilin-myc (A). The sortilin constructs were detected by anti-myc antibody, followed by incubation with a secondary antibody conjugated to Alexa 488 (green). The cells were also labeled for LAMP-1 (red). When compared to the wild-type sortilin (A), both the Y14A (B) and L17A (C) mutations produced a decrease in the number of punctate structures labeled with LAMP-1. The scale bars shown equal 8 μm and apply to all panels.

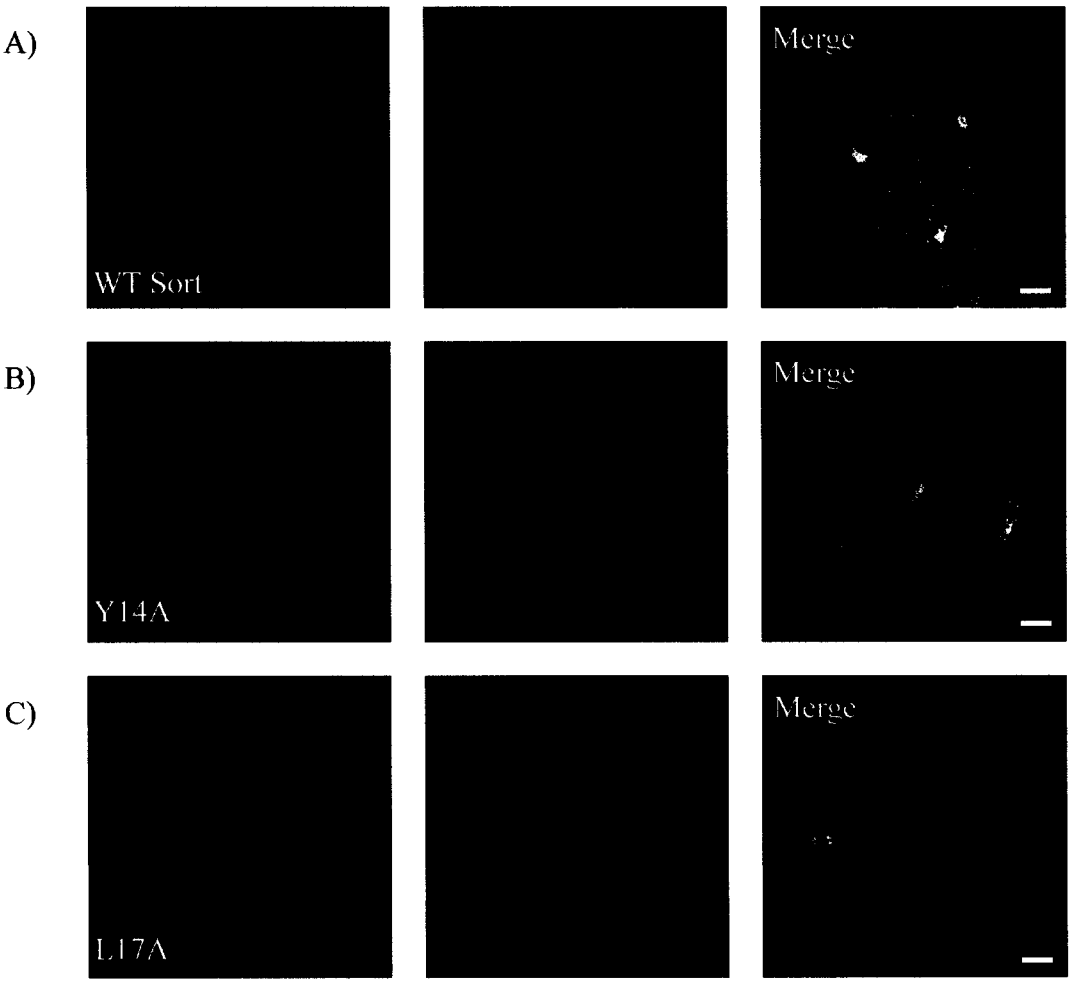
A)
WT Sort
Merge
B)
Y14A
Merge
C)
L17A
Merge

Figure 31. Retromer and AP-1 RNAi Controls. To verify the inhibition of retromer and AP-1 by siRNA, western blotting and confocal microscopy were performed. Both of these siRNA possessed 3'-Alexa Fluor 488 tags that permitted visualization via confocal microscopy (A and B). Cells expressing either siRNA had no Vps26 or γ-adaptin expression, as demonstrated by the absence of any red staining (A and B). These images were compared to COS-7 cells transfected with a nonspecific negative control siRNA (A and B). Control cells show a normal expression pattern of Vps26 and γ-adaptin in perinuclear and punctate structures. Additionally, inhibition was assessed by western blot. siRNA specific to either Vps26 or γ-adaptin, specifically inhibited expression of their respective targets as is seen by the absence of bands at 35 kDa and 90 kDa. Conversely, the loading control β-actin is unchanged (A and B). The stability of sortilin was assessed under these conditions by a cycloheximide chase experiment (C). After treatment with 40 μg/ml of cycloheximide, the cells were collected and the lysates were probed with anti-sortilin antibody and the results shown here (C). The scale bars shown equal 8 μm and apply to all panels.

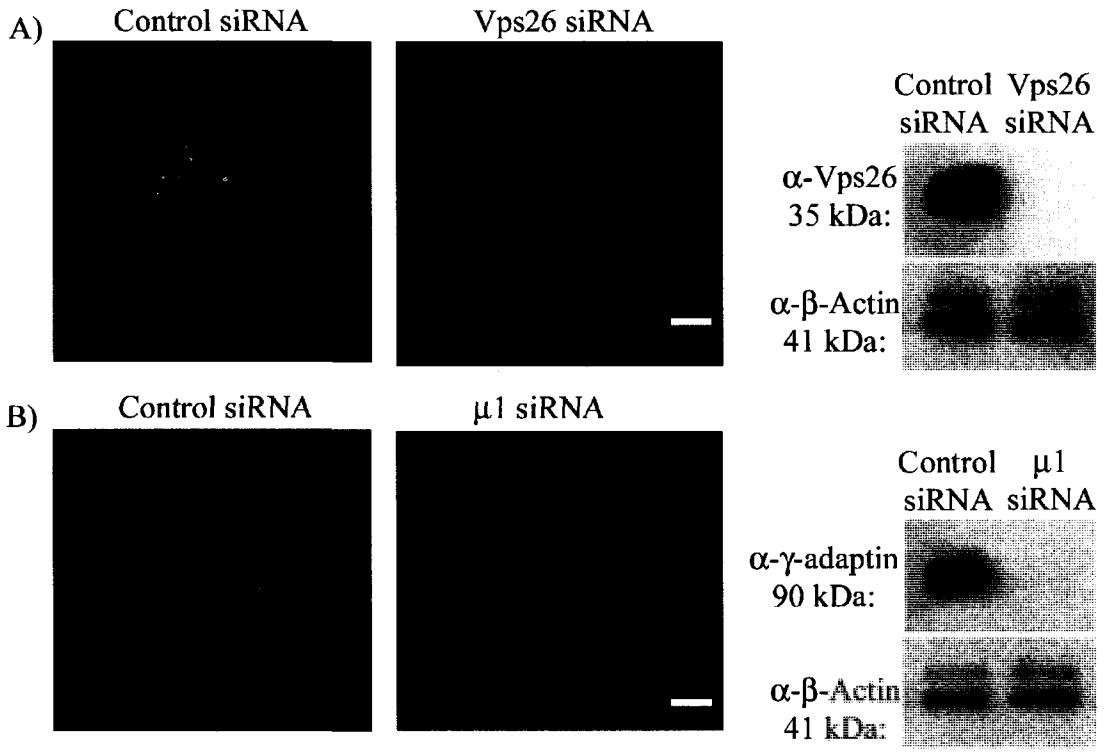
A)
Control siRNA
Vps26 siRNA
Control Vps26
siRNA siRNA
α-Vps26
35 kDa:
α-β-Actin
41 kDa:
B)
Control siRNA
μ1 siRNA
Control μ1
siRNA siRNA
α-γ-adaptin
90 kDa:
α-β-Actin
41 kDa:
C)
Control siRNA μ1 siRNA Vps26 siRNA
0 2 4 6 0 2 4 6 0 2 4 6
α-Sortilin
100 kDa:
α-β-Actin
41 kDa:

Figure 32. RNAi Inhibited Transport of Sortilin Cargo. To determine the effects of Vps26 and μ1 inhibition by 3'-Alexa Fluor 488 tagged siRNA on transport of cargo proteins, confocal microscopy was performed. COS-7 cells were transfected with either Vps26 or μ1 siRNA, prepared for immuno-microscopy and stained for sortilin-myc, cathepsin B, prosaposin, or LAMP-1 followed by incubation with their respective Alexa 594 conjugated secondary antibodies (A, B, C, D). Sortilin staining was reduced in the perinuclear region and increased in punctate lysosomal structures when cells were transfected with Vps26 siRNA (A). Sortilin-myc was localized solely to the perinuclear Golgi region when cells expressed μ1 siRNA (A). Prosaposin staining was absent entirely from cells expressing either Vps26 or μ1 siRNA (C). Similarly, the localization of cathepsin B was disrupted by both Vps26 and μ1 siRNA (B). LAMP-1 expression was examined as a negative control (D). LAMP-1 staining was unaffected by either Vps26 or μ1 siRNA (D). The scale bars shown equal 8 μm and apply to all panels.

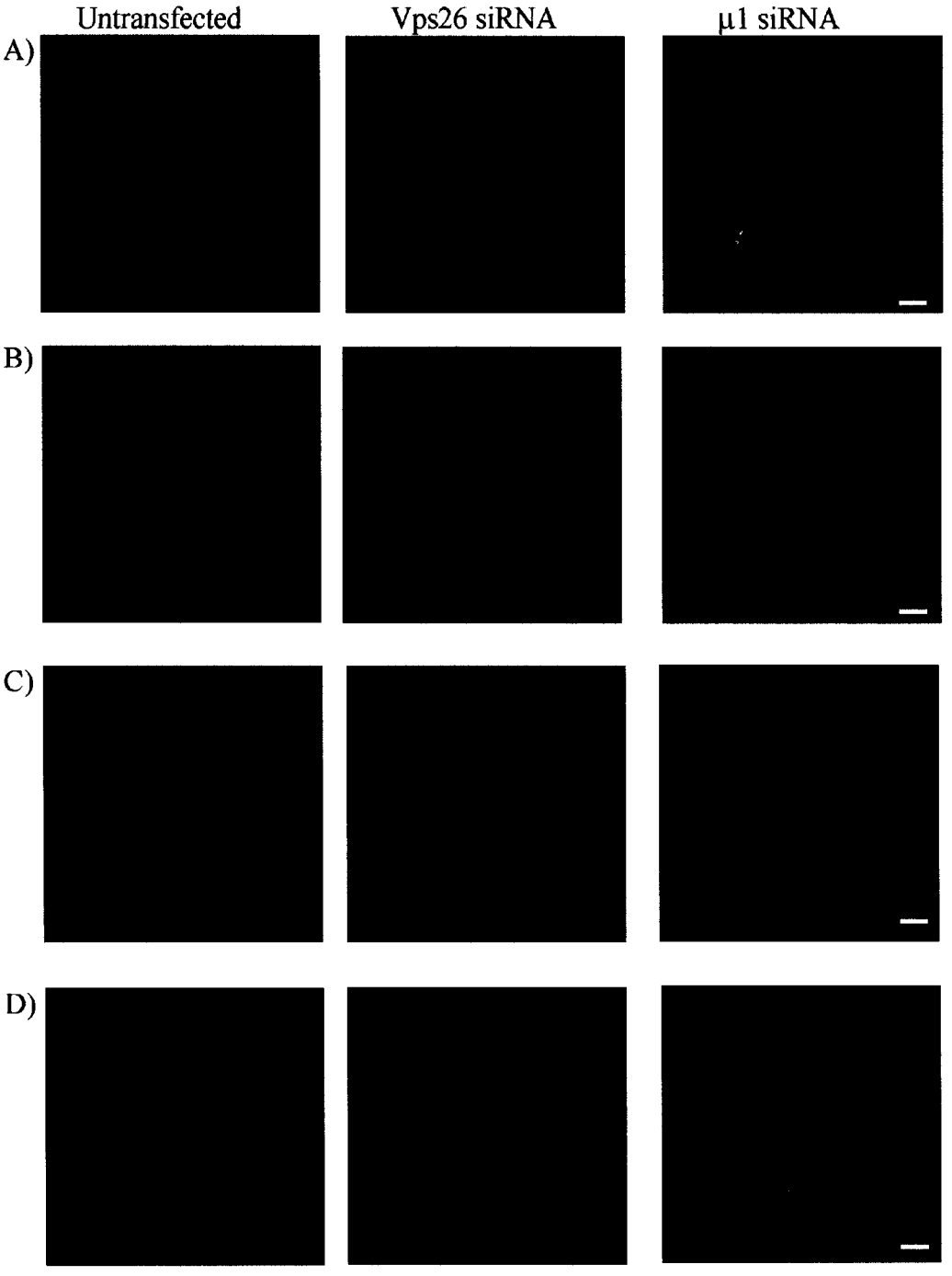
Untransfected
Vps26 siRNA
μ1 siRNA
A)
B)
C)
D)

Figure 33. Metabolic Labeling of Retromer and AP-1 Depleted Cells. COS-7 cells were transfected with negative control, Vps26, or μ1 targeted siRNA. Cells were pulse labelled with [^{35}S] methionine, chased for 30 minutes and the culture media immunoprecipitated with anti-cathepsin B, or anti-prosaposin antibody at 0, 30, 60, and 90 minutes (A, B). The inhibition of both Vps26 and μ1 by siRNA resulted in the increased presence of cathepsin B and prosaposin in the culture media (A, B). Quantification of 3 separate experiments is illustrated on right panels.

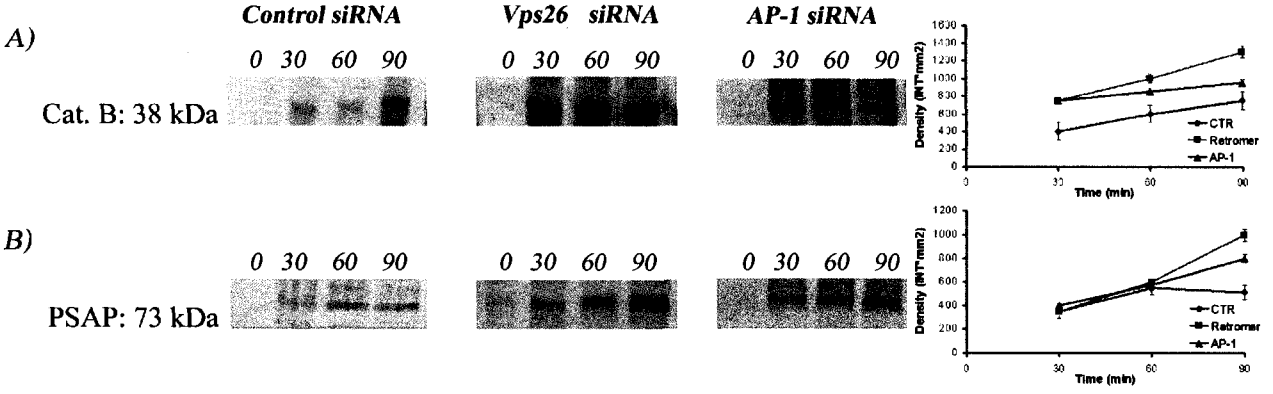
A)
Control siRNA
Vps26 siRNA
AP-1 siRNA
0 30 60 90
0 30 60 90
0 30 60 90
Cat. B: 38 kDa
Density (INT*mm2)
Time (min)
CTR
Retromer
AP-1
B)
0 30 60 90
0 30 60 90
0 30 60 90
PSAP: 73 kDa
Density (INT*mm2)
Time (min)
CTR
Retromer
AP-1

Chapter 6: Discussion

Part 1: Luminal Interaction of Sortilin with Soluble Hydrolases

One the main objectives of the present investigation was to test the hypothesis that sortilin mediates the sorting and trafficking of certain soluble hydrolases in addition to its known role in the transport of the non-enzymic sphingolipid activator proteins. Part 1 of the discussion deals with this hypothesis and with the mechanisms that mediate these interactions.

Sortilin Interacts with Cathepsins D and H

Although the majority of soluble lysosomal proteins are trafficked to the lysosomes by the M6PR (Lobel et al., 1989), several lines of evidence suggest that an alternative mechanism exists to mediate the lysosomal routing of certain cathepsins (Rijnboutt et al, 1991). This notion is supported by the observation that the lysosomes of ICD fibroblasts contain certain cathepsins, as well as other soluble proteins, in the absence of a functional M6PR pathway (Reitman et al., 1981; Rijnboutt et al., 1991a; Rijnboutt et al., 1991b). Hepatocytes, Kupffer cells, and lymphocytes, from ICD patients have near normal levels of several M6PR-dependent soluble lysosomal proteases (Gabel et al., 1983; Glickman and Kornfeld, 1993; Rijnboutt et al., 1991b). One specific cathepsin, cathepsin D, which has been previously suggested to traffic to the lysosomes via the M6PR, is found at approximately 45 % of its normal amounts in the lysosomes of ICD B lymphoblastoid cell lines (Glickman and Kornfeld, 1993). This result indicates the existence of a trafficking mechanism independent of the M6PR pathway for at least this protease.

Additionally, a variety of biochemical studies suggest the existence of an M6PR-independent sorting pathway for other soluble lysosomal proteins. Although cathepsin H may contain M6P residues, there is no correlate targeting to the lysosomes in primary cultures of rat hepatocytes (Tanaka et al., 2000). Similarly, when M6P was exogenously added to CHO cells, the subcellular localization of cathepsin K was unaffected (Claveau and Riendeau, 2001). Different lines of evidence also suggest that cathepsin L also traffics to the lysosomes independently of the M6PR. While cathepsin L also possesses an M6P tag it has been demonstrated to have extremely low affinity for the M6PR (Gottesman, 1978). Thus, the first objective of the present investigation was to test the hypothesis that the M6PR-independent transport of cathepsins D, H, K, and L to the lysosomes is carried out by an alternative sorting and trafficking receptor, presumably sortilin.

Sortilin is a novel lysosomal sorting receptor that has a remarkable homology to the yeast VPS10p sorting receptor (Nielsen et al., 2001). Sortilin has been shown to bind and traffic to the lysosomes the sphingolipid activator proteins (SAPs), prosaposin and $G_{M2}AP$ (Lefrancois et al., 2003). Unlike cathepsins which are soluble hydrolases, SAPs are non-enzymic proteins required to solubilize sphingolipids, presumably from luminal vesicles of multivesicular bodies (Morales et al., 1995).

To test the hypothesis that cathepsins D, H, K, and L are targeted to the lysosomes by the alternative sorting receptor, sortilin, the interaction of the cathepsins in question with sortilin was first investigated by Co-IP assay. The interaction of the cathepsins with the M6PR was also confirmed by Co-IP. The results showed that the M6PR was immunoprecipitated by cathepsins D, K, and L, but not by cathepsin H

(Figures 2, 3, and 4). These results indicate that cathepsin H is not an interactive partner of the MP6R whereas cathepsins D, K, and L are. Conversely, when anti-cathepsin D, H, K, or L antibodies were used to pull down sortilin, cathepsins D and H but not K or L were capable of pulling down both wild type and truncated sortilin-myc (Figure 2, 3, and 4). These results demonstrated that cathepsins D and H are interactive partners of sortilin and that this interaction was unaffected by truncation of the cytosolic domain of sortilin.

To examine whether or not sortilin played a role in the lysosomal targeting of cathepsins D, H, K, or L, immunofluorescent staining was conducted in untransfected cells or cells transfected with truncated sortilin-myc (Figures 8, 9, 10, and 11). The truncated sortilin-myc construct has previously been characterized and has been shown to act as a dominant-negative competitor of endogenous sortilin that induces the retention of sortilin in the Golgi apparatus (Figure 5) and inhibits the targeting of SAPs to the lysosomes (Lefrancois et al., 2003).

In untransfected cells, cathepsins D, H, K, and L were found in punctate lysosomal structures labeled with LAMP-1. However, when the cells were transfected with dominant-negative truncated sortilin-myc, anti-cathepsin D and H antibodies stained only the perinuclear region. Thus, truncated sortilin bound to both cathepsins D and H and caused their retention within the Golgi apparatus, indicating that the transport of cathepsins D and H to the lysosomes was disrupted by inhibition of the sortilin pathway (Figures 10 and 11). Therefore, in the case of cathepsin D, the truncated sortilin-myc construct not only competed with the endogenous sortilin but with the M6PR as well since cathepsin D was excluded from the lysosomes. Our

results also suggest that fluid-phase endocytosis does not play a major role in the uptake of cathepsin D or cathepsin H since the dominant-negative sortilin completely blocked the transport of cathepsin D and H to the lysosomes.

Alternatively, in cells transfected with truncated sortilin-myc, the localization of cathepsins K and L to punctate lysosomal structures labeled with LAMP-1 was unaltered as compared to cells in which the sortilin pathway was intact (Figures 8 and 9). This result suggests that while cathepsins K and L may attain the lysosomes independently of the M6PR, the alternative pathway employed is not via the sortilin receptor. The M6PR-independent trafficking of cathepsins K and L may be accounted for by fluid-phase endocytosis or another sorting receptor. Additional potential sorting receptors include members of the Vsp10 family such as SorLA or SorC1-3. These Vsp10-domain receptors have been shown to have a cytoplasmic tail capable of interacting with the adaptor proteins necessary for vesicular formation (Hermey et al., 1999; Nielsen et al., 2007). It can be speculated that these homologous receptors have evolved in accordance with the different expression patterns of their ligands since while some cathepsins are ubiquitously expressed, others, such as cathepsin K, are more restricted in their expression (Claveau and Riendeau, 2001).

Since cathepsin B has been demonstrated to utilize the M6PR to reach the lysosomes, truncated sortilin did not alter the punctate staining yielded by the anti-cathepsin B antibody (Figure 7) (Mort and Buttle, 1997). This indicates that our experimental manipulation did not alter the M6PR pathway.

The Absence of a Sortilin Pathway Affects the Trafficking of Cathepsins D and H

To determine the effect of the inactivation of sortilin on the lysosomal transport of cathepsins D, H, K, and L, COS-7 cells stably expressing sortilin shRNA were examined by confocal microscopy and pulse-chase analysis (Figures 15-18). Under this condition of sortilin ablation, the punctate staining of cathepsin H was abolished (Figure 16). In addition, pulse-chase experiments showed that the inactivation of sortilin induced the secretion of cathepsin H (Figure 16). Thus, these results indicate that the stable expression of sortilin shRNA inhibited the lysosomal transport of cathepsin H and resulted in the preferential secretion of cathepsin H into the extracellular milieu. On the other hand, the effect of the inactivation of sortilin on cathepsin D differed from the dominant-negative experiment. While dominant-negative truncated sortilin abrogated the trafficking of cathepsin D to the lysosomes, the sortilin shRNA did not (Figure 15). These results suggest that in cells in which sortilin expression was abrogated by the sortilin shRNA, the M6PR continued to traffic cathepsin D to the lysosomes. In addition, the secretion of cathepsin D also appears to be unaffected by sortilin ablation suggesting that in the absence of sortilin, the M6PR compensates the targeting of cathepsin D to the lysosomes (Figure 15).

In accordance with the results obtained using a truncated sortilin construct, inhibition of the sortilin pathway using shRNA produced similar effects on the sorting of cathepsins K and L (Figures 17 and 18). Analysis of cathepsin K and L localization by confocal microscopy and secretion pulse-chase showed no differences when shRNA expressing cells were compared to mock treated cells. These results further

substantiate the idea that the M6PR-independent trafficking of cathepsins K and L to the lysosomes is not due to the sortilin pathway.

M6PR and Sortilin Traffic Cathepsin D to the Lysosomes

The transport of cathepsins D, H, K, and L was also examined in ICD fibroblasts which have a disrupted M6PR pathway. Cathepsin B, a well characterized M6PR ligand, is excluded from the lysosomes of ICD cells due to the inability of the M6PR to recognize cargo that lacks M6P residues (Lobel et al., 1989). Cathepsin B staining of lysosomes ICD fibroblasts is therefore abolished (Figure 20). Under similar conditions, transport of cathepsin D to the lysosomes is partially inhibited and it has been estimated that only 45 % of cathepsin D reaches the lysosomes (Rijnboutt et al., 1991b). Accordingly, we found cathepsin D present in punctate lysosomal structures positively-stained with LAMP-1 confirming that cathepsin D can attain the lysosomes independently of the M6PR (Figure 23).

The sorting of cathepsins H, K, and L in ICD fibroblasts was not previously examined. When we incubated ICD fibroblasts with anti-cathepsins H, K, or L antibodies followed by Alexa tagged secondary antibodies, staining for all three cathepsins was observed in LAMP-1 labeled granules (Figures 21, 22, and 24). These results confirm that cathepsins H, K, and L are delivered to the lysosomes independently of the M6PR.

To observe the subcellular localization of cathepsins in the absence of both the M6PR and sortilin sorting pathways, ICD fibroblasts were transfected with the truncated sortilin-myc construct. Under these conditions the staining patterns of

cathepsins K, and L were unaltered confirming the hypothesis that the transport of these cathepsins to the lysosomes can occur independently of both the sortilin and M6PR pathways (Figures 21 and 22). However, abolishment of the sortilin sorting pathways by transfection with the truncated sortilin-myc construct inhibited the transport of cathepsins D and H to lysosomes (Figures 23 and 24). This result demonstrates not only that transport of cathepsin D to the lysosomes occurs through both the sortilin and M6PR sorting pathways, but the result suggests that the normal trafficking of cathepsin D in cells in which sortilin expression has been abrogated is due to M6PR-dependent trafficking of cathepsin D.

DRMs Play a Selective Role in the Interaction of Sortilin and its Ligands

It is well known that the endoplasmic reticulum (ER) produces the precursors of lipid-rafts (i.e., cholesterol and ceramide) which are then exported to the Golgi apparatus. In the Golgi, ceramide serves as a precursor for the synthesis of sphingomyelin. Consequently, sphingomyelin is produced relatively late in the process of membrane synthesis by enzymes located in the Golgi lumen. Thus, sphingomyelin is located exclusively in the noncytosolic leaflet of the lipid bilayer.

Results from our laboratory have shown that a sortilin ligand, prosaposin, requires sphingomyelin to be targeted from the Golgi apparatus to the lysosomes. Based on this result, it was postulated that the interaction of prosaposin with sphingomyelin brings this ligand in close proximity to the Golgi membrane to facilitate its binding to sortilin (Lefrancois et al., 2002). In fact, depletion of sphingomyelin with specific biochemical inhibitors results in the misrouting of

prosaposin to the secretory pathway (Lefrancois et al., 1999). Sphingomyelin is one of the main components of DRM microdomains (Simons and Ikonen, 1997).

DRMs have been postulated to exist in the TGN and to function as sorting platforms (Simons and Ikonen, 1997; Simons and van Meer, 1988). Of interest, sortilin has been demonstrated to bind G proteins present in lipid rafts at the plasma membrane (Gkantiragas et al., 2001; Martin et al., 2002). Thus, in an attempt to better understand the mechanism of lysosomal transport via the sortilin sorting receptor, we investigated here whether sortilin and its ligands are found associated to DRM microdomains in TM4 Sertoli cells. TM4 Sertoli cells were therefore transfected with wild-type sortilin-myc 24 hours prior to homogenization and fractionation by sucrose gradient centrifugation.

Our results from TM4 Sertoli cell fractionation show that sortilin, and its ligands, prosaposin, cathepsin D and cathepsin H are found within detergent resistant membrane fractions as was flotillin-1, a lipid raft marker (Figure 25). In support of this finding, recent evidence obtained with a novel proteomics approach has demonstrated that flotillin-1 and flotillin-2 represent a significant portion of the lysosomal membrane (Bagshaw et al., 2005). However, the M6PR and its ligand, cathepsin B, were not found in fractions known to contain lipid-rafts (Figure 25). This suggests the existence of two classes of soluble lysosomal proteins, one that uses the M6PR to reach the lysosomes independently of DRM microdomains and a second class which uses sortilin and requires DRM microdomains. The findings for cathepsin D suggest that, similar to the truncated sortilin-myc construct, under conditions in which wild-type sortilin was over-expressed, the M6PR was out-competed. We

therefore reason that in TM4 cells over-expressing wild-type sortilin, sortilin recruited cathepsin D away from the M6PR and into the DRM fractions.

Given that our results and previous reports from our laboratory suggest a role for sphingomyelin in the transport of prosaposin to the lysosomes, we next attempted to identify the regions (if any) within prosaposin that mediate its interaction with sphingomyelin. Due to published and unpublished data from our laboratory demonstrating that while the C-terminus of prosaposin alone mediates its interaction with sortilin, the D-domain of prosaposin is required for its lysosomal targeting (Lefrancois et al., 2002). Moreover, it was hypothesized that the role of the D-domain was to mediate the conditional interaction between the C-terminus of prosaposin and sortilin by first interacting with sphingomyelin (Figure C) (Lefrancois et al., 2002; Lefrancois et al., 2003). Thus we tested the hypothesis that the D-domain of prosaposin mediates its localization to sphingomyelin in DRMs.

DRM fractions from COS-7 cells expressing chimeric constructs consisting of albumin and both the D-domain and C-terminus of prosaposin were observed herein to contain the chimeric construct (Figure 26). While this initial result substantiates the aforementioned hypothesis, further investigation using a chimeric construct consisting of albumin and the C-terminus of prosaposin alone suggests otherwise since it was also present in DRM fractions (Figure 26). Likewise, a chimeric construct consisting of albumin and exclusively the D-domain of prosaposin was found to be excluded from DRM fractions (Figure 26).

These findings were further substantiated by our mutational analysis of the prosaposin D domain which explored the potential interaction of this domain with

sphingomyelin. Accordingly, based on the fact that sphingomyelin possesses positively charged headgroups, negatively charged amino acid residues in prosaposin were mutated to positively charged amino acids in an attempt to disrupt the interaction of prosaposin and sphingomyelin in DRMs. However, when specific negatively charged amino acid residues (E463 and E491) in prosaposin were mutated to positive residues (E463K and E491L) no effect was observed on the localization of prosaposin to DRMs (Figure 27). This finding shows that the amino acids selected for mutation did not mediate the interaction of prosaposin and DRMs and suggests that the localization of prosaposin to DRMs is not charge-dependent. Conversely, unpublished confocal microscopy data from our laboratory show that these mutations partially inhibit the trafficking of prosaposin from the TGN to the lysosomes. Together these findings have led us to propose that prosaposin must be properly folded in order to interact efficiently with the luminal domain of sortilin. Disruption of the charged amino acid residues and/or removal of the entire prosaposin D domain may therefore alter the conformation and affinity of the C-terminus to sortilin and in turn decrease the trafficking of the modified chimeric constructs to the lysosomes. Furthermore, the localization of sortilin, and not the M6PR to DRMs may prove to be an important feature in distinguishing the two sorting receptors, their ligands, and sorting pathways.

Further to this, our findings indicate that the interaction of prosaposin with DRMs must occur either through its C-terminus or indirectly through an association with sortilin which is localized to DRM microdomains. However, it is more likely that the localization of prosaposin to DRMs is the result of its interaction with sortilin since the C-terminus of prosaposin has not been demonstrated to bind sphingomyelin

directly. This was confirmed herein by investigating the localization of the wild-type albumin-D-domain-C-terminus chimera in cells in which sortilin was depleted by shRNA (Figure 27). In conclusion, our results show that the C-terminus, and not the D-domain, is implicated in the localization of prosaposin to DRMs. A plausible interpretation that reconciles the results of the present and past investigations is that the D domain of prosaposin plays a conformational role that favors the interaction of the C-terminus with sortilin. In fact, a closer analysis of the results initially published by (Zhao and Morales, 2000), shows some granular distribution around the Golgi apparatus of the albumin/prosaposin C-terminus chimeric construct. This observation indicates that the C-terminus of prosaposin partially restored the trafficking of the chimeric construct to the lysosomes. Additionally, the ability of saposin D and of the other saposins to bind sphingomyelin may be solely of functional significance in the lysosomes where saposins act as non-enzymic biological detergents.

Clearly the functional significance of raft domains in lysosomal transport remains to be clarified. However, it is tempting to speculate that raft domains may function as a structural scaffold for transport proteins or as a recruitment device for ligand-receptor complexes and accessory cytoplasmic proteins. Proteomic assessment of the Golgi lipid-rafts will help to identify the components of this putative platform involved in the lysosomal transport of some soluble proteases.

Part 2: Cytoplasmic Interaction of Sortilin with Adaptor Proteins

Based on the fact that the cytosolic tail of sortilin possesses a high degree of structural and functional similarities to the cytosolic tail of the M6P receptor, the second major objective of this investigation was to test the hypothesis that sortilin and the M6PR share an evolutionary conserved mechanism of trafficking between the TGN and the endosome. Part 2 deals with this hypothesis and with the mechanisms that mediate the interaction of sortilin with relevant cytoplasmic adaptor and accessory proteins.

A YXXΦ Sorting Motif Mediates the Interaction between Sortilin and Adaptor Proteins

Given the functional homology between the sortilin and M6P receptors, we next examined whether the adaptor proteins and complexes implicated in the trafficking of the M6PR also interact with full-length sortilin (Arighi et al., 2004; Seaman, 2007). The adaptor proteins and complexes of interest here were namely AP-1 and retromer. The multimeric adaptor, AP-1A has been found to play a role in sorting events at the TGN that involve the M6PR specifically through an interaction of the μ subunit (Meyer et al., 2000; Ohno et al., 1995; Owen and Evans, 1998). The pentameric retromer complex has more recently been implicated in the endosomal recycling of both the M6PR and a CD8 chimeric construct of the cytosolic tail of sortilin. The same report suggests that an FLV motif in the cytosolic domain of sortilin mediates the interaction with the Vps35 subunit of the retromer complex (Seaman, 2007).

Here, using a Co-IP assay, we show that full-length sortilin is capable of interacting with and immunoprecipitating both AP-1 (γ-adaptin) and retromer (Vps26) (Figure 28). Additionally, our Yeast Two-Hybrid analysis of the interaction between retromer or AP-1 and sortilin C-terminal deletion constructs demonstrated that sortilin interacts with both Vps35 (retromer) and μ1 (AP-1). Specifically, amino acid residues 789-799 were shown here to be essential for the binding of sortilin to Vps35 and μ1 (Figure 28). These results are consistent with what has been observed with CD8 chimeric sortilin with the exception that the FLV motif believed to mediate the interaction between sortilin and Vps35 occurs outside the 789-799 region identified here (Seaman, 2007). Rather the stretch of amino acids we identified contains another common sorting motif, YXXΦ. To examine if this motif is implicated in the interaction and trafficking of full-length sortilin by AP-1 and/or retromer, we introduced mutations into the YSVL motif in sortilin (Figure 29).

Our results showed that while mutating either Y14A or L17A inhibited the interaction of the cytosolic tail of sortilin with Vps35/Vps26, the interaction with γ-adaptin was unaffected (Figure 29). This result strongly indicates that the interaction between sortilin and retromer is dependent upon the YSVL sequence. However, the interaction of sortilin with AP-1 may rely on an entirely distinct sequence within residues 779 to 789 of sortilin, or more likely, since AP-1 also binds dileucine motifs, it is feasible that AP-1 binds to the dileucine motif of sortilin further downstream of the tyrosine motif.

Similarly, when the Y14A and L17A sortilin constructs were studied by confocal microscopy, our results suggested a role for these two amino acid residues in

the trafficking of sortilin (Figure 30). As compared to wild-type sortilin, the presence of both the Y14A and L17A constructs in LAMP-1 labeled lysosomes was found to be diminished. These results suggest that while Y14 and L17 may be essential for the interaction of sortilin with retromer, these amino acid residues are also important in mediating the exit of sortilin from the TGN, possibly via an interaction with AP-1.

Sortilin and its Ligands are Mis-sorted in the Absence of Retromer and AP-1

To further characterize the role of AP-1 and retromer in the trafficking of sortilin, cells in which AP-1 and retromer expression was abrogated by siRNA were studied by confocal microscopy and pulse-chase.

While attenuation of Vps26 expression caused depletion of sortilin in the perinuclear region, abrogation of μ1 expression resulted in the retention of sortilin in the perinuclear Golgi region (Figure 32). This result would indicate that in the absence of a functional retromer complex, sortilin accumulates in the endosomal system and is depleted from the Golgi complex, but that without AP-1 sortilin cannot exit the TGN. Therefore our results would indicate that AP-1 is implicated in the anterograde transport of sortilin from the TGN to the endosomal compartments, while retromer mediates the retrograde transport of sortilin from the endosomal compartments back to the TGN. Furthermore, when the stability of sortilin was examined in retromer or AP-1 siRNA treated cells, we observed a decrease in the expression of sortilin in cells lacking retromer (Figure 31). This finding would lead us to hypothesize that without retromer, sortilin is transferred from the endosomal compartments to the lysosomes where it is degraded, thereby resulting in the

decreased expression of this receptor and emphasizing the importance of receptor recycling.

The fate prosaposin and cathepsin B, ligands of sortilin and the M6PR respectively, in cells deficient in either retromer or AP-1 was also examined by confocal microscopy and pulse-chase. By confocal immunomicroscopy, the staining of both prosaposin and cathepsin B in cells transfected with retromer or AP-1 siRNA was abolished (Figure 32). The lack of prosaposin and cathepsin B within these cells appears to be a consequence of the defects in sortilin and M6PR sorting, which in turn, could have caused the release of prosaposin and cathepsin B to the extracellular space.

This was confirmed by a pulse-chase experiment that revealed that in similarly treated cells, prosaposin and cathepsin B were increasingly secreted into the extracellular milieu (Figure 33). The results obtained from the pulse-chase analysis indicate that the absence of functional sorting pathways in the Golgi causes secretion of soluble lysosomal proteins from the cell. Additionally, the similarity between prosaposin and cathepsin B indicates that sortilin and the M6P receptor use similar trafficking mechanisms to shuttle between the Golgi apparatus and the endosomes. In conclusion, the above results demonstrate a critical role for both retromer and AP-1 in the trafficking of full-length sortilin.

Part 3: General Conclusions

The efficient delivery of soluble lysosomal proteins from the TGN to the lysosomes requires sorting receptors (Kornfeld, 1986). Defects in the canonical M6PR sorting pathway result in LSDs such as mucolipidosis II (ICD) and

mucolipidosis III (Reitman et al., 1981). While the multimeric AP-1 adaptor protein and retromer sorting complex have been implicated in mediating the transport of the M6PR to and from the endosomes, we show here for the first time that these same adaptors are important for the trafficking of sortilin (Arighi et al., 2004; Meyer et al., 2000). Furthermore we have herein identified a new set of amino acids (YSVL) in the cytosolic tail of the sortilin sorting receptor that are required and essential for the interaction of sortilin with retromer.

This finding is important given that the proper sorting and function of soluble lysosomal proteases is essential for efficient lysosomal and cellular functioning. There is growing evidence that imbalance in the localization of cathepsins is related to familial forms of Alzheimer's disease (Urbanelli et al., 2006). Increased levels of cathepsin H in sera have also been identified as a marker in colorectal cancer (Schweiger et al., 2004). The results of this investigation support the hypothesis that cathepsins D and H are transported to the lysosomes in a manner that requires the sortilin sorting receptor. In the case of cathepsin H, sortilin appears to be the sole receptor required for lysosomal translocation. Alternately, the efficient transport of cathepsin D to the lysosomes requires both the M6PR and sortilin.

An additional feature that distinguishes sorting by sortilin and the M6P receptor that we have herein identified is DRM microdomains. Sortilin and its ligands are localized to DRMs whereas the M6PR and its ligands are not. These novel findings represent an important step towards the elucidation and differentiation of the pathways involved in sorting soluble lysosomal proteins and support the notion that sortilin functions as an alternative receptor to the M6PR. Additionally, these results

suggest that there are important similarities and differences between the sortilin and M6PR sorting pathways.

The explanation for the existence of two such sorting pathways may be evolutionary. Interestingly, the sortilin sorting pathway may represent an evolutionarily older mechanism for lysosomal transport than the M6PR pathway. Sortilin is a member of the Vps10 family of sorting receptors which also includes Vps10p, SorLA, and SorCS1-3. This family of proteins is characterized by luminal Vps10 domains that were first identified as a sorting motif in yeast (Hampe et al., 2001; Marcusson et al., 1994). Vps10 domain containing proteins are found in a variety of simple organisms including *Dictyostelium*, *Neurospora,* and *Metarhizium* (Hampe et al., 2001).

While the yeast Vps10p receptor is often described as a yeast analogue of the M6PR, it in fact possesses more similarities to sortilin than the M6PR. Both sortilin and the Vps10p receptor contain Vps10 domains (1 in sortilin and 2 in the Vps10p), while the M6PR has no Vps10 domain (Petersen et al., 1997). Although it has been well established that the M6PR recognizes its ligands through an added oligosaccharide side-chain (the M6P tag), both the Vps10p and sortilin receptors interact with ligands through proteinaceous interactions (Kornfeld and Kornfeld, 1985; Marcusson et al., 1994; Tauris et al., 1998). While the residues implicated in the interaction of Vps10 domains and cargo proteins have not yet been characterized, it should be noted that all of the known lysosomal cargo proteins possess prominent α-helices (Baldwin et al., 1993; Guncar et al., 1998; Wright et al., 2000; Zhao et al., 1998).

Together, this information would suggest that the M6PR pathway is a more specific mechanism for sorting soluble lysosomal proteins than is the sortilin pathway. The appearance of this new pathway may also explain why soluble lysosomal proteins differentially traffic via these two different receptors. In spite of the development of this new sorting mechanism, sortilin continues to be a unique sorting receptor that is evolving new functions essential in embryonic development, neural function and apoptosis (Hermans-Borgmeyer et al., 1999; Mazella and Vincent, 2006; Nelson and Alkon, 2007), while still is retaining its capacity to sort of certain soluble proteins (Lefrancois et al., 2003; Ni and Morales, 2006).

The results of this investigation also show that the cytoplasmic domain of sortilin and the M6PR possesses a high degree of structural and functional similarities characterized by the utilization of similar adaptor and accessory proteins to shuttle between the TGN and endosome. To the list of adaptor proteins implicated in the transport of both sorting receptors from the TGN to the endosome, we now add AP-1 complex. Additionally, this investigation confirms that the retromer complex is not exclusive to the M6PR, but also recycles sortilin from the endosomes (Arighi et al., 2004). These findings support our hypothesis that sortilin and the M6PR share an evolutionary conserved mechanism of trafficking between the TGN and the endosomal compartment.

Thus, the present investigation disclosed new aspects of the mechanism and function sortilin, and indirectly of the M6PR, which are significant for the understanding of lysosomal function and of lysosomal storage disorders that result from the impaired trafficking of lysosomal proteins.

Figure C. Model for the Interaction of Prosaposin with Sortilin in DRMs. According to the previously proposed model, prosaposin interacts with sphingomyelin found in the inner leaflet of the TGN membrane. The interaction of prosaposin (blue) with sphingomyelin according to this model occurs through the D-domain of prosaposin and mediates the interaction of the C-terminus of prosaposin with the luminal domain of sortilin (red). Subsequent to this binding, sortilin mediates the transport of prosaposin to the lysosomes via an interaction with the cytosolic GGA adaptor proteins (purple) (Lefrancois et al., 2003).

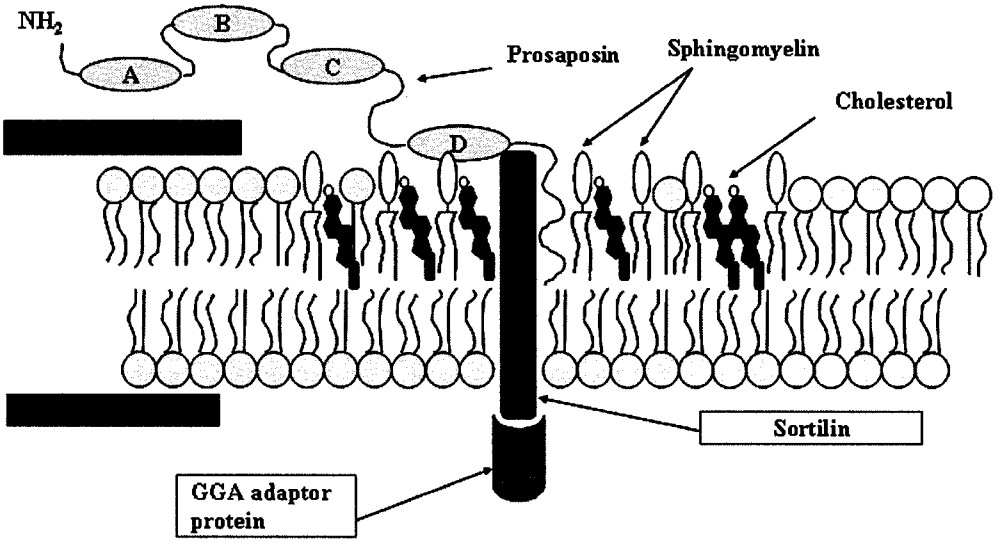
NH2
A
B
C
D
Prosaposin
Sphingomyelin
Cholesterol
Sortilin
GGA adaptor protein

Chapter 7: Original Contributions

We have shown that sortilin binds to cathepsins D and H, but not to cathepsins K and L.

We have demonstrated that inhibition of the sortilin pathway using a dominant-negative truncated sortilin construct results in the mis-sorting of cathepsins D and H, but not cathepsins K or L.

Similarly, by abrogating the expression of sortilin using shRNA, we have confirmed that cathepsin H, but not cathepsins D, K, or L were mis-sorted.

By examining DRM fractions we presented evidence that sortilin and its ligands (prosaposin, cathepsin D, and cathepsin H) reside in DRM microdomains, whereas the M6PR and its ligands (cathepsin B) do not.

Using site directed mutagenesis and a deletion strategy in conjunction with DRM fractionation we have demonstrated that prosaposin is localized to DRMs due to the interaction of its C-terminus with sortilin.

We have demonstrated for the first time important similarities between sortilin and the M6PR.

Using co-immunoprecipitation assays we have shown that sortilin interacts with AP-1 and retromer.

By means of confocal microscopy and RNA inhibition we have demonstrated that AP-1 and retromer are required for the trafficking of sortilin.

We have also identified the YSVL sorting motif in the cytosolic tail of sortilin as an important mediator of the interaction of sortilin and retromer.

In conclusion, our results presented herein demonstrate for the first time that sortilin is an alternative sorting receptor to the M6PR for certain soluble lysosomal

proteins. Based on our data, we propose a model in which sortilin interacts with its ligands through alpha-helical motifs and that this interaction occurs in DRM microdomains present in the TGN membrane. Subsequent to receptor-ligand binding, the interaction of sortilin with AP-1 then helps to mediate its endosomal transport. Finally, via the retromer complex, the sortilin sorting receptor is recycled to the TGN where it may once again interact with and deliver cargo to the endosomes.

Chapter 8: References

Ahle, S., Mann, A., Eichelsbacher, U., and Ungewickell, E. (1988) Structural relationships between clathrin assembly proteins from the Golgi and the plasma membrane. Embo J *7*, 919-929

Arighi, C. N., Hartnell, L. M., Aguilar, R. C., Haft, C. R., and Bonifacino, J. S. (2004) Role of the mammalian retromer in sorting of the cation-independent mannose 6-phosphate receptor. J Cell Biol *165*, 123-133

Azuma, N., Seo, H. C., Lie, O., Fu, Q., Gould, R. M., Hiraiwa, M., Burt, D. W., Paton, I. R., Morrice, D. R., O'Brien, J. S., and Kishimoto, Y. (1998) Cloning, expression and map assignment of chicken prosaposin. Biochem J *330 (Pt 1)*, 321-327

Bach, G. (2001) Mucolipidosis type IV. Mol Genet Metab *73*, 197-203

Bagshaw, R. D., Mahuran, D. J., and Callahan, J. W. (2005a) Lysosomal membrane proteomics and biogenesis of lysosomes. Mol Neurobiol *32*, 27-41

Bagshaw, R. D., Mahuran, D. J., and Callahan, J. W. (2005b) A proteomic analysis of lysosomal integral membrane proteins reveals the diverse composition of the organelle. Mol Cell Proteomics *4*, 133-143

Bainton, D. F. (1981) The discovery of lysosomes. J Cell Biol *91*, 66s-76s

Baldwin, E. T., Bhat, T. N., Gulnik, S., Hosur, M. V., Sowder, R. C., 2nd, Cachau, R. E., Collins, J., Silva, A. M., and Erickson, J. W. (1993) Crystal structures of native and inhibited forms of human cathepsin D: implications for lysosomal targeting and drug design. Proc Natl Acad Sci U S A *90*, 6796-6800

Barak, Y., and Nir, E. (1987) Chediak-Higashi syndrome. Am J Pediatr Hematol Oncol *9*, 42-55

Barlowe, C., Orci, L., Yeung, T., Hosobuchi, M., Hamamoto, S., Salama, N., Rexach, M. F., Ravazzola, M., Amherdt, M., and Schekman, R. (1994) COPII: a membrane coat formed by Sec proteins that drive vesicle budding from the endoplasmic reticulum. Cell *77*, 895-907

Barriocanal, J. G., Bonifacino, J. S., Yuan, L., and Sandoval, I. V. (1986) Biosynthesis, glycosylation, movement through the Golgi system, and transport to lysosomes by an N-linked carbohydrate-independent mechanism of three lysosomal integral membrane proteins. J Biol Chem *261*, 16755-16763

Bennett, M. K., Garcia-Arraras, J. E., Elferink, L. A., Peterson, K., Fleming, A. M., Hazuka, C. D., and Scheller, R. H. (1993) The syntaxin family of vesicular transport receptors. Cell *74*, 863-873

Besterman, J. M., Airhart, J. A., Woodworth, R. C., and Low, R. B. (1981) Exocytosis of pinocytosed fluid in cultured cells: kinetic evidence for rapid turnover and compartmentation. J Cell Biol *91*, 716-727

Beutler, E., Grabowski, GA (1991) Gaucher Disease, In The Metabolic and Molecular Basis of Inherited Disease, S. W. Scriver C, Child B, Beaudet AL, Valle D, Kinzler KW, Vogelstein B, ed. (Columbus: McGraw-Hill Inc), pp. 3635-3668

Bock, J. B., Lin, R. C., and Scheller, R. H. (1996) A new syntaxin family member implicated in targeting of intracellular transport vesicles. J Biol Chem *271*, 17961-17965

Bohley, P., and Seglen, P. O. (1992) Proteases and proteolysis in the lysosome. Experientia *48*, 151-157

Boman, A. L. (2001) GGA proteins: new players in the sorting game. J Cell Sci *114*, 3413-3418

Boman, A. L., Zhang, C., Zhu, X., and Kahn, R. A. (2000) A family of ADP-ribosylation factor effectors that can alter membrane transport through the trans-Golgi. Mol Biol Cell *11*, 1241-1255

Bonifacino, J. S. (2004) The GGA proteins: adaptors on the move. Nat Rev Mol Cell Biol *5*, 23-32

Bonifacino, J. S., and Glick, B. S. (2004) The mechanisms of vesicle budding and fusion. Cell *116*, 153-166

Bradova, V., Smid, F., Ulrich-Bott, B., Roggendorf, W., Paton, B. C., and Harzer, K. (1993) Prosaposin deficiency: further characterization of the sphingolipid activator protein-deficient sibs. Multiple glycolipid elevations (including lactosylceramidosis), partial enzyme deficiencies and ultrastructure of the skin in this generalized sphingolipid storage disease. Hum Genet *92*, 143-152

Braun, M., Waheed, A., and von Figura, K. (1989) Lysosomal acid phosphatase is transported to lysosomes via the cell surface. Embo J *8*, 3633-3640

Buckmaster, M. J., Lo Braico, D., Jr., Ferris, A. L., and Storrie, B. (1987) Retention of pinocytized solute by CHO cell lysosomes correlates with molecular weight. Cell Biol Int Rep *11*, 501-507

Cai, H., Reinisch, K., and Ferro-Novick, S. (2007) Coats, tethers, Rabs, and SNAREs work together to mediate the intracellular destination of a transport vesicle. Dev Cell *12*, 671-682

Chen, Y. A., and Scheller, R. H. (2001) SNARE-mediated membrane fusion. Nat Rev Mol Cell Biol *2*, 98-106

Christomanou, H., Aignesberger, A., and Linke, R. P. (1986) Immunochemical characterization of two activator proteins stimulating enzymic sphingomyelin degradation in vitro. Absence of one of them in a human Gaucher disease variant. Biol Chem Hoppe Seyler *367*, 879-890

Clark, R., and Griffiths, G. M. (2003) Lytic granules, secretory lysosomes and disease. Curr Opin Immunol *15*, 516-521

Claveau, D., and Riendeau, D. (2001) Mutations of the C-terminal end of cathepsin K affect proenzyme secretion and intracellular maturation. Biochem Biophys Res Commun *281*, 551-557

Clermont, Y., Morales, C., and Hermo, L. (1987) Endocytic activities of Sertoli cells in the rat. Ann N Y Acad Sci *513*, 1-15

Collins, B. M., Skinner, C. F., Watson, P. J., Seaman, M. N., and Owen, D. J. (2005) Vps29 has a phosphoesterase fold that acts as a protein interaction scaffold for retromer assembly. Nat Struct Mol Biol *12*, 594-602

Collins, B. M., Watson, P. J., and Owen, D. J. (2003) The structure of the GGA1-GAT domain reveals the molecular basis for ARF binding and membrane association of GGAs. Dev Cell *4*, 321-332

Conticello, S. G., Kowalsman, N. D., Jacobsen, C., Yudkovsky, G., Sato, K., Elazar, Z., Petersen, C. M., Aronheim, A., and Fainzilber, M. (2003) The prodomain of a secreted hydrophobic mini-protein facilitates its export from the endoplasmic reticulum by hitchhiking on sorting receptors. J Biol Chem *278*, 26311-26314

Conzelmann, E., and Sandhoff, K. (1978) AB variant of infantile GM2 gangliosidosis: deficiency of a factor necessary for stimulation of hexosaminidase A-catalyzed degradation of ganglioside GM2 and glycolipid GA2. Proc Natl Acad Sci U S A *75*, 3979-3983

Cooper, A. A., and Stevens, T. H. (1996) Vps10p cycles between the late-Golgi and prevacuolar compartments in its function as the sorting receptor for multiple yeast vacuolar hydrolases. J Cell Biol *133*, 529-541

D'Azzo, A., Hoogeveen, A., Reuser, A. J., Robinson, D., and Galjaard, H. (1982) Molecular defect in combined beta-galactosidase and neuraminidase deficiency in man. Proc Natl Acad Sci U S A *79*, 4535-4539

d'Azzo, A., Andria, G., Strisciuglio, G., and Galjaard, H. (2001), In Metabolic and Molecular Bases of Inherited Disease, C. R. Scriver, Beaudet, A. L., Sly, W. S., and Valle, D.,, ed. (New York: McGraw-Hill Inc), pp. 3811–3826

Dahms, N. M., Lobel, P., Breitmeyer, J., Chirgwin, J. M., and Kornfeld, S. (1987) 46 kd mannose 6-phosphate receptor: cloning, expression, and homology to the 215 kd mannose 6-phosphate receptor. Cell *50*, 181-192

Damen, E., Krieger, E., Nielsen, J. E., Eygensteyn, J., and van Leeuwen, J. E. (2006) The human Vps29 retromer component is a metallo-phosphoesterase for a cation-independent mannose 6-phosphate receptor substrate peptide. Biochem J *398*, 399-409

Dell'Angelica, E. C., Mullins, C., Caplan, S., and Bonifacino, J. S. (2000a) Lysosome-related organelles. Faseb J *14*, 1265-1278

Dell'Angelica, E. C., Puertollano, R., Mullins, C., Aguilar, R. C., Vargas, J. D., Hartnell, L. M., and Bonifacino, J. S. (2000b) GGAs: a family of ADP ribosylation

factor-binding proteins related to adaptors and associated with the Golgi complex. J Cell Biol *149*, 81-94

Dell'Angelica, E. C., Shotelersuk, V., Aguilar, R. C., Gahl, W. A., and Bonifacino, J. S. (1999) Altered trafficking of lysosomal proteins in Hermansky-Pudlak syndrome due to mutations in the beta 3A subunit of the AP-3 adaptor. Mol Cell *3*, 11-21

Diaz, E., and Pfeffer, S. R. (1998) TIP47: a cargo selection device for mannose 6-phosphate receptor trafficking. Cell *93*, 433-443

Doray, B., Bruns, K., Ghosh, P., and Kornfeld, S. (2002a) Interaction of the cation-dependent mannose 6-phosphate receptor with GGA proteins. J Biol Chem *277*, 18477-18482

Doray, B., Ghosh, P., Griffith, J., Geuze, H. J., and Kornfeld, S. (2002b) Cooperation of GGAs and AP-1 in packaging MPRs at the trans-Golgi network. Science *297*, 1700-1703

Elleder, M., Jerabkova, M., Befekadu, A., Hrebicek, M., Berna, L., Ledvinova, J., Hulkova, H., Rosewich, H., Schymik, N., Paton, B. C., and Harzer, K. (2005) Prosaposin deficiency -- a rarely diagnosed, rapidly progressing, neonatal neurovisceral lipid storage disease. Report of a further patient. Neuropediatrics *36*, 171-180

Eskelinen, E. L., Tanaka, Y., and Saftig, P. (2003) At the acidic edge: emerging functions for lysosomal membrane proteins. Trends Cell Biol *13*, 137-145

Fabbro, D., and Grabowski, G. A. (1991) Human acid beta-glucosidase. Use of inhibitory and activating monoclonal antibodies to investigate the enzyme's catalytic mechanism and saposin A and C binding sites. J Biol Chem *266*, 15021-15027

Feng, Y., Press, B., and Wandinger-Ness, A. (1995) Rab 7: an important regulator of late endocytic membrane traffic. J Cell Biol *131*, 1435-1452

Fernandes Filho, J. A., and Shapiro, B. E. (2004) Tay-Sachs disease. Arch Neurol *61*, 1466-1468

Forgac, M. (1999) Structure and properties of the vacuolar (H+)-ATPases. J Biol Chem *274*, 12951-12954

Frattini, A., Orchard, P. J., Sobacchi, C., Giliani, S., Abinun, M., Mattsson, J. P., Keeling, D. J., Andersson, A. K., Wallbrandt, P., Zecca, L., *et al.* (2000) Defects in TCIRG1 subunit of the vacuolar proton pump are responsible for a subset of human autosomal recessive osteopetrosis. Nat Genet *25*, 343-346

Fukuda, M. (1991) Lysosomal membrane glycoproteins. Structure, biosynthesis, and intracellular trafficking. J Biol Chem *266*, 21327-21330

Furst, W., and Sandhoff, K. (1992) Activator proteins and topology of lysosomal sphingolipid catabolism. Biochim Biophys Acta *1126*, 1-16

Gabel, C. A., Goldberg, D. E., and Kornfeld, S. (1983) Identification and characterization of cells deficient in the mannose 6-phosphate receptor: evidence for an alternate pathway for lysosomal enzyme targeting. Proc Natl Acad Sci U S A *80*, 775-779

Geuze, H. J., Slot, J. W., Strous, G. J., Lodish, H. F., and Schwartz, A. L. (1983) Intracellular site of asialoglycoprotein receptor-ligand uncoupling: double-label immunoelectron microscopy during receptor-mediated endocytosis. Cell *32*, 277-287

Ghosh, P., and Kornfeld, S. (2004) The GGA proteins: key players in protein sorting at the trans-Golgi network. Eur J Cell Biol *83*, 257-262

Giehl, A., Lemm, T., Bartelsen, O., Sandhoff, K., and Blume, A. (1999) Interaction of the GM2-activator protein with phospholipid-ganglioside bilayer membranes and with monolayers at the air-water interface. Eur J Biochem *261*, 650-658

Gieselmann, V. (2003) Metachromatic leukodystrophy: recent research developments. J Child Neurol *18*, 591-594

Gieselmann, V., Franken, S., Klein, D., Mansson, J. E., Sandhoff, R., Lullmann Rauch, R., Hartmann, D., Saravanan, V. P., De Deyn, P. P., D'Hooge, R., *et al.* (2003) Metachromatic leukodystrophy: consequences of sulphatide accumulation. Acta Paediatr Suppl *92*, 74-79; discussion 45

Gieselmann, V., Hasilik, A., and von Figura, K. (1984) Tartrate-inhibitable acid phosphatase. Purification from placenta, characterization and subcellular distribution in fibroblasts. Hoppe Seylers Z Physiol Chem *365*, 651-660

Gkantiragas, I., Brugger, B., Stuven, E., Kaloyanova, D., Li, X. Y., Lohr, K., Lottspeich, F., Wieland, F. T., and Helms, J. B. (2001) Sphingomyelin-enriched microdomains at the Golgi complex. Mol Biol Cell *12*, 1819-1833

Glew, R. H., Basu, A., LaMarco, K. L., and Prence, E. M. (1988) Mammalian glucocerebrosidase: implications for Gaucher's disease. Lab Invest *58*, 5-25

Glickman, J. N., and Kornfeld, S. (1993) Mannose 6-phosphate-independent targeting of lysosomal enzymes in I-cell disease B lymphoblasts. J Cell Biol *123*, 99-108

Gordon, R. M., and Marchese, T. (2004) Mucolipidosis type IV a rare genetic disorder: new addition to the Ashkenazi Jewish panel. J Midwifery Womens Health *49*, 359-360

Gottesman, M. M. (1978) Transformation-dependent secretion of a low molecular weight protein by murine fibroblasts. Proc Natl Acad Sci U S A *75*, 2767-2771

Gottschalk, S., Waheed, A., Schmidt, B., Laidler, P., and von Figura, K. (1989) Sequential processing of lysosomal acid phosphatase by a cytoplasmic thiol proteinase and a lysosomal aspartyl proteinase. Embo J *8*, 3215-3219

Gravel RA, C. J., Kaback MM, Mahuran D, Sandhoff K, Suzuki K (1995) The GM2 gangliosidoses, In The Metabolic and Molecular Bases of Inherited Disease, B. a. S. W. Scriver C, Valle D, ed. (New York: McGraw-Hill), pp. 2839-2879

Griffiths, G. M., and Isaaz, S. (1993) Granzymes A and B are targeted to the lytic granules of lymphocytes by the mannose-6-phosphate receptor. J Cell Biol *120*, 885-896

Guncar, G., Podobnik, M., Pungercar, J., Strukelj, B., Turk, V., and Turk, D. (1998) Crystal structure of porcine cathepsin H determined at 2.1 A resolution: location of the mini-chain C-terminal carboxyl group defines cathepsin H aminopeptidase function. Structure *6*, 51-61

Haft, C. R., de la Luz Sierra, M., Bafford, R., Lesniak, M. A., Barr, V. A., and Taylor, S. I. (2000) Human orthologs of yeast vacuolar protein sorting proteins Vps26, 29, and 35: assembly into multimeric complexes. Mol Biol Cell *11*, 4105-4116

Hammer, J. A., 3rd, and Wu, X. S. (2002) Rabs grab motors: defining the connections between Rab GTPases and motor proteins. Curr Opin Cell Biol *14*, 69-75

Hampe, W., Rezgaoui, M., Hermans-Borgmeyer, I., and Schaller, H. C. (2001) The genes for the human VPS10 domain-containing receptors are large and contain many small exons. Hum Genet *108*, 529-536

Hancock, M. K., Haskins, D. J., Sun, G., and Dahms, N. M. (2002) Identification of residues essential for carbohydrate recognition by the insulin-like growth factor II/mannose 6-phosphate receptor. J Biol Chem *277*, 11255-11264

Harter, C., and Mellman, I. (1992) Transport of the lysosomal membrane glycoprotein lgp120 (lgp-A) to lysosomes does not require appearance on the plasma membrane. J Cell Biol *117*, 311-325

Harzer, K., Paton, B. C., Poulos, A., Kustermann-Kuhn, B., Roggendorf, W., Grisar, T., and Popp, M. (1989) Sphingolipid activator protein deficiency in a 16-week-old atypical Gaucher disease patient and his fetal sibling: biochemical signs of combined sphingolipidoses. Eur J Pediatr *149*, 31-39

Hasilik, A. (1992) The early and late processing of lysosomal enzymes: proteolysis and compartmentation. Experientia *48*, 130-151

Hasilik, A., Waheed, A., and von Figura, K. (1981) Enzymatic phosphorylation of lysosomal enzymes in the presence of UDP-N-acetylglucosamine. Absence of the activity in I-cell fibroblasts. Biochem Biophys Res Commun *98*, 761-767

Hassan, A. J., Zeng, J., Ni, X., and Morales, C. R. (2004) The trafficking of prosaposin (SGP-1) and GM2AP to the lysosomes of TM4 Sertoli cells is mediated by sortilin and monomeric adaptor proteins. Mol Reprod Dev *68*, 476-483

Helms, J. B., and Zurzolo, C. (2004) Lipids as targeting signals: lipid rafts and intracellular trafficking. Traffic *5*, 247-254

Hermans-Borgmeyer, I., Hermey, G., Nykjaer, A., and Schaller, C. (1999) Expression of the 100-kDa neurotensin receptor sortilin during mouse embryonal development. Brain Res Mol Brain Res *65*, 216-219

Hermey, G., Riedel, I. B., Hampe, W., Schaller, H. C., and Hermans-Borgmeyer, I. (1999) Identification and characterization of SorCS, a third member of a novel receptor family. Biochem Biophys Res Commun *266*, 347-351

Hinek, A., Pshezhetsky, A. V., von Itzstein, M., and Starcher, B. (2006) Lysosomal sialidase (neuraminidase-1) is targeted to the cell surface in a multiprotein complex that facilitates elastic fiber assembly. J Biol Chem *281*, 3698-3710

Hirst, J., Lindsay, M. R., and Robinson, M. S. (2001) GGAs: roles of the different domains and comparison with AP-1 and clathrin. Mol Biol Cell *12*, 3573-3588

Hirst, J., Lui, W. W., Bright, N. A., Totty, N., Seaman, M. N., and Robinson, M. S. (2000) A family of proteins with gamma-adaptin and VHS domains that facilitate trafficking between the trans-Golgi network and the vacuole/lysosome. J Cell Biol *149*, 67-80

Ho, M. W., and O'Brien, J. S. (1971) Gaucher's disease: deficiency of 'acid' -glucosidase and reconstitution of enzyme activity in vitro. Proc Natl Acad Sci U S A *68*, 2810-2813

Holtschmidt, H., Sandhoff, K., Kwon, H. Y., Harzer, K., Nakano, T., and Suzuki, K. (1991) Sulfatide activator protein. Alternative splicing that generates three mRNAs and a newly found mutation responsible for a clinical disease. J Biol Chem *266*, 7556-7560

Hong, W. (2005) SNAREs and traffic. Biochim Biophys Acta *1744*, 493-517

Honing, S., and Hunziker, W. (1995) Cytoplasmic determinants involved in direct lysosomal sorting, endocytosis, and basolateral targeting of rat lgp120 (lamp-I) in MDCK cells. J Cell Biol *128*, 321-332

Honing, S., Sosa, M., Hille-Rehfeld, A., and von Figura, K. (1997) The 46-kDa mannose 6-phosphate receptor contains multiple binding sites for clathrin adaptors. J Biol Chem *272*, 19884-19890

Hulkova, H., Cervenkova, M., Ledvinova, J., Tochackova, M., Hrebicek, M., Poupetova, H., Befekadu, A., Berna, L., Paton, B. C., Harzer, K., *et al.* (2001) A novel mutation in the coding region of the prosaposin gene leads to a complete deficiency of prosaposin and saposins, and is associated with a complex sphingolipidosis dominated by lactosylceramide accumulation. Hum Mol Genet *10*, 927-940

Ikonen, E. (2001) Roles of lipid rafts in membrane transport. Curr Opin Cell Biol *13*, 470-477

Inui, K., and Wenger, D. A. (1984) Biochemical, immunological, and structural studies on a sphingolipid activator protein (SAP-1). Arch Biochem Biophys *233*, 556-564

Jacobsen, L., Madsen, P., Jacobsen, C., Nielsen, M. S., Gliemann, J., and Petersen, C. M. (2001) Activation and functional characterization of the mosaic receptor SorLA/LR11. J Biol Chem *276*, 22788-22796

Jacobsen, L., Madsen, P., Moestrup, S. K., Lund, A. H., Tommerup, N., Nykjaer, A., Sottrup-Jensen, L., Gliemann, J., and Petersen, C. M. (1996) Molecular characterization of a novel human hybrid-type receptor that binds the alpha2-macroglobulin receptor-associated protein. J Biol Chem *271*, 31379-31383

Jahn, R., and Grubmuller, H. (2002) Membrane fusion. Curr Opin Cell Biol *14*, 488-495

Jahn, R., and Scheller, R. H. (2006) SNAREs--engines for membrane fusion. Nat Rev Mol Cell Biol *7*, 631-643

Jahraus, A., Storrie, B., Griffiths, G., and Desjardins, M. (1994) Evidence for retrograde traffic between terminal lysosomes and the prelysosomal/late endosome compartment. J Cell Sci *107 (Pt 1)*, 145-157

Janvier, K., and Bonifacino, J. S. (2005) Role of the endocytic machinery in the sorting of lysosome-associated membrane proteins. Mol Biol Cell *16*, 4231-4242

Jatzkewitz, H. (1958) [Two types of cerebroside sulfates as so-called prelipids and storage substances in leukodystrophy of type Scholz (metachromatic form of diffuse sclerosis).]. Hoppe Seylers Z Physiol Chem *311*, 279-282

Johnson, K. F., and Kornfeld, S. (1992) The cytoplasmic tail of the mannose 6-phosphate/insulin-like growth factor-II receptor has two signals for lysosomal enzyme sorting in the Golgi. J Cell Biol *119*, 249-257

Johnson, L. M., Bankaitis, V. A., and Emr, S. D. (1987) Distinct sequence determinants direct intracellular sorting and modification of a yeast vacuolar protease. Cell *48*, 875-885

Kang, J. X., Li, Y., and Leaf, A. (1997) Mannose-6-phosphate/insulin-like growth factor-II receptor is a receptor for retinoic acid. Proc Natl Acad Sci U S A *94*, 13671-13676

Kaplan, A., Fischer, D., Achord, D., and Sly, W. (1977) Phosphohexosyl recognition is a general characteristic of pinocytosis of lysosomal glycosidases by human fibroblasts. J Clin Invest *60*, 1088-1093

Kelly, T. E., Thomas, G. H., Taylor, H. A., Jr., McKusick, V. A., Sly, W. S., Glaser, J. H., Robinow, M., Luzzatti, L., Espiritu, C., Feingold, M., *et al.* (1975) Mucolipidosis III (pseudo-Hurler polydystrophy): Clinical and laboratory studies in a series of 12 patients. Johns Hopkins Med J *137*, 156-175

Kolter, T., and Sandhoff, K. (1998) Glycosphingolipid degradation and animal models of GM2-gangliosidoses. J Inherit Metab Dis *21*, 548-563

Kornfeld, R., and Kornfeld, S. (1985) Assembly of asparagine-linked oligosaccharides. Annu Rev Biochem *54*, 631-664

Kornfeld, S. (1986) Trafficking of lysosomal enzymes in normal and disease states. J Clin Invest *77*, 1-6

LaPlante, J. M., Falardeau, J., Sun, M., Kanazirska, M., Brown, E. M., Slaugenhaupt, S. A., and Vassilev, P. M. (2002) Identification and characterization of the single channel function of human mucolipin-1 implicated in mucolipidosis type IV, a disorder affecting the lysosomal pathway. FEBS Lett *532*, 183-187

Le Borgne, R., Schmidt, A., Mauxion, F., Griffiths, G., and Hoflack, B. (1993) Binding of AP-1 Golgi adaptors to membranes requires phosphorylated cytoplasmic domains of the mannose 6-phosphate/insulin-like growth factor II receptor. J Biol Chem *268*, 22552-22556

Lee, S. J., and Nathans, D. (1988) Proliferin secreted by cultured cells binds to mannose 6-phosphate receptors. J Biol Chem *263*, 3521-3527

Lefrancois, S., May, T., Knight, C., Bourbeau, D., and Morales, C. R. (2002) The lysosomal transport of prosaposin requires the conditional interaction of its highly conserved d domain with sphingomyelin. J Biol Chem *277*, 17188-17199

Lefrancois, S., Michaud, L., Potier, M., Igdoura, S., and Morales, C. R. (1999) Role of sphingolipids in the transport of prosaposin to the lysosomes. J Lipid Res *40*, 1593-1603

Lefrancois, S., Zeng, J., Hassan, A. J., Canuel, M., and Morales, C. R. (2003) The lysosomal trafficking of sphingolipid activator proteins (SAPs) is mediated by sortilin. Embo J *22*, 6430-6437

LeRoy, J. G., and Demars, R.I. (1967) Mutant enzymatic and cytological phenotypes in cultured human fibroblasts. Science *157*, 804-806

Leroy, J. G., and Spranger, J. W. (1970) I-cell disease. N Engl J Med *283*, 598-599

Li, S. C., Sonnino, S., Tettamanti, G., and Li, Y. T. (1988) Characterization of a nonspecific activator protein for the enzymatic hydrolysis of glycolipids. J Biol Chem *263*, 6588-6591

Li, Y. T., Li, S. C., Hasegawa, A., Ishida, H., Kiso, M., Bernardi, A., Brocca, P., Raimondi, L., and Sonnino, S. (1999) Structural basis for the resistance of Tay-Sachs ganglioside GM2 to enzymatic degradation. J Biol Chem *274*, 10014-10018

Liang, F., Seyrantepe, V., Landry, K., Ahmad, R., Ahmad, A., Stamatos, N. M., and Pshezhetsky, A. V. (2006) Monocyte differentiation up-regulates the expression of the lysosomal sialidase, Neu1, and triggers its targeting to the plasma membrane via major histocompatibility complex class II-positive compartments. J Biol Chem *281*, 27526-27538

Lobel, P., Fujimoto, K., Ye, R. D., Griffiths, G., and Kornfeld, S. (1989) Mutations in the cytoplasmic domain of the 275 kd mannose 6-phosphate receptor differentially alter lysosomal enzyme sorting and endocytosis. Cell *57*, 787-796

Ludwig, T., Munier-Lehmann, H., Bauer, U., Hollinshead, M., Ovitt, C., Lobel, P., and Hoflack, B. (1994) Differential sorting of lysosomal enzymes in mannose 6-phosphate receptor-deficient fibroblasts. Embo J *13*, 3430-3437

Lukong, K. E., Elsliger, M. A., Mort, J. S., Potier, M., and Pshezhetsky, A. V. (1999) Identification of UDP-N-acetylglucosamine-phosphotransferase-binding sites on the lysosomal proteases, cathepsins A, B, and D. Biochemistry *38*, 73-80

Lukong, K. E., Seyrantepe, V., Landry, K., Trudel, S., Ahmad, A., Gahl, W. A., Lefrancois, S., Morales, C. R., and Pshezhetsky, A. V. (2001) Intracellular distribution of lysosomal sialidase is controlled by the internalization signal in its cytoplasmic tail. J Biol Chem *276*, 46172-46181

MacDonald, R. G., Pfeffer, S. R., Coussens, L., Tepper, M. A., Brocklebank, C. M., Mole, J. E., Anderson, J. K., Chen, E., Czech, M. P., and Ullrich, A. (1988) A single receptor binds both insulin-like growth factor II and mannose-6-phosphate. Science *239*, 1134-1137

Mahuran, D. J. (1998) The GM2 activator protein, its roles as a co-factor in GM2 hydrolysis and as a general glycolipid transport protein. Biochim Biophys Acta *1393*, 1-18

Malsam, J., Satoh, A., Pelletier, L., and Warren, G. (2005) Golgin tethers define subpopulations of COPI vesicles. Science *307*, 1095-1098

Marcusson, E. G., Horazdovsky, B. F., Cereghino, J. L., Gharakhanian, E., and Emr, S. D. (1994) The sorting receptor for yeast vacuolar carboxypeptidase Y is encoded by the VPS10 gene. Cell *77*, 579-586

Marks, M. S., Roche, P. A., van Donselaar, E., Woodruff, L., Peters, P. J., and Bonifacino, J. S. (1995) A lysosomal targeting signal in the cytoplasmic tail of the beta chain directs HLA-DM to MHC class II compartments. J Cell Biol *131*, 351-369

Marks, S. C., Jr. (1989) Osteoclast biology: lessons from mammalian mutations. Am J Med Genet *34*, 43-54

Martin, S., Navarro, V., Vincent, J. P., and Mazella, J. (2002) Neurotensin receptor-1 and -3 complex modulates the cellular signaling of neurotensin in the HT29 cell line. Gastroenterology *123*, 1135-1143

Matanis, T., Akhmanova, A., Wulf, P., Del Nery, E., Weide, T., Stepanova, T., Galjart, N., Grosveld, F., Goud, B., De Zeeuw, C. I., *et al.* (2002) Bicaudal-D regulates COPI-independent Golgi-ER transport by recruiting the dynein-dynactin motor complex. Nat Cell Biol *4*, 986-992

Matsuda, J., Kido, M., Tadano-Aritomi, K., Ishizuka, I., Tominaga, K., Toida, K., Takeda, E., Suzuki, K., and Kuroda, Y. (2004) Mutation in saposin D domain of sphingolipid activator protein gene causes urinary system defects and cerebellar Purkinje cell degeneration with accumulation of hydroxy fatty acid-containing ceramide in mouse. Hum Mol Genet *13*, 2709-2723

Matsuda, J., Vanier, M. T., Saito, Y., Tohyama, J., Suzuki, K., and Suzuki, K. (2001) A mutation in the saposin A domain of the sphingolipid activator protein (prosaposin) gene results in a late-onset, chronic form of globoid cell leukodystrophy in the mouse. Hum Mol Genet *10*, 1191-1199

Maxfield, F. R. (1982) Weak bases and ionophores rapidly and reversibly raise the pH of endocytic vesicles in cultured mouse fibroblasts. J Cell Biol *95*, 676-681

Mazella, J., and Vincent, J. P. (2006) Internalization and recycling properties of neurotensin receptors. Peptides *27*, 2488-2492

Mazella, J., Zsurger, N., Navarro, V., Chabry, J., Kaghad, M., Caput, D., Ferrara, P., Vita, N., Gully, D., Maffrand, J. P., and Vincent, J. P. (1998) The 100-kDa neurotensin receptor is gp95/sortilin, a non-G-protein-coupled receptor. J Biol Chem *273*, 26273-26276

Meier, E. M., Schwarzmann, G., Furst, W., and Sandhoff, K. (1991) The human GM2 activator protein. A substrate specific cofactor of beta-hexosaminidase A. J Biol Chem *266*, 1879-1887

Meikle, P. J., Hopwood, J. J., Clague, A. E., and Carey, W. F. (1999) Prevalence of lysosomal storage disorders. Jama *281*, 249-254

Mellman, I. (1996) Endocytosis and molecular sorting. Annu Rev Cell Dev Biol *12*, 575-625

Metzelaar, M. J., Wijngaard, P. L., Peters, P. J., Sixma, J. J., Nieuwenhuis, H. K., and Clevers, H. C. (1991) CD63 antigen. A novel lysosomal membrane glycoprotein, cloned by a screening procedure for intracellular antigens in eukaryotic cells. J Biol Chem *266*, 3239-3245

Meyer, C., Eskelinen, E. L., Guruprasad, M. R., von Figura, K., and Schu, P. (2001) Mu 1A deficiency induces a profound increase in MPR300/IGF-II receptor internalization rate. J Cell Sci *114*, 4469-4476

Meyer, C., Zizioli, D., Lausmann, S., Eskelinen, E. L., Hamann, J., Saftig, P., von Figura, K., and Schu, P. (2000) mu1A-adaptin-deficient mice: lethality, loss of AP-1 binding and rerouting of mannose 6-phosphate receptors. Embo J *19*, 2193-2203

Misra, S., Beach, B. M., and Hurley, J. H. (2000) Structure of the VHS domain of human Tom1 (target of myb 1): insights into interactions with proteins and membranes. Biochemistry *39*, 11282-11290

Miyatake, T., and Suzuki, K. (1972) Globoid cell leukodystrophy: additional deficiency of psychosine galactosidase. Biochem Biophys Res Commun *48*, 539-543

Morales, C. R., el-Alfy, M., Zhao, Q., and Igdoura, S. (1995) Molecular role of sulfated glycoprotein-1 (SGP-1/prosaposin) in Sertoli cells. Histol Histopathol *10*, 1023-1034

Morales, C. R., Fuska, J., Zhao, Q., and Lefrancois, S. (2001) Biogenesis of lysosomes in marshall cells and in cells of the male reproductive system. Mol Reprod Dev *59*, 54-66

Morales, C. R., Zhao, Q., and Lefrancois, S. (1999) Biogenesis of lysosomes by endocytic flow of plasma membrane. Biocell *23*, 149-160

Morgan, D. O., Edman, J. C., Standring, D. N., Fried, V. A., Smith, M. C., Roth, R. A., and Rutter, W. J. (1987) Insulin-like growth factor II receptor as a multifunctional binding protein. Nature *329*, 301-307

Morimoto, S., Martin, B. M., Kishimoto, Y., and O'Brien, J. S. (1988) Saposin D: a sphingomyelinase activator. Biochem Biophys Res Commun *156*, 403-410

Morimoto, S., Martin, B. M., Yamamoto, Y., Kretz, K. A., O'Brien, J. S., and Kishimoto, Y. (1989) Saposin A: second cerebrosidase activator protein. Proc Natl Acad Sci U S A *86*, 3389-3393

Morinville, A., Martin, S., Lavallee, M., Vincent, J. P., Beaudet, A., and Mazella, J. (2004) Internalization and trafficking of neurotensin via NTS3 receptors in HT29 cells. Int J Biochem Cell Biol *36*, 2153-2168

Mort, J. S., and Buttle, D. J. (1997) Cathepsin B. Int J Biochem Cell Biol *29*, 715-720

Nakano, T., Sandhoff, K., Stumper, J., Christomanou, H., and Suzuki, K. (1989) Structure of full-length cDNA coding for sulfatide activator, a Co-beta-glucosidase and two other homologous proteins: two alternate forms of the sulfatide activator. J Biochem (Tokyo) *105*, 152-154

Nalini, A., and Christopher, R. (2004) Cerebral glycolipidoses: clinical characteristics of 41 pediatric patients. J Child Neurol *19*, 447-452

Nelson, T. J., and Alkon, D. L. (2007) Protection against beta-amyloid induced apoptosis by peptides interacting with beta-amyloid. J Biol Chem

Nguyen, G. (2006) Renin/prorenin receptors. Kidney Int *69*, 1503-1506

Ni, X., and Morales, C. R. (2006) The lysosomal trafficking of acid sphingomyelinase is mediated by sortilin and mannose 6-phosphate receptor. Traffic *7*, 889-902

Nielsen, M. S., Jacobsen, C., Olivecrona, G., Gliemann, J., and Petersen, C. M. (1999) Sortilin/neurotensin receptor-3 binds and mediates degradation of lipoprotein lipase. J Biol Chem *274*, 8832-8836

Nielsen, M. S., Madsen, P., Christensen, E. I., Nykjaer, A., Gliemann, J., Kasper, D., Pohlmann, R., and Petersen, C. M. (2001) The sortilin cytoplasmic tail conveys Golgi-endosome transport and binds the VHS domain of the GGA2 sorting protein. Embo J *20*, 2180-2190

Nolan, C. M., and Sly, W.S. (1989) I-cell disease and pseudo-hurler polydystrophy: disorders of lysosomal enzyme phosphorylation and localization, In The Metabolic basis of Inherited Disease, C. R. Schriver, Beaudet, A.L., Sly, W.S. & Valle, D., ed. (New York: McGraw-Hill), pp. 1589–1601

Nykjaer, A., Christensen, E. I., Vorum, H., Hager, H., Petersen, C. M., Roigaard, H., Min, H. Y., Vilhardt, F., Moller, L. B., Kornfeld, S., and Gliemann, J. (1998) Mannose 6-phosphate/insulin-like growth factor-II receptor targets the urokinase receptor to lysosomes via a novel binding interaction. J Cell Biol *141*, 815-828

Nykjaer, A., Lee, R., Teng, K. K., Jansen, P., Madsen, P., Nielsen, M. S., Jacobsen, C., Kliemannel, M., Schwarz, E., Willnow, T. E., *et al.* (2004) Sortilin is essential for proNGF-induced neuronal cell death. Nature *427*, 843-848

O'Brien, J. S., and Kishimoto, Y. (1991) Saposin proteins: structure, function, and role in human lysosomal storage disorders. Faseb J *5*, 301-308

O'Brien, J. S., Kretz, K. A., Dewji, N., Wenger, D. A., Esch, F., and Fluharty, A. L. (1988) Coding of two sphingolipid activator proteins (SAP-1 and SAP-2) by same genetic locus. Science *241*, 1098-1101

Oesterreicher, S., Blum, W. F., Schmidt, B., Braulke, T., and Kubler, B. (2005) Interaction of insulin-like growth factor II (IGF-II) with multiple plasma proteins: high affinity binding of plasminogen to IGF-II and IGF-binding protein-3. J Biol Chem *280*, 9994-10000

Ogata, S., and Fukuda, M. (1994) Lysosomal targeting of Limp II membrane glycoprotein requires a novel Leu-Ile motif at a particular position in its cytoplasmic tail. J Biol Chem *269*, 5210-5217

Ohno, H., Aguilar, R. C., Fournier, M. C., Hennecke, S., Cosson, P., and Bonifacino, J. S. (1997) Interaction of endocytic signals from the HIV-1 envelope glycoprotein complex with members of the adaptor medium chain family. Virology *238*, 305-315

Ohno, H., Stewart, J., Fournier, M. C., Bosshart, H., Rhee, I., Miyatake, S., Saito, T., Gallusser, A., Kirchhausen, T., and Bonifacino, J. S. (1995) Interaction of tyrosine-based sorting signals with clathrin-associated proteins. Science *269*, 1872-1875

Okada, S., and O'Brien, J. S. (1969) Tay-Sachs disease: generalized absence of a beta-D-N-acetylhexosaminidase component. Science *165*, 698-700

Owen, D. J., and Evans, P. R. (1998) A structural explanation for the recognition of tyrosine-based endocytotic signals. Science *282*, 1327-1332

Parkinson-Lawrence, E., Fuller, M., Hopwood, J. J., Meikle, P. J., and Brooks, D. A. (2006) Immunochemistry of Lysosomal Storage Disorders. Clin Chem

Paton, B. C., Schmid, B., Kustermann-Kuhn, B., Poulos, A., and Harzer, K. (1992) Additional biochemical findings in a patient and fetal sibling with a genetic defect in the sphingolipid activator protein (SAP) precursor, prosaposin. Evidence for a deficiency in SAP-1 and for a normal lysosomal neuraminidase. Biochem J *285 (Pt 2)*, 481-488

Pearse, B. M. (1975) Coated vesicles from pig brain: purification and biochemical characterization. J Mol Biol *97*, 93-98

Pelham, H. R., and Rothman, J. E. (2000) The debate about transport in the Golgi--two sides of the same coin? Cell *102*, 713-719

Peters, C., Braun, M., Weber, B., Wendland, M., Schmidt, B., Pohlmann, R., Waheed, A., and von Figura, K. (1990) Targeting of a lysosomal membrane protein: a tyrosine-

containing endocytosis signal in the cytoplasmic tail of lysosomal acid phosphatase is necessary and sufficient for targeting to lysosomes. Embo J *9*, 3497-3506

Peters, S. P., Coyle, P., Coffee, C. J., and Glew, R. H. (1977) Purification and properties of a heat-stable glucocerebrosidase activating factor from control and Gaucher spleen. J Biol Chem *252*, 563-573

Petersen, C. M., Nielsen, M. S., Nykjaer, A., Jacobsen, L., Tommerup, N., Rasmussen, H. H., Roigaard, H., Gliemann, J., Madsen, P., and Moestrup, S. K. (1997) Molecular identification of a novel candidate sorting receptor purified from human brain by receptor-associated protein affinity chromatography. J Biol Chem *272*, 3599-3605

Probst, O. C., Ton, P., Svoboda, B., Gannon, A., Schuhmann, W., Wieser, J., Pohlmann, R., and Mach, L. (2006) The 46-kDa mannose 6-phosphate receptor does not depend on endosomal acidification for delivery of hydrolases to lysosomes. J Cell Sci *119*, 4935-4943

Pshezhetsky, A. V., and Ashmarina, M. (2001) Lysosomal multienzyme complex: biochemistry, genetics, and molecular pathophysiology. Prog Nucleic Acid Res Mol Biol *69*, 81-114

Puertollano, R., Aguilar, R. C., Gorshkova, I., Crouch, R. J., and Bonifacino, J. S. (2001) Sorting of mannose 6-phosphate receptors mediated by the GGAs. Science *292*, 1712-1716

Qi, X., Leonova, T., and Grabowski, G. A. (1994) Functional human saposins expressed in Escherichia coli. Evidence for binding and activation properties of saposins C with acid beta-glucosidase. J Biol Chem *269*, 16746-16753

Radin, N. S. (1984) Biosynthesis of the sphingoid bases: a provocation. J Lipid Res *25*, 1536-1540

Reitman, M. L., Varki, A., and Kornfeld, S. (1981) Fibroblasts from patients with I-cell disease and pseudo-Hurler polydystrophy are deficient in uridine 5'-diphosphate-N-acetylglucosamine: glycoprotein N-acetylglucosaminylphosphotransferase activity. J Clin Invest *67*, 1574-1579

Renfrew, C. A., and Hubbard, A. L. (1991) Degradation of epidermal growth factor receptor in rat liver. Membrane topology through the lysosomal pathway. J Biol Chem *266*, 21265-21273

Rijnboutt, S., Aerts, H. M., Geuze, H. J., Tager, J. M., and Strous, G. J. (1991a) Mannose 6-phosphate-independent membrane association of cathepsin D, glucocerebrosidase, and sphingolipid-activating protein in HepG2 cells. J Biol Chem *266*, 4862-4868

Rijnboutt, S., Kal, A. J., Geuze, H. J., Aerts, H., and Strous, G. J. (1991b) Mannose 6-phosphate-independent targeting of cathepsin D to lysosomes in HepG2 cells. J Biol Chem *266*, 23586-23592

Robinson, M. S. (1987) 100-kD coated vesicle proteins: molecular heterogeneity and intracellular distribution studied with monoclonal antibodies. J Cell Biol *104*, 887-895

Robinson, M. S. (2004) Adaptable adaptors for coated vesicles. Trends Cell Biol *14*, 167-174

Robinson, M. S., and Bonifacino, J. S. (2001) Adaptor-related proteins. Curr Opin Cell Biol *13*, 444-453

Rohrer, J., Schweizer, A., Russell, D., and Kornfeld, S. (1996) The targeting of Lamp1 to lysosomes is dependent on the spacing of its cytoplasmic tail tyrosine sorting motif relative to the membrane. J Cell Biol *132*, 565-576

Romano, P. S., Jofre, G., Carvelli, L., Lopez, A. C., Sartor, T., and Sosa, M. A. (2006) Changes in phosphomannosyl ligands correlate with cation-dependent mannose-6-phosphate receptors in rat liver during perinatal development. Biochem Biophys Res Commun *344*, 605-611

Rybin, V., Ullrich, O., Rubino, M., Alexandrov, K., Simon, I., Seabra, M. C., Goody, R., and Zerial, M. (1996) GTPase activity of Rab5 acts as a timer for endocytic membrane fusion. Nature *383*, 266-269

Sachs, B. (1896) A family form of idiocy, generally fatal, associated with early blindness (amaurotic family idiocy). J Nerv Ment Dis *21*, 475-479

Saint-Pol, A., Yelamos, B., Amessou, M., Mills, I. G., Dugast, M., Tenza, D., Schu, P., Antony, C., McMahon, H. T., Lamaze, C., and Johannes, L. (2004) Clathrin adaptor epsinR is required for retrograde sorting on early endosomal membranes. Dev Cell *6*, 525-538

Sandhoff, K. (1969) Variation of beta-N-acetylhexosaminidase-pattern in Tay-Sachs disease. FEBS Lett *4*, 351-354

Sandhoff, K. (2001) The GM2-gangliosidoses and the elucidation of the beta-hexosaminidase system. Adv Genet *44*, 67-91

Sandhoff, K., and Kolter, T. (1996) Topology of glycosphingolipid degradation. Trends Cell Biol *6*, 98-103

Sandoval, I. V., Arredondo, J. J., Alcalde, J., Gonzalez Noriega, A., Vandekerckhove, J., Jimenez, M. A., and Rico, M. (1994) The residues Leu(Ile)475-Ile(Leu, Val, Ala)476, contained in the extended carboxyl cytoplasmic tail, are critical for targeting of the resident lysosomal membrane protein LIMP II to lysosomes. J Biol Chem *269*, 6622-6631

Schmid, B., Paton, B. C., Sandhoff, K., and Harzer, K. (1992) Metabolism of GM1 ganglioside in cultured skin fibroblasts: anomalies in gangliosidoses, sialidoses, and sphingolipid activator protein (SAP, saposin) 1 and prosaposin deficient disorders. Hum Genet *89*, 513-518

Schweiger, A., Christensen, I. J., Nielsen, H. J., Sorensen, S., Brunner, N., and Kos, J. (2004) Serum cathepsin H as a potential prognostic marker in patients with colorectal cancer. Int J Biol Markers *19*, 289-294

Scott, G. K., Fei, H., Thomas, L., Medigeshi, G. R., and Thomas, G. (2006) A PACS-1, GGA3 and CK2 complex regulates CI-MPR trafficking. Embo J *25*, 4423-4435

Seaman, M. N. (2004) Cargo-selective endosomal sorting for retrieval to the Golgi requires retromer. J Cell Biol *165*, 111-122

Seaman, M. N. (2007) Identification of a novel conserved sorting motif required for retromer-mediated endosome-to-TGN retrieval. J Cell Sci *120*, 2378-2389

Seaman, M. N., Marcusson, E. G., Cereghino, J. L., and Emr, S. D. (1997) Endosome to Golgi retrieval of the vacuolar protein sorting receptor, Vps10p, requires the function of the VPS29, VPS30, and VPS35 gene products. J Cell Biol *137*, 79-92

Seaman, M. N., McCaffery, J. M., and Emr, S. D. (1998) A membrane coat complex essential for endosome-to-Golgi retrograde transport in yeast. J Cell Biol *142*, 665-681

Seyrantepe, V., Poupetova, H., Froissart, R., Zabot, M. T., Maire, I., and Pshezhetsky, A. V. (2003) Molecular pathology of NEU1 gene in sialidosis. Hum Mutat *22*, 343-352

Shorter, J., Beard, M. B., Seemann, J., Dirac-Svejstrup, A. B., and Warren, G. (2002) Sequential tethering of Golgins and catalysis of SNAREpin assembly by the vesicle-tethering protein p115. J Cell Biol *157*, 45-62

Simmen, T., Honing, S., Icking, A., Tikkanen, R., and Hunziker, W. (2002) AP-4 binds basolateral signals and participates in basolateral sorting in epithelial MDCK cells. Nat Cell Biol *4*, 154-159

Simons, K., and Ikonen, E. (1997) Functional rafts in cell membranes. Nature *387*, 569-572

Simons, K., and Toomre, D. (2000) Lipid rafts and signal transduction. Nat Rev Mol Cell Biol *1*, 31-39

Simons, K., and van Meer, G. (1988) Lipid sorting in epithelial cells. Biochemistry *27*, 6197-6202

Soldati, T., Rancano, C., Geissler, H., and Pfeffer, S. R. (1995) Rab7 and Rab9 are recruited onto late endosomes by biochemically distinguishable processes. J Biol Chem *270*, 25541-25548

Soldati, T., Shapiro, A. D., Svejstrup, A. B., and Pfeffer, S. R. (1994) Membrane targeting of the small GTPase Rab9 is accompanied by nucleotide exchange. Nature *369*, 76-78

Sonnichsen, B., De Renzis, S., Nielsen, E., Rietdorf, J., and Zerial, M. (2000) Distinct membrane domains on endosomes in the recycling pathway visualized by multicolor imaging of Rab4, Rab5, and Rab11. J Cell Biol *149*, 901-914

Spranger, J. W., and Wiedemann, H. R. (1970) The genetic mucolipidoses. Diagnosis and differential diagnosis. Humangenetik *9*, 113-139

Springer, S., Spang, A., and Schekman, R. (1999) A primer on vesicle budding. Cell *97*, 145-148

Steinman, R. M., Mellman, I. S., Muller, W. A., and Cohn, Z. A. (1983) Endocytosis and the recycling of plasma membrane. J Cell Biol *96*, 1-27

Stevens, R. L., Fluharty, A. L., Kihara, H., Kaback, M. M., Shapiro, L. J., Marsh, B., Sandhoff, K., and Fischer, G. (1981) Cerebroside sulfatase activator deficiency induced metachromatic leukodystrophy. Am J Hum Genet *33*, 900-906

Stevens, T. H., and Forgac, M. (1997) Structure, function and regulation of the vacuolar (H+)-ATPase. Annu Rev Cell Dev Biol *13*, 779-808

Stoka, V., Turk, B., and Turk, V. (2005) Lysosomal cysteine proteases: structural features and their role in apoptosis. IUBMB Life *57*, 347-353

Storrie, B., and Desjardins, M. (1996) The biogenesis of lysosomes: is it a kiss and run, continuous fusion and fission process? Bioessays *18*, 895-903

Suter, A., Everts, V., Boyde, A., Jones, S. J., Lullmann-Rauch, R., Hartmann, D., Hayman, A. R., Cox, T. M., Evans, M. J., Meister, T., *et al.* (2001) Overlapping functions of lysosomal acid phosphatase (LAP) and tartrate-resistant acid phosphatase (Acp5) revealed by doubly deficient mice. Development *128*, 4899-4910

Suzuki, K. (2003) Globoid cell leukodystrophy (Krabbe's disease): update. J Child Neurol *18*, 595-603

Suzuki, K., and Suzuki, Y. (1970) Globoid cell leucodystrophy (Krabbe's disease): deficiency of galactocerebroside beta-galactosidase. Proc Natl Acad Sci U S A *66*, 302-309

Suzuki, Y. (1995) [Lysosomal enzymes, sphingolipid activator proteins, and protective protein]. Nippon Rinsho *53*, 2887-2891

Takatsu, H., Katoh, Y., Shiba, Y., and Nakayama, K. (2001) Golgi-localizing, gamma-adaptin ear homology domain, ADP-ribosylation factor-binding (GGA) proteins interact with acidic dileucine sequences within the cytoplasmic domains of sorting receptors through their Vps27p/Hrs/STAM (VHS) domains. J Biol Chem *276*, 28541-28545

Tanaka, Y., Tanaka, R., and Himeno, M. (2000) Lysosomal cysteine protease, cathepsin H, is targeted to lysosomes by the mannose 6-phosphate-independent system in rat hepatocytes. Biol Pharm Bull *23*, 805-809

Tang, B. L., Low, D. Y., Lee, S. S., Tan, A. E., and Hong, W. (1998a) Molecular cloning and localization of human syntaxin 16, a member of the syntaxin family of SNARE proteins. Biochem Biophys Res Commun *242*, 673-679

Tang, B. L., Low, D. Y., Tan, A. E., and Hong, W. (1998b) Syntaxin 10: a member of the syntaxin family localized to the trans-Golgi network. Biochem Biophys Res Commun *242*, 345-350

Tang, X. M., Clermont, Y., and Hermo, L. (1988) Origin and fate of autophagosomes in Leydig cells of normal adult rats. J Androl *9*, 284-293

Tauris, J., Ellgaard, L., Jacobsen, C., Nielsen, M. S., Madsen, P., Thogersen, H. C., Gliemann, J., Petersen, C. M., and Moestrup, S. K. (1998) The carboxy-terminal domain of the receptor-associated protein binds to the Vps10p domain of sortilin. FEBS Lett *429*, 27-30

Tay, W. (1884) A third instance in the same family of symmetrical changes in the region of the yellow spot in each eye of an infant, closely resembling those of embolism. Trans Opthalmol Soc UK *4*, 158-159

Terman, A., and Brunk, U. T. (2005) The aging myocardium: roles of mitochondrial damage and lysosomal degradation. Heart Lung Circ *14*, 107-114

Tong, P. Y., and Kornfeld, S. (1989) Ligand interactions of the cation-dependent mannose 6-phosphate receptor. Comparison with the cation-independent mannose 6-phosphate receptor. J Biol Chem *264*, 7970-7975

Traub, L. M. (2005) Common principles in clathrin-mediated sorting at the Golgi and the plasma membrane. Biochim Biophys Acta *1744*, 415-437

Traub, L. M., Bannykh, S. I., Rodel, J. E., Aridor, M., Balch, W. E., and Kornfeld, S. (1996) AP-2-containing clathrin coats assemble on mature lysosomes. J Cell Biol *135*, 1801-1814

Tsuji, A., Omura, K., and Suzuki, Y. (1988) I-cell disease: evidence for a mannose 6-phosphate independent pathway for translocation of lysosomal enzymes in lymphoblastoid cells. Clin Chim Acta *176*, 115-121

Turk, B., and Stoka, V. (2007) Protease signalling in cell death: caspases versus cysteine cathepsins. FEBS Lett *581*, 2761-2767

Turk, B., Turk, D., and Salvesen, G. S. (2002) Regulating cysteine protease activity: essential role of protease inhibitors as guardians and regulators. Curr Pharm Des *8*, 1623-1637

Turk, B., Turk, D., and Turk, V. (2000) Lysosomal cysteine proteases: more than scavengers. Biochim Biophys Acta *1477*, 98-111

Turk, V., Turk, B., and Turk, D. (2001) Lysosomal cysteine proteases: facts and opportunities. Embo J *20*, 4629-4633

Turley, S. J., Inaba, K., Garrett, W. S., Ebersold, M., Unternaehrer, J., Steinman, R. M., and Mellman, I. (2000) Transport of peptide-MHC class II complexes in developing dendritic cells. Science *288*, 522-527

Ullrich, A., Gray, A., Tam, A. W., Yang-Feng, T., Tsubokawa, M., Collins, C., Henzel, W., Le Bon, T., Kathuria, S., Chen, E., and et al. (1986) Insulin-like growth factor I receptor primary structure: comparison with insulin receptor suggests structural determinants that define functional specificity. Embo J *5*, 2503-2512

Ullrich, K., and von Figura, K. (1979) Endocytosis of beta-N-acetylglucosaminidase from sections of mucolipidosis-II and-III fibroblasts by non-parenchymal rat liver cells. Biochem J *182*, 245-247

Ullrich, O., Horiuchi, H., Bucci, C., and Zerial, M. (1994) Membrane association of Rab5 mediated by GDP-dissociation inhibitor and accompanied by GDP/GTP exchange. Nature *368*, 157-160

Urbanelli, L., Emiliani, C., Massini, C., Persichetti, E., Orlacchio, A., Pelicci, G., Sorbi, S., Hasilik, A., Bernardi, G., and Orlacchio, A. (2006) Cathepsin D expression is decreased in Alzheimer's disease fibroblasts. Neurobiol Aging

Vaccaro, A. M., Salvioli, R., Barca, A., Tatti, M., Ciaffoni, F., Maras, B., Siciliano, R., Zappacosta, F., Amoresano, A., and Pucci, P. (1995) Structural analysis of saposin C and B. Complete localization of disulfide bridges. J Biol Chem *270*, 9953-9960

Vaccaro, A. M., Tatti, M., Ciaffoni, F., Salvioli, R., Maras, B., and Barca, A. (1993) Function of saposin C in the reconstitution of glucosylceramidase by phosphatidylserine liposomes. FEBS Lett *336*, 159-162

Valdez, A. C., Cabaniols, J. P., Brown, M. J., and Roche, P. A. (1999) Syntaxin 11 is associated with SNAP-23 on late endosomes and the trans-Golgi network. J Cell Sci *112 (Pt 6)*, 845-854

Valls, L. A., Hunter, C. P., Rothman, J. H., and Stevens, T. H. (1987) Protein sorting in yeast: the localization determinant of yeast vacuolar carboxypeptidase Y resides in the propeptide. Cell *48*, 887-897

van der Spoel, A., Bonten, E., and d'Azzo, A. (1998) Transport of human lysosomal neuraminidase to mature lysosomes requires protective protein/cathepsin A. Embo J *17*, 1588-1597

Varki, A., and Kornfeld, S. (1980) Identification of a rat liver alpha-N-acetylglucosaminyl phosphodiesterase capable of removing "blocking" alpha-N-acetylglucosamine residues from phosphorylated high mannose oligosaccharides of lysosomal enzymes. J Biol Chem *255*, 8398-8401

Varki, A. P., Reitman, M. L., and Kornfeld, S. (1981) Identification of a variant of mucolipidosis III (pseudo-Hurler polydystrophy): a catalytically active N-acetylglucosaminylphosphotransferase that fails to phosphorylate lysosomal enzymes. Proc Natl Acad Sci U S A *78*, 7773-7777

Vega, M. A., Rodriguez, F., Segui, B., Cales, C., Alcalde, J., and Sandoval, I. V. (1991a) Targeting of lysosomal integral membrane protein LIMP II. The tyrosine-lacking carboxyl cytoplasmic tail of LIMP II is sufficient for direct targeting to lysosomes. J Biol Chem *266*, 16269-16272

Vega, M. A., Segui-Real, B., Garcia, J. A., Cales, C., Rodriguez, F., Vanderkerckhove, J., and Sandoval, I. V. (1991b) Cloning, sequencing, and expression of a cDNA encoding rat LIMP II, a novel 74-kDa lysosomal membrane protein related to the surface adhesion protein CD36. J Biol Chem *266*, 16818-16824

Vinogradova, M. V., Michaud, L., Mezentsev, A. V., Lukong, K. E., El-Alfy, M., Morales, C. R., Potier, M., and Pshezhetsky, A. V. (1998) Molecular mechanism of lysosomal sialidase deficiency in galactosialidosis involves its rapid degradation. Biochem J *330 (Pt 2)*, 641-650

Vladutiu, G. D., and Rattazzi, M. C. (1979) Excretion-reuptake route of beta-hexosaminidase in normal and I-cell disease cultured fibroblasts. J Clin Invest *63*, 595-601

von Figura, K., and Hasilik, A. (1986) Lysosomal enzymes and their receptors. Annu Rev Biochem *55*, 167-193

Waguri, S., Tomiyama, Y., Ikeda, H., Hida, T., Sakai, N., Taniike, M., Ebisu, S., and Uchiyama, Y. (2006) The luminal domain participates in the endosomal trafficking of the cation-independent mannose 6-phosphate receptor. Exp Cell Res *312*, 4090-4107

Waheed, A., Braulke, T., Junghans, U., and von Figura, K. (1988) Mannose 6-phosphate/insulin like growth factor II receptor: the two types of ligands bind

simultaneously to one receptor at different sites. Biochem Biophys Res Commun *152*, 1248-1254

Waheed, A., Pohlmann, R., Hasilik, A., von Figura, K., van Elsen, A., and Leroy, J. G. (1982) Deficiency of UDP-N-acetylglucosamine:lysosomal enzyme N-acetylglucosamine-1-phosphotransferase in organs of I-cell patients. Biochem Biophys Res Commun *105*, 1052-1058

Ward, D. M., Shiflett, S. L., Huynh, D., Vaughn, M. B., Prestwich, G., and Kaplan, J. (2003) Use of expression constructs to dissect the functional domains of the CHS/beige protein: identification of multiple phenotypes. Traffic *4*, 403-415

Waters, M. G., Serafini, T., and Rothman, J. E. (1991) 'Coatomer': a cytosolic protein complex containing subunits of non-clathrin-coated Golgi transport vesicles. Nature *349*, 248-251

Westergaard, U. B., Sorensen, E. S., Hermey, G., Nielsen, M. S., Nykjaer, A., Kirkegaard, K., Jacobsen, C., Gliemann, J., Madsen, P., and Petersen, C. M. (2004) Functional organization of the sortilin Vps10p domain. J Biol Chem *279*, 50221-50229

Winchester, B. (2005) Lysosomal metabolism of glycoproteins. Glycobiology *15*, 1R-15R

Wright, C. S., Li, S. C., and Rastinejad, F. (2000) Crystal structure of human GM2-activator protein with a novel beta-cup topology. J Mol Biol *304*, 411-422

Xie, B., Rigat, B., Smiljanic-Georgijev, N., Deng, H., and Mahuran, D. (1998) Biochemical characterization of the Cys138Arg substitution associated with the AB variant form of GM2 gangliosidosis: evidence that Cys138 is required for the

recognition of the GM2 activator/GM2 ganglioside complex by beta-hexosaminidase A. Biochemistry *37*, 814-821

Zhao, Q., Bell, A. W., El-Alfy, M., and Morales, C. R. (1998) Mouse testicular sulfated glycoprotein-1: sequence analysis of the common backbone structure of prosaposins. J Androl *19*, 165-174

Zhao, Q., and Morales, C. R. (2000) Identification of a novel sequence involved in lysosomal sorting of the sphingolipid activator protein prosaposin. J Biol Chem *275*, 24829-24839

Zhu, Y., Doray, B., Poussu, A., Lehto, V. P., and Kornfeld, S. (2001) Binding of GGA2 to the lysosomal enzyme sorting motif of the mannose 6-phosphate receptor. Science *292*, 1716-1718

Appendix: Research Compliance Certificates